Synchrotron Microanalysis of Gallium Maltolate as a Potential Novel Therapy for *Escherichia coli* Urinary Tract Infections

A Dissertation Submitted to the College of Graduate Studies and Research

in Partial Fulfillment of the Requirements for the Degree Doctor of Philosophy

in the Graduate Program of Veterinary Biomedical Sciences

University of Saskatchewan

Saskatoon

Katherine R. Ball

Permission to Use

In presenting this thesis in partial fulfilment of the requirements for a postgraduate degree from the University of Saskatchewan, I agree that the Libraries of this University may make it freely available for inspection. I further agree that permission for copying of this thesis in any manner, in whole or in part, for scholarly purposes may be granted by the professors who supervised my thesis work or, in their absence, by the Head of the Department or the Dean of the College in which my thesis work was done. It is understood that any copying or publication or use of this thesis or parts thereof for financial gain shall not be allowed without my written permission. It is also understood that due recognition shall be given to me and to the University of Saskatchewan in any scholarly use which may be made of any material in my thesis.

Requests for permission to copy or to make other use of material in this thesis in whole or part should be addressed to:

Head of the Department of Veterinary Biomedical Sciences

University of Saskatchewan

Saskatoon, Saskatchewan S7N 5B4

Abstract

Most urinary tract infections in humans and dogs are caused by uropathogenic strains of *Escherichia coli*, and increasing antimicrobial resistance among these pathogens has created a need for a novel approach to therapy. Bacterial iron uptake and metabolism are potential targets for novel antimicrobial therapy, as iron is a limiting factor in *E. coli* growth during infection. As a trivalent metal of similar atomic size to iron (III), gallium can interact with a wide variety of biomolecules that normally contain or interact with iron. Gallium compounds disrupt bacterial iron metabolism, are known to accumulate at sites of infection and inflammation in mammals, exert antimicrobial activity against multiple bacterial pathogens in vitro, and may be good candidates as novel antimicrobial drugs. We assessed the suitability of orally administered gallium maltolate as a potential new antimicrobial therapy for urinary tract infections by evaluating its distribution into the bladder, its activity against uropathogenic *E. coli* in vitro, and its pharmacokinetics and efficacy in a mouse cystitis model. Using a novel application of synchrotron-based analytical methods, we confirmed the distribution of gallium to the bladder mucosa and characterized the relationship between iron and gallium distribution in the bladder.

In vitro experiments with human and canine uropathogenic *E. coli* isolates demonstrated that gallium maltolate exerts antimicrobial effects in a time-dependent, bacteriostatic manner. Minimum inhibitory concentrations ranged from 0.144 µmol/mL to >9.20 µmol/mL with a median of 1.15 µmol/mL. Isolates resistant to ampicillin, ciprofloxacin, or with decreased susceptibility to cephalothin were susceptible to the antimicrobial activity of gallium maltolate, suggesting that resistance to conventional antimicrobials does not predict resistance to gallium maltolate.

Pharmacokinetic studies in healthy mice and in a mouse model of urinary tract infection confirmed that gallium is absorbed into systemic circulation after oral administration of gallium maltolate. Gallium is slowly eliminated from the body, with a trend toward longer terminal half-lives in blood and bladder for infected mice relative to healthy mice. This study did not reveal any statistically significant effect of infection status on maximum blood gallium concentrations (4.46 nmol/mL, 95% confidence interval 2.75 nmol/mL – 6.18 nmol/mL and 4.80 nmol/mL, 95% confidence interval 2.53 nmol/mL – 7.06 nmol/mL in healthy and infected mice, respectively) or total gallium exposure in blood and kidney as represented by area under the concentration vs. time curves. Gallium exposure in the bladder was significantly greater for mice with urinary tract infections than for healthy mice.

The investigation of gallium distribution within tissues represented a novel application of synchrotron-based analytical techniques to antimicrobial pharmacokinetics. Prior to analysing tissue samples, a library of x-ray absorption spectra was assembled for gallium compounds in both the hard and soft x-ray ranges. The suitability of hard x-ray fluorescence imaging and scanning and transmission x-ray microscopy for localizing and speciating trace elements in tissues was subsequently assessed. Of these methods, only hard x-ray microprobe analysis was well-suited to the analysis and was successfully used for this application. This approach confirmed that gallium arrives at the bladder mucosa after oral administration of gallium maltolate. Furthermore, comparison of iron and gallium distribution within the bladder mucosa indicated that these elements are similarly but not identically distributed and that they do not

significantly inhibit one another's distribution. This finding suggests that gallium may be distributed in part via pathways that do not involve iron.

Despite the favorable distribution characteristics of gallium and the persistence of gallium in target tissues following the oral administration of gallium maltolate, its efficacy in a mouse model of urinary tract infection was disappointing. In this study, no statistically significant difference was detected between gallium maltolate, ciprofloxacin and sham treatments in their ability to eliminate bacteria in the urinary tracts. The failure of ciprofloxacin treatment to render bladder tissue culture-negative for an organism that is classified as ciprofloxacin-susceptible in vitro is consistent with observations from other research groups. The similar lack of efficacy observed for gallium maltolate may be related to the large gap between minimum inhibitory concentrations observed in vitro and gallium concentrations observed in tissues from treated mice, but may also be related to the small study size if the effect size of gallium maltolate treatment is small. Given the magnitude of the difference between tissue concentrations and minimum inhibitory concentrations, it may not be possible to increase the dose sufficiently to achieve therapeutic concentrations without causing toxicity.

While the results of these experiments suggest that orally administered gallium maltolate may not be a reasonable antimicrobial drug candidate for treating urinary tract infections caused by uropathogenic *E. coli*, it may be useful for other applications. Other bacterial pathogens may be more susceptible to the antimicrobial effects of gallium maltolate, and local or topical administration could produce much higher concentrations than we observed following oral administration. Continued development of the synchrotron-based analytical techniques used in

these experiments could provide new and important opportunities to investigate antimicrobial distribution and metabolism within cells and tissues, particularly for metal-based drugs.

Acknowledgements

I am sincerely grateful to all of the people who assisted me during my studies, research, and writing. I wish to thank my supervisors, Dr. D. Hamilton and Dr. J. Thompson for providing advice, assistance and encouragement while also giving me the opportunity to work independently. I must also thank my committee members for their unique contributions. Dr. P. Dowling invited me to pursue graduate studies and a veterinary clinical pharmacology residency at the University of Saskatchewan, and helped me to remember the importance of "real world" applications of pharmacology. I am greatly indebted to Dr. J. Alcorn for the many hours she spent mentoring me in pharmacokinetics. Dr. J. Boison, Dr. G. Muir, and Dr. B. Singh ensured that this work met their exacting standards and helped navigate the administrative complexities of graduate studies.

Many other talented individuals provided help and advice, including Monique Burmester and the WCVM Animal Care Unit staff, Sarah Caldwell, Jesse Invik, Dr. L. Bernstein, Dr. C. Karunakaran and the staff scientists at the Canadian Light Source, and Dr. R. Gordon at the Advanced Photon Source. Dr. M. Chirino-Trejo provided bacterial isolates and critical advice for the microbiological studies. Dr. R. Blyth provided access to the SGM beamline at the Canadian Light Source and spent countless hours explaining x-ray interactions with matter. Dr. T.K. Sham provided excellent advice and mentorship, as well as providing facility access at the Advanced Photon Source.

My colleagues and friends Dr. F. Sampieri, Dr. J. Rubin, Dr. A. Chicoine, Dr. J.Y. Ko and Dr. B.B. Ling were an important source of good suggestions, hands-on help, constructive criticism and friendly encouragement.

This research was supported by the Canadian Institutes of Health Research, the Natural Sciences and Engineering Research Council, and the Western College of Veterinary Medicine Companion Animal Health Fund. I was personally supported by an Interprovincial Graduate Student Fellowship.

I am grateful to my parents, Max and Cheryl, my grandmother Jean Ball, Val Bandas and my aunts, uncles and cousins for their never-ending support and encouragement during my studies. This work would have been impossible in the absence of friends and family, and would be meaningless to me without their presence in my life.

To each of these people, and to the many more that are not listed here, I extend my sincere thanks.

Dedication

Some of my elders wished to complete high school or post-secondary studies, but were prevented from doing so by financial hardship or gender discrimination. This work is dedicated to each family member who was not able to access the education they desired.

Table of Contents

List of Tables

List of Figures

Abbreviations

ABBC	Area between the microbial growth curve and the microbial kill curve for a particular antimicrobial compound and pathogen combination
ABC	ATP Binding Cassette
ATCC	American type culture collection
ATCC 700336	UPEC type strain originally isolated from a human pyelonephritis case; commonly known as J96
ATCC 700928	UPEC type strain originally isolated from a human pyelonephritis case; commonly known as CFT073
AUC	Area under the concentration vs. time curve; subscripts may be used to indicate the associated time range
CFT073	UPEC type strain ATCC 700928
CLSI	Clinical and Laboratory Standards Institute
C_{max}	Maximum concentration of analyte observed in the target matrix in samples collected over a defined range of times
DMT1	Divalent metal transporter 1
EXAFS	Extended x-ray absorption fine structure (spectra or spectroscopy)
FimH	Type 1 fimbriae which contribute to UPEC adhesion to urothelial cells
$Ga(NO_3)_3$	Gallium nitrate
Ga_2O_3	Gallium oxide
GaD_3	Tris(dimethylamido) gallium (III)
GaM	Gallium maltolate
GaQ_3	Tris(8-hydroxyquinolinato) gallium (III)
IBC	Intracellular bacterial community
IC_{50}	Inhibitory concentration; concentration of the test compound which inhibits enzyme function by 50%

IL	Interleukin
J96	UPEC type strain ATCC 700336
LD_{50}	Lethal dose-50; the median lethal dose
LLOQ	Lower limit of quantification
MIC	Minimum inhibitory concentration
MMHA	4,4'-methylenebis(2-methylcyclohexylamine)
MPC	Mutant prevention concentration
NGF	Nerve growth factor
PD	Pharmacodynamic
PMMA	Poly(methylmethacrylate)
PTH	Parathyroid hormone
ST131	Sequence type 131; an epidemiologically important UPEC strain bearing multiple virulence factor and antimicrobial resistance genes
STXM	Scanning and transmission x-ray microscopy
TEM	Transmission electron microscopy
TFR1	Transferrin receptor 1
TFR2	Transferrin receptor 2
T_{max}	The time at which the maximum analyte concentration is observed, usually reported relative to the time of drug administration
TPD	N,N'-bis(3-methylphenyl)-N,N'-diphenylbenzidine
TTE	Trimethylolpropane triglycidal ether-4,4'-methylenebis(2-methylcyclohexylamine)
UPEC	Uropathogenic *Escherichia coli*
UTI	Urinary tract infection
UTI89	UPEC type strain isolated from a human case of recurrent cystitis

XANES	X-ray absorption near-edge spectra (or spectroscopy)
XAS	X-ray absorption spectroscopy
XRF	Synchrotron radiation-induced x-ray fluorescence

Chapter 1. Introduction

1.1. **Urinary tract infections**

Urinary tract infections occur when microbial pathogens overcome mammalian host defenses and invade the urinary bladder, ureter, or kidney. Lower urinary tract infections affect the bladder, while infections of the ureter and kidney are considered upper urinary tract infections (Lane and Takhar, 2011). Urinary tract infections are of clinical importance in human and veterinary medicine because in addition to patient discomfort and economic burdens from treatment costs and lost work time, failure to cure these infections can lead to serious complications including pyelonephritis and septicaemia (Ling, 1984; Foxman and Brown, 2003; Chang et al., 2011; Lee et al., 2011).

1.1.1. **Pathology**

While the pathogenesis of urinary tract infections has been extensively studied in mouse models and in humans, only limited canine-specific research is reported. Similar pathogen prevalence and clinical presentation suggest that human and canine urinary tract infections closely resemble one another in pathogenesis (Zhanel et al., 2006; Ball et al., 2008a; Karlowsky et al., 2011). This is also supported by the genetic similarity in *Escherichia coli* isolated from canine and human infections, along with the growing evidence for transmission of uropathogenic *E. coli* clones between humans and dogs (Johnson et al., 2001; Johnson et al., 2003; Johnson and Clabots, 2006; Johnson et al., 2008).

1.1.1.2. **Host defenses against urinary tract infection**

1.1.1.2.1. **Unidirectional urine flow**

Urine produced by the kidney flushes the urinary tract, dislodging debris and bacteria which are not affixed to local structures. Normally, the urine flow is unidirectional and thus impedes ascension of bacteria into the urinary tract. The direction of flow is maintained by a series of anatomic and physiologic features. First, urine arriving at the renal pelvis flows down a pressure gradient into the ureters, where it is moved toward the bladder by peristaltic activity. The oblique course of the ureter through the bladder wall in the trigone region makes the ureterovesicular junction susceptible to compression during bladder distension, thereby passively restricting retrograde urine flow (Roshani et al., 1996). Developmental anomalies such as ectopic ureter and duplex kidney interfere with this function by decreasing the length of the ureter's path through the submucosa, predisposing the individual to vesico-ureteral reflux (Bhat et al., 2011; Hunziker et al., 2011). These phenomena are most commonly diagnosed early in life, and are associated with hydronephrosis, pyelonephritis and renal scarring in children (Sung and Skoog, 2011). Neoplastic disease such as transitional cell carcinoma and prostatic hyperplasia can interfere with bladder emptying and urethral sphincter competence (Heyns, 2011).

1.1.1.2.2. **Urine composition**

The protection afforded by unidirectional urine flow is complimented by urine composition that discourages pathogens from establishing infections. The inhibitory effect of urine on bacterial growth is widely recognized, and is a result of multiple factors (Kaye, 1968). Canine and human urine are normally acidic, and the antimicrobial activity of urine increases as pH decreases (Kaye, 1968). Although this effect occurs independently, it is more pronounced in the presence

of nitrite (Carlsson et al., 2001). Under acidic conditions, nitrite generated through bacterial metabolism is more efficiently converted to nitric oxide which has antimicrobial activity of its own (Carlsson et al., 2001). Urine can become alkalinized following changes in diet, administration of sodium bicarbonate, or administration of carbonic anhydrase inhibitors such as acetazolamide (Sterrett et al., 2008). High urea concentrations and high urine osmolality also contribute to bacterial growth inhibition (Kaye, 1968; Cicmanec et al., 1985).

1.1.1.2.3. **Antimicrobial proteins and peptides**

Several macromolecules contribute to urinary tract defense against infection. Tamm-Horsfall protein, a glycoprotein secreted in the thick ascending limb of the loop of Henle, inhibits bacterial adhesion to transitional epithelial cells by binding to bacterial pathogens, particularly uropathogenic *Escherichia coli* (Zasloff, 2007; Ali et al., 2009). Lactoferrin, an iron-binding protein present at numerous mucosal surfaces including the bladder mucosa, inhibits bacterial growth by reducing iron availability (Ali et al., 2009). Defensins and cathelicidins are cationic antimicrobial peptides produced in multiple locations in the body, particularly at mucosal surfaces (Ali et al., 2009). While α-defensins are well-known as secretory products of small intestinal paneth cells and as agents of non-oxidative microbial killing within neutrophils, they are also expressed in the kidney, ureters and bladder (Ali et al., 2009; Spencer et al., 2012). The β-defensin HBD-1 is constitutively expressed in the renal tubules, and it is hypothesized to exert antimicrobial activity at the mucosal surface as concentrations achieved in urine are insufficient to produce antimicrobial effects (Ali et al., 2009). In contrast, expression of the β-defensin HBD-2 in the renal tubules is inducible by chronic renal infection (Zasloff, 2007). In high concentrations, HBD-2 decreases the bacterial load of uropathogenic *Escherichia coli* in urine

and bladder in a rat model of urinary tract infection (Zhao et al., 2011). Cathelicidins, particularly LL-37, interfere with bacterial invasion of the urinary tract by exerting antimicrobial activity against a variety of bacterial pathogens (Nielubowicz and Mobley, 2010). This activity is a result of bacterial membrane disruption by the cathelicidin (Chromek et al., 2006). LL-37 secretion is strongly upregulated in response to type 1- or p-fimbriae-associated lipopolysaccharide interaction with toll-like receptor 4 in urothelial cells of the renal tubules and proximal ureter (Chromek and Brauner, 2008).

1.1.1.3. **Host response to infection**

Urinary tract infections are established when invading bacteria overcome the defenses of the urinary tract. In most cases, bacteria gain access to the urinary tract by ascension through the urethra. The gastrointestinal tract and perineum are reservoirs of potential uropathogens, resulting in ongoing exposure of the urethral meatus to potential pathogens (Foxman, 2010). Risk factors such as sexual intercourse and urethral catheterization facilitate introduction of bacteria to the urethra (Foxman and Brown, 2003). Nosocomial infections caused by contamination of urinary catheters are also common (Foxman, 2010).

As uropathogenic strains of *Escherichia coli* (UPEC) are the most common cause of urinary tract infections and are the most thoroughly characterized with respect to host-pathogen interactions, the following review will focus on the pathogenesis of *E. coli* infections (Ball et al., 2008a; Karlowsky et al., 2011).

Bacteria in the bladder must have the ability to resist the flushing action of urine flow to establish an infection. Interaction between FimH type 1 fimbriae and uroplakin Ia on the surface of urothelial cells allows UPEC to adhere to the urothelium in the presence of urine flow (Wu et al., 1996; Nilsson et al., 2007; Wu et al., 2009). The extent of binding between type 1 fimbriae and urothelial cells is significantly greater in diabetic patients than in non-diabetic people, which is likely attributable to shortened polysaccharide components of the uroplakins and likely contributes to the increased risk of urinary tract infections associated with diabetes mellitus (Geerlings et al., 2002; Taganna et al., 2011). While the FimH uroplakin-linked polysaccharide binding target differs from that of UPEC, *Klebsiella pneumoniae* strains bearing FimH also use this mechanism to adhere to the urothelium and establish infection (Stahlhut et al., 2009). Interaction between FimH and uroplakin III and between lipopolysaccharide and toll-like receptor 4 lead to apoptosis of the urothelial cell, which is ultimately shed into the urine (Klumpp et al., 2006; Khandelwal et al., 2009; Thumbikat et al., 2009). Bacterial production of hemolysin further contributes to mucosal damage by accelerating urothelial exfoliation and evoking the inflammatory response (Smith et al., 2008).

Bacterial invasion of the urinary tract leads to a complex inflammatory response. Toll-like receptor 4 can interact with FimH, lipopolysaccharide and P-fimbriae, activating lymphocytes, initiating the synthesis of inflammatory mediators interleukin (IL) -8 and IL-6 and up-regulating cyclooxygenase-2 synthesis (Scherberich and Hartinger, 2008; Hannan et al., 2010; Chen et al., 2011). Neutrophil recruitment and migration into the bladder lumen occurs in response to IL-8 secretion, and is an essential component of host defense (Haraoka et al., 1999; Ingersoll et al., 2008). The inflammatory response is further amplified when mast cells in the bladder mucosa

degranulate upon exposure to FimH, releasing histamine, tumor necrosis factor α, leukotrienes and neutrophil chemoattractants (Malaviya et al., 2004).

The inflammatory response alters bladder neurophysiology. Pain in the pelvic abdomen is common in human patients with cystitis. This is a multifactorial phenomenon. Prostaglandins and inflammatory mediators stimulate nociceptors, activating the unmyelinated C-fibres to produce pain sensation (Beckel and Holstege, 2011). Toll-like receptor 4 stimulation by lipopolysaccharide also contributes to pain sensation (Rudick et al., 2010). Increased tissue concentrations of IL-6 trigger the production of inducible nitric oxide synthase (iNOS), which contributes to the increased bladder contractility and pollakiuria associated with cystitis (Weng et al., 2009). Nerve growth factor (NGF) production by bladder tissues increases in response to infection and inflammation, further increasing detrusor contractility, sensitizing afferent sensory fibres and contributing to pain sensations (Ochodnický et al., 2011).

1.1.2. **Diagnosis**

Urinary tract infections can be recurrent, persistent, complicated, or uncomplicated. Recurrent infections are diagnosed by isolation of the same bacterial strain(s) on multiple occasions with periods of remission following treatment (Foxman et al., 2000; Seguin et al., 2003). Infections are classified as persistent when the pathogens are not cleared from the urinary tract such that the same strain can be isolated on numerous occasions without remission of clinical signs (Seguin et al., 2003; Drazenovich et al., 2004). Cases where patients experience multiple infections caused by different bacterial strains are considered re-infection (Seguin et al., 2003). Uncomplicated urinary tract infections occur in the absence of concurrent urological anomalies (Foxman and

Brown, 2003). Infections in patients with conditions such as prostatitis, ectopic ureters, bladder cancers, spinal cord injuries, and indwelling medical devices are classified as complicated. Complicated infections can represent a greater treatment challenge due to increased pathogen access to the urinary tract via catheters, altered host characteristics that may influence bacterial adhesion and bacterial reservoir formation in biofilms (Geerlings et al., 1999; Geerlings, 2008; Niveditha et al., 2012).

Appropriate clinical management of urinary tract infections requires timely and accurate diagnosis including pathogen identification. Clinical signs and symptoms noted during history-taking or observed during clinical examination are important prompts for clinicians to proceed with diagnostic tests. Pollakiuria, dysuria and hematuria are often observed in canine and human patients with lower urinary tract infections (Bartges, 2004; Lane and Takhar, 2011). Adult humans often report a sensation of urinary urgency, likely related to increased NGF production (Ochodnický et al., 2011). Inappropriate urination is observed in dogs with lower urinary tract infections, and may be caused by a similar mechanism as urgency sensation in humans (Bartges, 2004). Pelvic abdominal pain is a common presenting complaint in human patients (Lane and Takhar, 2011). Upper urinary tract infections are more commonly associated with hematuria, abdominal pain, vomiting and pyrexia in both humans and dogs (Bartges, 2004; Lane and Takhar, 2011). In human patients, the presence of gross hematuria has the greatest specificity among clinical signs for predicting urinary tract infections, while dysuria, pollakiuria and urgency are the most sensitive measures in this context (Giesen et al., 2010).

On urinalysis, detection of nitrites with urine dipsticks is the most specific predictor of urinary tract infections in male and female human patients (Koeijers et al., 2007; Medina-Bombardo and Jover-Palmer, 2011). As several bacterial uropathogens do not metabolize nitrate to nitrite, infections caused by these species cannot be predicted using this test. Furthermore, urine dipstick nitrite indicators produce unreliable results with canine urine and should not be used as a predictive instrument in this species (Klausner et al., 1976; Reine and Langston, 2005).

Microscopic detection of pyuria and a positive dipstick test for leukocyte esterase are additional positive predictors for urinary tract infection, particularly when combined with observations of dysuria, pollakiuria and positive nitrate urine dipstick test results (Giesen et al., 2010; Medina-Bombardo and Jover-Palmer, 2011). In the absence of clinical signs such as pollakiuria and dysuria, microscopic detection of pyuria and dipstick tests for leukocyte esterase and nitrates become unreliable predictors of infection (Khasriya et al., 2010). While pyuria can lead to visible urine turbidity, visual inspection of urine clarity has very poor sensitivity and should not be used alone as a diagnostic test (Foley and French, 2011). In dogs, microscopic examination of urine sediment is required as dipstick tests for leukocyte esterase have poor sensitivity for detecting canine pyuria (Vail et al., 1986). Microscopic examination of urine sediment for bacterial cells is inconsistently reliable for identifying bacteriuria, particularly when bacterial numbers are low (Carroll et al., 1994; Arslan et al., 2002; Leman, 2002; Wilson and Gaido, 2004; dos Santos et al., 2007). The sensitivity and specificity of urine sediment examination are improved when the sediment is stained (Swenson et al., 2004; Wiwanitkit et al., 2005).

Urine culture is the gold standard test for diagnosing urinary tract infections in a clinical setting (Bartges, 2004; Lane and Takhar, 2011). Sample collection methods can substantially influence the value of information gained from urine cultures as sample contamination can obscure results and prevent meaningful interpretation (Platt, 1983; Ling et al., 2001). When completed without inadvertent puncture of bowel loops, ante-pubic cystocentesis is the sample collection method least susceptible to contamination, and is the method of choice for urine collection from veterinary patients (Platt, 1983). Urine collected by this method is ordinarily sterile in healthy individuals. Urethral catheterization following cleansing of the urethral meatus and surrounding tissue is a reasonable alternative to cystocentesis, but the greater probability of sample contamination is reflected in the interpretation criterion where bacteriuria is only considered significant at $\geq 10^5$ colony-forming units/mL (Platt, 1983; Bartges, 2004). Free-catch or voided specimens are often the most conveniently collected samples from human and veterinary patients, but are susceptible to contamination during collection. Culture results from these samples are interpreted similarly to results from urine collected by urethral catheterization (Platt, 1983; Bartges, 2004).

1.1.3. **Epidemiology**

Urinary tract infections are among the most common bacterial diseases in dogs and humans (Ling et al., 1984; Foxman, 2010). Over half of all women and approximately 10% of men experience at least one bout of cystitis, the most common type of urinary tract infection, by their mid-thirties (Foxman and Brown, 2003). These infections account for approximately 1% of all outpatient visits in the United States, with costs estimated at $2.3 billion (US dollars) in 2010, excluding prescription drug expenses (Foxman, 2003; Foxman, 2010). Losses in productivity add

to the economic burden of urinary tract infection. In young women outpatients with urinary tract infections, the mean duration of activity restriction during infection was approximately 2 days, with a mean of 1.2 days lost from work or study (Foxman and Frerichs, 1985). Urinary tract infections are also the most common type of hospital-acquired infection in Canada and worldwide, resulting in prolonged hospital stays and significantly increased treatment costs (Gravel et al., 2007; Wagenlehner et al., 2011a; Weber et al., 2011). Increasing the probability of therapeutic success before the infection progresses to where hospitalization is indicated could improve patient quality of life and reduce the economic burden of urinary tract infections. New antimicrobial therapies with mechanisms of action unrelated to currently available antimicrobial drugs will likely play an important role in managing infections in the face of increasing antimicrobial resistance.

1.1.3.1. **Pathogen prevalence in humans**

Uropathogenic *E. coli* are the most common uropathogens in both uncomplicated urinary tract infections and healthcare-associated infections worldwide (Gales et al., 2002; Turnidge et al., 2002; Streit et al., 2004; Akram et al., 2007; Masinde et al., 2009; Schito et al., 2009; Mwaka et al., 2011; Wagenlehner et al., 2011a). While regional differences exist in their relative prevalence, *Klebsiella* spp., *Enterococcus* spp., and *Proteus* spp. are the next most common uropathogens in healthcare-associated infections worldwide (Wagenlehner et al., 2011a). After UPEC, *Staphylococcus* spp., *Proteus* spp., *Klebsiella* spp. and *Enterococcus* spp. are the next most common pathogens in uncomplicated urinary tract infections, with regional variations in order of prevalence (Schito et al., 2009; Mwaka et al., 2011). Compared with observations for uncomplicated infections in outpatients, *Pseudomonas aeruginosa* and *Enterococcus* spp. along

with other opportunistic pathogens tend to occupy higher prevalence ranks in healthcare-associated infections, infections diagnosed in intensive care units and infections diagnosed at tertiary care facilities (Gordon and Jones, 2003; Streit et al., 2004; Zhanel et al., 2005; Schito et al., 2009; Mwaka et al., 2011; Wagenlehner et al., 2011a).

In Canada, approximately 70% of community-acquired urinary tract infections and 23% of urinary tract infections acquired in hospital intensive care units are caused by uropathogenic *Escherichia coli* (UPEC) (Laupland et al., 2005; Laupland et al., 2007). When all patient categories are considered, UPEC are isolated from the urine samples of approximately 54% of all patients with urinary tract infections at Canadian tertiary care facilities (Karlowsky et al., 2011). In descending order of prevalence, *Klebsiella* spp., *Enterococcus* spp., and group B streptococci are the next most common uropathogens in Canadian outpatients after UPEC (Laupland et al., 2007). In cases of infections acquired in intensive care units, *Candida* spp., *Enterococcus* spp. *Pseudomonas* spp. and *Klebsiella* spp. are the next most prevalent pathogens following UPEC (Laupland et al., 2005).

1.1.3.2. **Pathogen prevalence in dogs**

Uropathogenic *E. coli* are consistently noted as the most common pathogen in dogs with uncomplicated and complicated urinary tract infections (Bush, 1976; Wooley and Blue, 1976; Wierup, 1978; Feria et al., 2000; Ling et al., 2001; Seguin et al., 2003; Ogeer-Gyles et al., 2006; Ball et al., 2008a). *Staphylococcus pseudintermedius* (8.1 – 16.5% of isolates), *Enterococcus* spp. (4.5 – 10.2% of isolates), *Proteus* spp. (5.9 - 11.7% of isolates) and *Klebsiella* spp. (1.1 – 9.1%) are the next most common uropathogens, with rank orders varying between study

locations (Ling et al., 2001; Bubenik et al., 2007; Ball et al., 2008a). The prevalence rankings of *Enterococcus* spp., *Klebsiella* spp., and *Pseudomonas aeruginosa* tend to be higher in complicated urinary tract infections, persistent infections, mixed infections and hospital-acquired infections relative to uncomplicated infections (Norris et al., 2000; Seguin et al., 2003; Ogeer-Gyles et al., 2006; Bubenik et al., 2007; Ball et al., 2008a). Increasing antimicrobial resistance among canine UPEC isolates has been reported at multiple centres in North America (Cohn et al., 2003; Ball et al., 2008a).

1.2. **Uropathogenic *Escherichia coli***

Uropathogenic *Escherichia coli* are a distinct pathotype of extraintestinal pathogenic *Escherichia coli* defined by their ability to invade and colonize the urinary tract (Russo and Johnson, 2000; Marrs et al., 2005). These strains typically possess one or more adaptations such as adhesion factors and supplementary iron uptake systems which facilitate survival within the urinary tract (Bidet et al., 2007; Lloyd et al., 2007). Despite the relatively low numbers of UPEC detectable in fecal cultures, the gastrointestinal tract is considered the principal reservoir of UPEC (Emody et al., 2003). In addition, the isolate responsible for urinary tract infection in a particular patient is usually present in fecal samples collected at the same time (Bower et al., 2005; Niki et al., 2011).

Escherichia coli have traditionally been classified by serotyping based on O-, K-, and H-antigens (Stenutz et al., 2006). While these antigens are not specific uropathogenic virulence factors, certain O-serotypes are more prevalent among UPEC (Stenutz et al., 2006; Bidet et al., 2007). Types O2, O4, O6, O14, O22, O75 and O83 are common among UPEC and they typically possess at least one UPEC virulence factor (Bidet et al., 2007; Yamamoto, 2007). It is important

to note that UPEC are distinct from enterohemorrhagic *E. coli* and do not include serotype O157 (Wiles et al., 2008). Strains of the O157 serotype, including the infamous causative agent of hemolytic uremic syndrome, *E. coli* O157:H7, produce shiga toxin associated with foodborne hemorrhagic colitis but are non-uropathogenic.

The increasing availability of multilocus sequence typing has facilitated epidemiological studies of global UPEC distribution and pathogenicity of particular clones (Maiden et al., 1998; Bidet et al., 2007). For example, uropathogenic *E. coli* of sequence type 131 (O25:H4:ST131) is of increasing global concern as it has been identified worldwide, is commonly fluoroquinolone-resistant and frequently possesses the gene coding for extended spectrum beta-lactamase CTX-M-15 along with multiple uropathogenic virulence factors (Nicolas-Chanoine et al., 2008; Rogers et al., 2011). This clone likely also has zoonotic potential, as it has been identified in dogs with urinary tract infections (Ewers et al., 2010).

1.2.1. **Transmission of uropathogenic *Escherichia coli***

Strains of UPEC can be transmitted between hosts by several routes. Potential pathogens can be introduced to the urethra through interpersonal contact. Particularly in women, recent sexual intercourse is a risk factor for urinary tract infections caused by UPEC among other less common uropathogens (Foxman and Frerichs, 1985; David et al., 1996). Interpersonal transmission resulting in carrier status or leading to overt urinary tract infection is observed among household members even in the absence of sexual contact (Johnson and Clabots, 2006). In addition, canine-human transmission and canine-feline transmission are possible, adding to the complexity of UPEC dissemination within a household (Johnson et al., 2008; Johnson et al., 2009b; Reeves et

al., 2011). As a result of multiple transmissions of UPEC among co-habiting people and dogs, clones can persist within households for years (Reeves et al., 2011). The genetic similarity between UPEC isolated from human and animal infections further supports the hypothesis that UPEC is a zoonotic pathogen (Kurazono et al., 2003; Johnson and Clabots, 2006; Ewers et al., 2010).

Uropathogenic *E. coli* and related strains can also be isolated from horses and food animals (Ewers et al., 2010). Isolation of *E. coli* from clonal groups associated with uropathogenicity (including ST131) from retail meat samples, prepared foods and produce suggests that food may be an important reservoir of UPEC (Moulin-Schouleur et al., 2007; Vincent et al., 2010). This is further supported by the ability of some UPEC-type strains isolated from retail meat to establish urinary tract infections in mouse models (Jakobsen et al., 2010; Xia et al., 2011). As intestinal colonization with UPEC is hypothesized to occur following oral exposure, the presence of epidemiologically important UPEC strains in rivers and water treatment plant effluents is also of potential public health concern (Boczek et al., 2007; Dhanji et al., 2011; Dolejska et al., 2011).

1.2.2. **Pathogenesis of *Escherichia coli* urinary tract infections**

1.2.2.1. **Mouse cystitis model**

Mice have been widely used to investigate the pathogenesis and treatment of urinary tract infections caused by *E. coli* (van den Bosch et al., 1981; Hagberg et al., 1983; Mulvey et al., 1998). Bacterial adhesion to the urothelium occurs with similar affinity between humans and mice, and intracellular infection events are also observed in both species (Hagberg et al., 1983;

Rosen et al., 2007). This may be a result of the strong conservation of uroplakin structure between mammalian species including humans and mice (Wu et al., 1994).

1.2.2.2. **Pathogenicity markers and virulence factors**

While no single gene has been identified that is specific only to UPEC, several groups of genes occur commonly among UPEC isolates and are predictive of virulence. Adhesion is critical for establishing urinary tract infections, and this is consistent with the high prevalence of type 1 fimbriae among UPEC (Mobley et al., 1987; Gunther IV et al., 2002). P-fimbriae, encoded by *pap* genes, are common adhesins in UPEC strains associated with pyelonephritis (Johnson and Russo, 2005). S-adhesins are inconsistently detected among UPEC, but *sfa* was present in 26% of UPEC isolated from inpatients and outpatients in Brazil (Narciso et al., 2011; Oliveira et al., 2011). F1C fimbriae, products of *foc*, also serve as adhesion factors in UPEC.

Iron is essential for UPEC survival, yet the urinary tract is an iron-poor environment. This is compounded by the mammalian defense strategy of iron-withholding (Ganz, 2009). An important bacterial strategy for acquiring iron during infection is the use of siderophore-mediated uptake.

Multiple siderophores, siderophore receptors and iron uptake mechanisms tend to be more prevalent in UPEC than in non-pathogenic *E. coli* and are considered virulence factors in UPEC. In addition to enterobactin, a siderophore present in most *E. coli*, aerobactin (*aer*) and its receptor IutA are common in clinical UPEC isolates and important predictors of virulence (Alteri and Mobley, 2007; Narciso et al., 2011; Oliveira et al., 2011). The glycosylated enterobactin,

salmochelin (*IroA*), and its receptor (*IroN*) are frequently expressed in clinical UPEC isolates and allow iron uptake while avoiding interference by host lipocalins (Wiles et al., 2008; Henderson et al., 2009).

The redundancy of iron uptake mechanisms in UPEC indicates that iron metabolism is of great importance to bacterial survival in the urinary tract. As no conventional antimicrobials interfere with bacterial iron uptake and metabolism, this may be a suitable target for novel antimicrobial drugs.

1.2.2.3. **Intracellular bacterial communities**

After gaining entry to the urinary bladder, UPEC attach to the urothelium through interaction between FimH and uroplakin Ia (Mulvey et al., 1998; Zhou et al., 2001). Following attachment, UPEC can use a zipper-like mechanism to invade the urothelial cell (Schwartz et al., 2011). Interaction between FimH and uroplakin III initiates a signal cascade leading to microtubule re-arrangement, generation of a phagocytic cup and ultimately internalization of the bacteria (Wang et al., 2008; Dhakal and Mulvey, 2009; Thumbikat et al., 2009). The UPEC then begin to divide and form a glycocalyx, generating a biofilm-like structure (intracellular bacterial community, IBC) in a FimH-dependent process (Anderson et al., 2003; Schwartz et al., 2011). Although toll-like receptor 4-mediated apoptosis is frequently triggered upon initial contact between UPEC and the urothelial cell surface, the intracellular bacteria can assume a filamentous form and re-emerge from the cell before the exfoliated cell is flushed from the bladder during micturition (Mulvey et al., 2001). The filamentous bacteria are able to evade phagocytosis by the neutrophils and invade neighbouring cells without contacting the urine (Justice et al., 2006; Rosen et al.,

2007; Loughman and Hunstad, 2011). Continuation of the IBC cycle requires reversion to ordinary bacillary morphology of the bacterial cells, which is also a requirement for virulence in vivo (Justice et al., 2006). Intracellular UPEC can also remain in quiescent intracellular reservoirs for months before re-emerging, contributing to chronic and apparently relapsing infections (Mysorekar and Hultgren, 2006; Schwartz et al., 2011). In addition to establishing intracellular infections in urothelial cells, UPEC can also form IBCs in human and mouse macrophages in vitro, suggesting that these cells may also provide additional opportunities for protected bacterial growth (Bokil et al., 2011). The formation of IBCs in macrophages in vivo with potential subsequent contribution to septicemia has not been established.

1.2.2.4. **Gene expression during infection**

Considering that most in vitro systems evaluate planktonic bacteria in media that vaguely approximate extracellular fluid conditions and that during infection UPEC can establish intracellular infections and form biofilm-like structures, it is not surprising that bacterial metabolism differs between these environments (Snyder et al., 2004; Vigil et al., 2011). Iron acquisition systems are notably up-regulated during infection in mice and humans, suggesting that iron uptake is a critical function during infection (Hagan et al., 2010). Other notable changes include increased expression of amino acid transporters and increased capacity for acetate excretion likely associated with abundant carbon nutrient resources (Hagan et al., 2010). Although adhesion factors are strongly up-regulated during infection in mice, this effect is not observed during human infection (Snyder et al., 2004; Hagan et al., 2010).

1.2.2.6. **Response to antimicrobial therapy**

For infections caused by UPEC, antimicrobial susceptibility has limited value for predicting therapeutic outcome and negative post-therapy urine cultures are observed despite bacterial persistence (Ferry et al., 1988; Schilling et al., 2002; Ejrnaes, 2011). Genetic fingerprinting techniques demonstrate that a substantial proportion of recurrent UPEC infections in humans are caused by the same strain despite initial apparent therapeutic success, suggesting bacterial persistence in the absence of bacteriuria and symptoms (Foxman et al., 2000; Ejrnaes et al., 2006).

Uropathogenic *E. coli* strain UTI89 is classified as susceptible to trimethoprim-sulfamethoxazole according to CLSI guidelines, but this is not reflected in therapeutic outcomes in a mouse infection model (Blango and Mulvey, 2010). After mice infected with UTI89 were treated with trimethoprim-sulfamethoxazole for 3 or 10 days, bacteria were eradicated from the urine yet persisted within bladder tissue (Schilling et al., 2002). Similar observations are reported for gentamicin, cefuroxime and mecillinam (Hvidberg et al., 2000; Kerrn et al., 2005). While therapeutic failures may be attributed to the failure of these drugs to penetrate urothelial cells, ciprofloxacin, sparfloxacin, and fosfomycin also fail to effect clinically relevant reductions in tissue UPEC counts (Blango and Mulvey, 2010). Although these treatments fail to cure UPEC infections in vivo, UPEC were clearly susceptible to the antimicrobials during conventional susceptibility testing, in urothelial cell cultures and in homogenized tissues (Blango and Mulvey, 2010). Antimicrobial compounds which penetrate urothelial cells and specifically target UPEC metabolic pathways that are active during infection may produce more acceptable clinical results, but none are currently available for clinical use.

1.2.3. **Epidemiology of antimicrobial resistance**

Similar to numerous other important bacterial pathogens, antimicrobial resistance is increasing among UPEC isolated from human and canine patients. Reported trends include increased resistance to trimethoprim-sulfamethoxazole, fluoroquinolones, aminoglycosides and aminopenicillins among UPEC isolated from humans and dogs (Ball et al., 2008a; Cullen et al., 2011; Karlowsky et al., 2011; Lagacé-Wiens et al., 2011). The increasingly prevalent serotype 131 contributes to growing antimicrobial resistance as it possesses the extended-spectrum beta-lactamase CTX-M-15 (conferring resistance to all beta-lactam antimicrobials) and is also resistant to fluoroquinolones and sulfonamides (Johnson et al., 2009a; Ewers et al., 2010; Rogers et al., 2011). New antimicrobials with unique mechanisms of action could reduce the likelihood of cross-resistance between conventional and novel antimicrobial drugs, facilitating treatment of multi-drug resistant infections.

1.3. **Iron metabolism in *Escherichia coli***

Iron is essential for *E. coli* growth and survival. It is incorporated into numerous of proteins where its ability to undergo oxidation and reduction under physiological conditions catalyze a wide variety of critical reactions (Andrews et al., 2003). Among UPEC, virulence is associated with siderophore production, particularly aerobactin, enterobactin, salmochelin and yersiniabactin (Emody et al., 2003; Wiles et al., 2008). The relationship between siderophore production and virulence suggests that iron acquisition is essential for UPEC survival in the urinary tract. Iron metabolism pathways may therefore be suitable therapeutic targets for treating UPEC infections, particularly since these pathways are not targeted by any currently available antimicrobials.

1.3.1. **Iron-bearing proteins**

Iron is nearly exclusively bound to proteins within the bacterial cell, as unbound iron poses a significant threat to cellular integrity. Moderately reactive oxygen species such as hydrogen peroxide and superoxide are generated during aerobic cellular metabolism. Unbound iron can participate in Fenton and Haber-Weiss reactions, converting moderately reactive hydrogen peroxide and superoxide to hydroxyl radicals (Figure 1.1.). This can ultimately lead to macromolecular damage and cellular dysfunction (Andrews et al., 2003).

Reduction of free iron (III)

$$Fe^{3+} + \cdot O_2^- \rightarrow Fe^{2+} + O_2$$

Fenton reaction

$$Fe^{2+} + H_2O_2 \rightarrow Fe^{3+} + OH^- + HO\cdot$$

Haber-Weiss reaction (net effect of free iron reduction and subsequent Fenton reaction)

$$\cdot O_2^- + H_2O_2 \xrightarrow{Fe\ reduction\ \&\ oxidation} O_2 + OH^- + HO\cdot$$

Figure 1.1. Fenton and Haber-Weiss reactions

The principal storage mechanism for iron is binding to ferritin, a strategy common to bacteria, archaea, plants, fungi and animals (Abdul-Tehrani et al., 1999). This spherical protein can accumulate between 2,000 and 4,000 iron atoms within its central cavity, where they are

incorporated into ferric phosphate (Andrews et al., 2003). Reduction and oxidation play prominent roles in ferritin function, as only iron(II) can be taken up by the protein yet it is stored as iron(III). This reaction occurs at the ferroxidase region within the ferritin. Reduction is required prior to iron release from the ferritin (Abdul-Tehrani et al., 1999). Bacterioferritins, found in *E. coli* and numerous other bacterial species, resemble ferritins but their iron storage capacity is increased by the presence of protoporphyrin IX (Andrews et al., 2003). The mechanism for the increased capacity is unknown.

1.3.2. **Heme iron acquisition**

Heme is a common prosthetic group for biologically important proteins, and is thus frequently encountered by bacteria as a potential iron source. Nearly all heme in the host environment is protein-bound. Hemolysins elaborated by UPEC liberate the heme from the host proteins, preparing it for bacterial uptake (Krewulak and Vogel, 2008; Wiles et al., 2008). It is actively transported across the outer membrane by a TonB-dependent transporter such as hma and chuA, both of which occur in UPEC and are expressed during infection (Hagan et al., 2010; Noinaj et al., 2010; Garcia et al., 2011). Heme transport across the inner cell membrane is mediated by ATP Binding Cassette (ABC) transporters (Andrews et al., 2003; Krewulak and Vogel, 2011).

1.3.3. **Non-heme iron acquisition**

The principal bacterial strategy for acquiring non-heme iron is the use of siderophore pathways. Siderophores are low molecular weight compounds with a strong affinity for binding iron(III) and are produced by most bacterial species including UPEC (Emery, 1986; Krewulak and Vogel, 2008). While a variety of molecules are elaborated as siderophores, the formation constant for

their iron complexes is typically at least 10^{30} (Neilands, 1995). The iron binding sites are typically octahedral with multiple oxygen atoms and follow a limited set of structural themes (Chu et al., 2010). Consequently, most siderophores can be classified as catecholate, hydroxyamate, α-hydroxycarboxylic acid, or heterocyclic types based on the nature of their iron binding site (Krewulak and Vogel, 2008). Uropathogenic *E. coli* produce various combinations of siderophores including the catecholates enterobactin and salmochelin; the mixed α-hydroxycarboxylic acid-hydroxyamate aerobactin; the hydroxyamate ferrichrome and the heterocyclic yersiniabactin (Neilands, 1995; Miller et al., 2006; Garcia et al., 2011).

Exposure to an iron-poor environment activates the ferric uptake regulator (fur) gene, which then up-regulates siderophore and siderophore receptor production (Chu et al., 2010). Once synthesized and secreted into the immediate environment, their extremely high iron affinity allows siderophores to scavenge iron from host proteins such as transferrins. While siderophores readily bind free iron (III), the extremely low concentrations within the host prevent its use as an important bacterial iron source. Iron-laden enterobactin is susceptible to host interference through lipocalin-2 binding; production of structurally different siderophores allows bacterial iron uptake to continue in the presence of lipocalins (Ganz, 2009).

Iron-laden siderophores gain entry to the bacterial cells via receptors on the outer cell membrane and are then actively transported to the periplasmic space with energy provided by TonB (Chu et al., 2010; Krewulak and Vogel, 2011). After complexing with its corresponding periplasmic binding protein, the siderophore complex is transported across the inner cell membrane by ABC transporters (Newton et al., 2010; Garénaux et al., 2011).

1.4. **Antimicrobial therapy of urinary tract infections**

Empirical therapy for uncomplicated urinary tract infections in women commonly involves fluoroquinolones, trimethoprim-sulfamethoxazole, or less frequently, nitrofurantoin (Yamamoto et al., 2010; Beveridge et al., 2011; Lane and Takhar, 2011; Wagenlehner et al., 2011b). Amoxicillin, with or without clavulanic acid, is commonly used in dogs with urinary tract infections. The dosing regimens for all of these compounds are well-established and are based on pharmacokinetic and pharmacodynamic principles.

1.4.1. **Pharmacokinetics and pharmacodynamics**

"Pharmacokinetics" refers to the time course of drug concentrations in the body. The processes of drug absorption, distribution, metabolism and excretion dictate drug concentrations in specific matrices over time. "Pharmacodynamics" (PD) refers to the action of the drug on the biological system. This action is generally mediated by an interaction between the drug and a receptor (target biomolecule). The receptor can be located on or in the patient's cells; in the case of antimicrobial therapy, it is located on or in the bacterial or fungal cells. The interaction between pharmacokinetics and pharmacodynamics produces the drug's clinical effects.

The pharmacokinetic parameters that are conventionally considered in drug dosage design are the area under the plasma concentration versus time curve (AUC) from 0 to 24 hours, the maximum plasma concentration (C_{max}), and the time the antimicrobial concentration exceeds a defined PD threshold (McKellar et al., 2004). The most commonly used pharmacodynamic parameter is the bacterial minimum inhibitory concentration (MIC), which is determined in vitro (Mouton et al., 2005). The minimum bactericidal concentration (MBC), a related parameter,

refers to the concentration of the antimicrobial required to reduce the bacterial population by 99.9% (Finberg et al., 2004; Levison and Levison, 2009). In relating pharmacokinetic and pharmacodynamic parameters to clinical efficacy, antimicrobial drugs are commonly classified as either concentration-dependent or time-dependent. For antimicrobials whose activity is concentration-dependent, high drug concentrations relative to the MIC of the pathogen and the area under the plasma concentration-time curve that is above the bacterial MIC during the dosage interval are the major determinants of clinical efficacy (McKellar et al., 2004). Dosing regimens for concentration-dependent antimicrobials are designed to maximize peak plasma or tissue concentrations, and to achieve a high ratio of AUC to MIC. Based on data from human and rodent fluoroquinolone studies, the target AUC to MIC ratio is commonly arbitrarily set at 100 or 125 for all pathogens (McKellar et al., 2004). The paucity of pathogen, patient and drug-specific data for predicting therapeutic outcome based on in vitro parameters precludes an ideal, more tailored approach to designing dosing regimens targeting specific optimized AUC to MIC ratios. Some concentration-dependent antimicrobial drugs also have prolonged post-antibiotic effects against select pathogens, which allows long dosing intervals while maintaining clinical efficacy (Walker and Dowling, 2006).

In contrast to the concentration-dependent antimicrobials, the major predictor of efficacy for the time-dependent antimicrobials is the proportion of the dosing interval where their plasma concentrations exceed the pathogen MIC. It is typically recommended that plasma concentrations should exceed the target MIC by 1-5 times for at least 40% of the dosing interval (McKellar et al., 2004). Antimicrobials are further categorized as bacteriostatic or bactericidal depending on the magnitude of population reduction upon drug exposure.

While ideal pharmacodynamic assessment of antimicrobial drugs would be conducted in the target patient species or at least in an animal model, this is often impractical. Consequently, time-kill experiments in vitro are commonly used to classify novel antimicrobials as time-dependent or concentration-dependent, bacteriostatic or bactericidal (Tam et al., 2005). Conventionally, an antimicrobial is classified as bactericidal if it causes at least a 1000-fold decrease in bacterial counts. Compounds that reduce bacterial counts at a lower magnitude of effect are considered bacteriostatic. Time-dependent or concentration-dependent classification is often based on visual analysis of time-kill plots or on linear regression analysis considering bacterial count as a function of time and drug concentration. Visual inspection of time-kill plots allows researchers to identify whether bacterial exposure to antimicrobial concentrations exceeding the MIC causes substantial increases in bacterial killing, thus allowing classification of the antimicrobial as concentration-dependent.

Conventional time-kill analyses are ill-equipped to address bacterial re-growth and the emergence of antimicrobial resistance during treatment. Area-based measures such as the area between the growth curve generated in the absence of antimicrobial exposure, and the kill curve generated in the presence of selected antimicrobial concentrations (ABBC), can account for bacterial re-growth and duration of effect (Firsov et al., 1997). Once active drug concentration ranges are established, dynamic in vitro systems allow drug concentrations to be adjusted over the course of the study, more closely mimicking the fluctuations observed in vivo and providing insight into emerging antimicrobial resistance during treatment (Campion et al., 2005a; Campion et al., 2005b).

The mutant prevention concentration (MPC), the antimicrobial concentration required to prevent all bacterial growth on agar plates inoculated with 10^{10} colony forming units, has been advanced as an alternative pharmacodynamic metric (Zhao and Drlica, 2002). The MPC and the MIC provide the upper and lower bounds of the mutant selection window, a range of antimicrobial concentrations likely to lead to selection for resistant mutants. Dosing regimens based on this premise are designed to minimize the amount of time where drug concentrations fall within the mutant selection window while maximizing microbial exposure to concentrations above the MPC. While the MPC value for a particular isolate will never be less than the MIC value, it is not a predictable multiple of the MIC and requires specific laboratory determination (Wetzstein, 2005). As this determination is highly labour- and resource-intensive, it is not typically conducted in diagnostic laboratories. This leaves clinicians to rely largely on published data which may not accurately reflect the scenarios encountered in practice. Furthermore, little information is available about the duration that antimicrobial concentrations must exceed the MPC in vivo to prevent mutant selection. The final barrier to clinical use of MPC data is that the majority of clinically useful antimicrobial drugs cannot be safely administered at the doses required to exceed the MPCs for many pathogens.

1.5. **Gallium**

Elemental gallium is a soft, shiny grey metal and is not found in nature. Various gallium compounds occur in trace amounts in aluminum and zinc ores (Sacks, 2003). Smaller quantities are released upon burning coal (Sacks, 2003). China and Japan are the leading producers of gallium worldwide, with China accounting for over 80% of global production (Anonymous,

2008). Gallium arsenide is principally used as a semiconductor in electronic devices, but is also a component of light-emitting diodes of commercial importance.

1.5.1. **Chemical properties**

Gallium has an atomic mass of 69.723 with melting and boiling points of 29.8°C and 2403°C. Its two stable isotopes, ^{69}Ga and ^{71}Ga, exist in molar fractions of 0.601 and 0.398, respectively (de Laeter et al., 2003). The five most stable of the gallium radioisotopes are ^{67}Ga, ^{68}Ga, ^{70}Ga, ^{72}Ga and ^{73}Ga, with half-lives of 3.3 days, 66 minutes, 20 minutes, 14 hours and 4.9 hours respectively (Sagane, 1939; McCown et al., 1948; King and Chou, 1993).

Of its three oxidation states, Ga(III) is the most stable as it is the only one without an unpaired electron in the highest energy orbital. Ga(III) cannot be reduced to Ga(I) under physiological conditions (Bernstein, 1998). Of the less stable oxidation states, Ga(I) is preferred as it leaves no unpaired electrons in the 3d orbital. Ga(II) is so unstable that it is considered effectively non-existent.

In the absence of a chelating agent, gallium will form gallate ions ($Ga(OH)_4^-$) and its insoluble hydroxide ($Ga(OH)_3$) in aqueous solution (Bernstein, 1998).

1.5.2. **Interaction with biomolecules**

As Ga(III) and Fe(III) are both trivalent with similar ionic radii, gallium can compete with iron to interact with numerous biomolecules that normally react with or contain iron (Harris and

Pecoraro, 1983; Bernstein, 1998). These interactions are hypothesized to contribute to gallium's effects on biological systems including antimicrobial and antineoplastic activity.

When gallium salts are added to human plasma, approximately 99% of the gallium binds to transferrin, with the remainder present as gallate ion (0.035%), gallium hydroxide (0.0014%), gallium citrate (0.0001%), and unbound trivalent gallium (in a fraction 1.3×10^{-16} of the total gallium concentration) (Jackson and Byrne, 1996).

1.5.2.1. **Mammalian transferrins**

Transferrins are a family of highly-conserved proteins with exquisite affinity for iron (Dunn et al., 2007). They are critical for iron distribution in the body, accompanying ferric iron through extracellular spaces and facilitating its cellular uptake (Chua et al., 2007). Proteins from this family are highly conserved and are found in a wide variety of vertebrates and invertebrates including insects, echinoderms, fish, reptiles, amphibians, birds and mammals (Lambert et al., 2005). Most transferrins are bilobed proteins with a single atom iron binding site on each lobe in an octahedral configuration (Sun et al., 1999). Proteins isolated from non-mammalian species can also occur as single or tri-lobed forms (Lambert, 2012). Iron binding is aided by the presence of bicarbonate ions, which substantially increase the binding affinity constants for both sites (Sun et al., 1999).

The principal mammalian transferrins are serum transferrin and lactoferrin. While serum transferrin is the principal iron carrier in blood and tissues, lactoferrin is typically present in mammary and pancreatic secretions, tears, saliva, bile and leukocytes (Sun et al., 1999).

Melanotransferrin is a bilobed membrane-bound protein with approximately 30% sequence homology to transferrin (Rahmanto et al., 2012). Unlike transferrin which has two binding sites, melanotransferrin possesses only one iron binding site (Sun et al., 1999). It exists in small quantities on most mammalian cells and abundant on neoplastic cells, particularly in melanoma cells (Sekyere et al., 2005; Rahmanto et al., 2012). While its role in iron uptake in most cell types is negligible, melanotransferrin may be important for delivering iron to neurons across the blood-brain barrier (Moroo et al., 2003).

Transferrin can interact with transferrin receptor 1 (TFR1) and transferrin receptor 2 (TFR2). The former is the principal route of non-heme iron entry into most cell types, but TFR2 contributes to iron uptake in the duodenum, liver, and erythroid cells (Lambert, 2012). Transferrin receptor 1 is expressed on the basolateral membranes of transitional epithelial cells and its expression is upregulated during UPEC infection and in response to iron deficiency via iron response elements associated with the TFR1 gene (Dunn et al., 2007; Reigstad et al., 2007). This receptor is a homodimer, with each monomer capable of binding two holotransferrin units (i.e., four iron atoms) (Sun et al., 1999). At physiological pH (7.4), TFR1 has an affinity for holotransferrin roughly three orders of magnitude greater than for apotransferrin, while at pH 5.5, these binding preferences are reversed. This property is exploited during cellular iron uptake after occupied transferrin receptors are internalized by endocytosis (Chua et al., 2007). Following endocytosis and endosome acidification, iron is released from the transferrin. Ferrireductases, particularly Steap3, reduce the iron(III) which is then transported into the cytosol by divalent metal transporter 1 (DMT1) (Ohgami et al., 2006; Chua et al., 2007).

In addition to iron transport, transferrin and its receptors contribute to non-iron metal trafficking (El Hage Chahine et al., 2012; Lambert, 2012). Although it has a strong preference for iron, transferrin can bind an array of non-iron metals including uranium, bismuth, cobalt and gallium (El Hage Chahine et al., 2012). The affinity constants for iron at the first and second binding sites of human transferrin (6.3×10^{22} and 3.2×10^{21} respectively) are approximately 400 and 200 times those for gallium (2.0×10^{20} and 2.0×10^{19} respectively) (Harris and Pecoraro, 1983). Metals bound to transferrin can be internalized by mammalian cells via TFR1, although the receptor's affinity for iron-transferrin is substantially greater than for transferrin bound to other metals (El Hage Chahine et al., 2012). This mechanism may account for the accumulation of gallium in endosomes within neoplastic cells, renal tubular cells and in lysosomes (Berry et al., 1984). However, uptake of gallium into the tissues of hypotransferrinemic animals suggests that transferrin-mediated uptake is not the sole mechanism of gallium distribution (Radunovic´ et al., 1997). The movement of gallium out of endosomes has not been evaluated but likely does not involve DMT1.

1.5.2.2. **Protoporphyrin IX**

Heme is an essential component of mammalian metabolic machinery, using iron to transport oxygen as part of hemoglobin in erythrocytes and myoglobin in myocytes. It is also a critical prosthetic group for an array of enzymes involved in oxidative metabolism including cytochromes P450, catalase and peroxidases (Layer et al., 2010). The final step of heme synthesis is the insertion of iron(II) into protoporphyrin IX, which is catalyzed by the enzyme ferrochelatase (Dailey et al., 2000). Ferrochelatase can bind a variety of non-iron divalent metals including cadmium(II), mercury(II), lead(II), copper(II), cobalt(II), manganese (II), nickel(II)

and zinc(II) (Dailey et al., 2000; Davidson et al., 2009). While ferrochelatase function is inhibited by non-iron divalent metals, it can successfully incorporate cobalt, zinc and nickel into protoporphyrin IX (Dailey et al., 2000; Medlock et al., 2009; Layer et al., 2010). This inhibition arises from the enzyme's inability to release non-iron protoporphyrin IX compounds (Medlock et al., 2009). While gallium-protoporphyrin IX can be synthesized under non-physiological conditions in the laboratory, ferrochelatase cannot successfully produce protoporphyrin IX compounds containing monovalent or trivalent metal ions and is unlikely to catalyze this reaction in vivo (Stojiljkovic et al., 1999; Dailey et al., 2000; Behnam Azad et al., 2012).

While it is unlikely that gallium is incorporated into protoporphyrin IX in vivo, it must be noted that it does inhibit the zinc metalloprotein porphobilinogen synthase (Goering and Rehm, 1990; Chitambar, 2010; Layer et al., 2010). Porphobilinogen synthase catalyzes the formation of porphobilinogen from two 5-aminolevulinic acid molecules, an essential early step in heme synthesis. Porphobilinogen molecules are then assembled to produce uroporphyrinogen III, the base pyrrole structure that is subsequently modified to produce protoporphyrin IX and heme (Layer et al., 2010). Similar to aluminum and indium, gallium reversibly displaces zinc from porphobilinogen synthase, inhibiting enzyme function (Rocha et al., 2004). This mechanism has been suggested as an explanation for the hypochromic microcytic anemia observed in rodents following chronic exposure to gallium arsenide (National Toxciology Program, 2000; Chitambar, 2010).

1.5.2.4. **Siderophores**

The catecholate siderophore enterobactin is ubiquitous in UPEC and is capable of binding gallium (Llinas et al., 1973; Henderson et al., 2009). Micacocidin, a siderophore produced by the plant pathogen *Ralstonia solanacearum*, binds gallium (III) (Kreutzer et al., 2011). As micacocidin differs from yersiniabactin only by the presence of a short side chain outside the iron binding site, it is likely that yersiniabactin and micacocidin bind to similar metals including gallium (Miller et al., 2006). Although little information is available on gallium binding by aerobactin, gallium binding by a wide range of other hydroxamates including ferrichrome and desferrioxamine suggests that aerobactin is capable of the same (Emery, 1986; Herscheid et al., 1986; Banin et al., 2008; Krewulak and Vogel, 2008).

1.5.3. **Current clinical use**

1.5.3.1. **Hypercalcemia**

Gallium nitrate is approved in the United States for treating hypercalcemia of malignancy (Leyland-Jones, 2004; United States Pharmacopeia, 2005; Legrand, 2011). Gallium nitrate administration decreases serum calcium concentrations by inhibiting osteoclastic bone resorption (Warrell et al., 1984; Verron et al., 2010). In addition to inhibiting mature osteoclast function, gallium also inhibits osteoclast differentiation without affecting viability (Verron et al., 2012).

The efficacy of gallium nitrate for decreasing serum calcium concentrations is similar to that of pamindronate, but it is maintained as a second- or third-line treatment due to its nephrotoxic potential (Apseloff, 1999; Cvitkovic et al., 2006; Lumachi et al., 2008; Legrand, 2011). Clinically, its greatest use is in patients where fluid therapy, diuresis and bisphosphonate

(particularly pamidronate and zoledronic acid) therapy have failed (Leyland-Jones, 2004; Legrand, 2011). This situation is most commonly encountered with tumours that produce large quantities of parathyroid hormone (Leyland-Jones, 2004). Mammary adenocarcinomas, non-Hodgkin's lymphoma, lung cancers, and adult T-cell leukemia frequently fall in this category (Lumachi et al., 2008; Clines, 2011).

1.5.3.2. **Medical imaging**

Gallium-67 has been used for scintigraphy since the 1970s for identifying tumors and focal infections, particularly in cases with fever of unknown origin (Deysine et al., 1974; Hegge et al., 1977; Hoffer et al., 1977; Tsan, 1985; Chen et al., 2012). Increased transferrin production and TFR1 expression at inflammatory foci lead to gallium accumulation, which allows lesion localization (Tsan, 1985; Apseloff, 1999; Yeh et al., 2011). Viable neoplastic cells typically express TFR1 abundantly, which is associated with gallium binding. Consequently, gallium-67 imaging is useful for discriminating between neoplasia and fibrosis (Weiner, 1996).

1.5.3.3. **Experimental applications**

Gallium compounds exert antineoplastic activity in vitro and in rodent models and have been extensively evaluated as potential cancer chemotherapy agents (Hart and Adamson, 1971; Weiner et al., 1996; Collery et al., 2002; Chua et al., 2006; Chitambar et al., 2007; Chitambar and Purpi, 2010). While gallium nitrate is known to disrupt cellular iron metabolism and inhibit ribonucleotide reductase by substituting for iron in one of the subunits of the enzyme in neoplastic cells in vitro, its mechanism of action has not been fully characterized (Chitambar and Seligman, 1986; Chitambar, 2010). When combined with vinblastine and ifosfamide, gallium

nitrate had antineoplastic effects against transitional cell carcinoma in a phase II clinical trial, but the specific contribution of gallium nitrate to this combination therapy could not be evaluated (Dreicer et al., 1997). Phase II clinical trials conducted using gallium nitrate had clinically insignificant antineoplastic activity against numerous human cancers including:

- Transitional cell carcinoma (Crawford et al., 1991; McCaffrey et al., 1997)
- Small cell lung cancer (Baselga et al., 1993)
- Non-small cell lung cancer (Chang et al., 1995; Webster et al., 2000)
- Cervical carcinomas (Malfetano et al., 1991b; Malfetano et al., 1995)
- Ovarian carcinoma (Malfetano et al., 1991a)
- Metastatic breast cancer (Jabboury et al., 1989)
- Metastatic prostatic adenocarcinoma (Senderowicz et al., 1999)

Nephrotoxicity and hematological toxicity (microcytic hypochromic anemia) were noted in multiple studies and further limit the clinical utility of gallium salts as cancer chemotherapy agents (Crawford et al., 1991; Baselga et al., 1993; Dreicer et al., 1997; Chitambar, 2010).

Gallium compounds are of interest as potential inhibitors of oxidative tissue damage, particularly in ocular tissues (Banin et al., 2000; Banin et al., 2003). Desferrioxamine-gallium may have military applications as it reduces oxidative damage in ocular tissues following nitrogen mustard (mechlorethamine) exposure (Banin et al., 2003). The researchers speculated that the higher affinity of desferrioxamine for iron led to gallium release and iron scavenging at the site of injury. The reduction in free iron concentrations coupled with gallium (III)'s resistance to reduction was hypothesized to mitigate free radical production and interrupt the progression of

oxidative injury (Banin et al., 2000; Banin et al., 2003). As oxidative damage accompanies inflammatory processes, local administration of desferrioxamine-gallium may also have applications in managing extra-ocular inflammatory diseases.

1.5.4. **Toxicity**

As with most metals, gallium is potentially toxic to mammalian systems. Compared with the other group IIIa elements aluminum, indium and thallium, gallium is a moderately potent toxin in mice. The conventional but clinically crude measure of LD_{50} (lethal dose-50) for gallium nitrate falls below that of aluminum nitrate but above both indium nitrate and thallium nitrate (Hart and Adamson, 1971).

1.5.4.1. **Nephrotoxicity**

Gallium's nephrotoxic potential is widely recognized. In an early clinical trial in patients with advanced lymphoma, six out of eight patients treated with gallium nitrate at 750 mg/m^2 developed abnormalities in markers of renal function. In addition to the elevated serum creatinine and blood urea nitrogen concentrations, two of these patients also developed renal tubular acidosis with hypokalemia and hypocalcemia. Osmotic diuresis initiated by mannitol treatment did not change gallium clearance but urinary gallium concentrations were reduced and only one out of nine patients developed nephrotoxicity. At higher doses, osmotic diuresis did not prevent nephrotoxicity (Krakoff et al., 1979). Similar effects were observed in rats, where saline diuresis prevented gallium nitrate nephrotoxicity (Whelan et al., 1994).

Microscopic examination of kidneys from rats treated with gallium nitrate revealed multiple pathological changes including nephritis, tubular necrosis, and tubular occlusion with amorphous and whorled calcium-containing precipitates (Newman et al., 1979). Osmotic diuresis during gallium administration led to decreased severity of lesions and prevented the formation of amorphous precipitates with no effect on gallium clearance (Newman et al., 1979). This finding suggests that nephrotoxicity occurs secondary to precipitation of gallium complexes from renal tubular fluid.

1.5.4.2. **Hepatotoxicity**

While hepatotoxicity is observed following exposure to gallium arsenide, biochemical and histopathological effects of other gallium compounds are minimal (Flora et al., 1998). Gallium sulfate administration does lead to inhibition of hepatic porphobilinogen synthase activity, suggesting that prolonged exposure could cause iatrogenic porphyria (Goering and Rehm, 1990).

In vitro testing of hepatocellular carcinoma cell lines suggests that hepatotoxicity may occur upon prolonged treatment. Gallium maltolate exposure for six days leads to apoptosis and growth inhibition in hepatocellular carcinoma cells with IC_{50} (inhibitory concentration which inhibits cell growth by 50%) values ranging from 27 – 111 µg/mL corresponding to gallium concentrations of 4.2 – 17.4 µg/mL (Chua et al., 2006). These effects are not observed after shorter exposures. Unfortunately, the study did not investigate the effects of gallium exposure on non-neoplastic hepatocytes, as the preferential distribution of gallium into hepatocellular carcinoma relative to normal liver tissue was assumed to produce antineoplastic effects prior to inducing hepatic failure (Nagasue, 1983; Chua et al., 2006). These concentrations are within an

order of magnitude of gallium concentrations observed in humans and dogs treated with a single oral dose of gallium maltolate at 500 mg and 10 mg/kg respectively (Bernstein et al., 2000). The effect of multiple-dose regimens on hepatic anatomy and physiology has not been investigated in vivo.

1.5.4.3. **Hematologic toxicity**

Gallium inhibits porphobilinogen synthase, which is hypothesized to cause the hypochromic microcytic anemia observed in rodents and humans treated with gallium nitrate (Hart and Adamson, 1971; Krakoff et al., 1979; Newman et al., 1979; Warrell et al., 1983). The inhibitory effect of gallium-transferrin on reticulocyte iron uptake further contributes to the pathogenesis of the hypochromic microcytic anemia (Chitambar and Zivkovic, 1987). As gallium treatment does not affect platelets and leukocytes, it is considered acceptable for managing hypercalcemia in neutropenic patients (Chitambar, 2010).

1.5.4.4. **Pulmonary toxicity**

Gallium arsenide exposure causes pulmonary inflammation and airway epithelial hyperplasia, but this effect is associated with the arsenic moiety and is unlikely to influence patients treated with other gallium compounds (National Toxciology Program, 2000; Chitambar, 2010).

1.5.4.5. **Gastrointestinal toxicity**

Diarrhea and vomiting were prominent adverse effects in clinical trials of gallium nitrate administered parenterally as an antineoplastic therapy after infusions of 200 - 750 mg/m^2 (Jabboury et al., 1989; Malfetano et al., 1991a; Malfetano et al., 1995; Senderowicz et al., 1999).

No speculations were made about the pathology of gallium nitrate-associated gastrointestinal upset. Diarrhea was not observed in foals following oral administration of gallium maltolate (Martens et al., 2010).

1.5.4.6. **Effects on calcium metabolism**

Gallium inhibits osteoclastic bone resorption and interferes with osteoclast differentiation, producing its antihypercalcemic effect (Warrell et al., 1984). By inhibiting osteoclast activation through the receptor activator of nuclear factor κB, gallium interferes with parathyroid hormone (PTH) or PTH-like protein effects on serum calcium concentrations (Verron et al., 2010; Clines, 2011; Verron et al., 2012). This may have clinically important consequences if gallium compounds are used to treat patients with hypocalcemia and hypoparathyroidism.

1.5.4.7. **Immunologic effects**

Gallium arsenide inhibits humoral and cell-mediated immune responses, interfering with macrophage antigen processing, IgM responses, and T-cell proliferation (Burns and Munson, 1993; Burns et al., 1994; Lewis et al., 1996). These effects are likely caused by the arsenic component of this compound (Burns et al., 1991).

Gallium nitrate inhibits T-cell proliferation, with minimal effects on humoral immune responses (Huang et al., 1994; Bernstein, 1998).

1.5.4.9. **Potential for ecological toxicity**

As gallium is principally eliminated in urine, therapeutic use of gallium compounds could lead to environmental contamination through inadequate sewage treatment. Using carp (*Cyprinus carpio*) as a model for fish toxicity, researchers observed multiple toxic effects of gallium exposure. Gallium exposure reduces growth rate of young fish despite normal feed consumption (Yang and Chen, 2003b). Biochemical changes included substantial decreases in plasma immunoglobulin concentrations and hypoproteinemia upon exposure to gallium nitrate (Betoulle et al., 2002). Gallium sulfate exposure for 28 days led to significantly increased blood urea nitrogen and creatinine, cholesterol and triglyceride concentrations along with decreased blood glucose concentrations (Yang and Chen, 2003a). Hematological changes included erythrocyte deformation and decreased leukocyte concentrations (Betoulle et al., 2002; Yang and Chen, 2003a). Histopathological changes include edema and hyperplasia of the gill epithelium, renal tubular necrosis and glomerular distension (Yang and Chen, 2003b). While these effects were observed at relatively high gallium concentrations (8 mg/L), lower concentrations could be of ecological concern if chronic exposure to low gallium concentrations influences fish health. A safe water concentration of 2 mg/L (elemental gallium) is suggested for carp, although the sensitivity of other fish species may vary (Yang and Chen, 2003a). Appropriate estimates of environmental contamination with follow-up toxicology studies for potentially vulnerable species are warranted should therapeutic gallium use become common.

1.5.5. **Antimicrobial activity of gallium compounds**

Gallium compounds exert antimicrobial activity against a variety of bacteria, including Gram-negative, Gram-positive, and intracellular pathogens. Antimicrobial activity is also observed in a

small number of animal infection models, suggesting that gallium compounds may be clinically useful antimicrobials. In vitro susceptibility test results must be compared with caution as media composition, particularly its iron concentration, can influence minimum inhibitory concentration measurements (Harrington et al., 2006; Kaneko et al., 2007). The antimicrobial effects of various gallium compounds in vitro are summarized in Table 1.1.

Gallium compound	Bacterial species	Antimicrobial effects	References
Desferrioxamine-gallium	*Pseudomonas aeruginosa*	MIC of 32 nmol/mL for a single laboratory strain during planktonic growth	(Banin et al., 2008)
Gallium maltolate	*Rhodococcus equi*	MICs for 98 clinical isolates ranged from 4 – 16 nmol/mL	(Coleman et al., 2010)
Gallium maltolate	*Staphylococcus aureus*	MIC for 10 isolates ranged from 845 – 3317 nmol/mL; bactericidal activity observed at or above 10x MIC	(Baldoni et al., 2010)
Gallium maltolate	*Staphylococcus epidermidis*	MIC for 10 isolates ranged from 211 – 422 nmol/mL; bactericidal activity observed at or above 10x MIC	(Baldoni et al., 2010)
Gallium nitrate	*Mycobacterium avium* and *Mycobacterium tuberculosis*	Growth of five strains inhibited by 50% at 1.25 – 2.5 nmol/mL	(Olakanmi et al., 2000)
Gallium nitrate	*Pseudomonas aeruginosa*	Planktonic growth inhibited at 1 nmol/mL	(Kaneko et al., 2007)
Gallium nitrate	*Rhodococcus equi*	Growth inhibition observed at 50 nmol/mL (no lower concentrations tested)	(Harrington et al., 2006)
Gallium-protoporphyrin IX	*Escherichia coli*	Minimum inhibitory concentrations less than 0.7 nmol/mL.	(Stojiljkovic et al., 1999)
Gallium-transferrin	*Mycobacterium avium* and *Mycobacterium tuberculosis*	Growth of five strains in macrophages inhibited by 50% at 125 nmol/mL (gallium basis)	(Olakanmi et al., 2000)
Gallium-transferrin	*Francisella tularensis*	Growth in macrophages inhibited at 10 nmol/mL (gallium basis); 80% reduction in growth rate at 100 nmol/mL (gallium basis)	(Olakanmi et al., 2010)

Table 1.1. Summary of antimicrobial effects reported for selected gallium compounds against various bacterial species in vitro

1.5.5.2. ***Escherichia coli***

Limited studies have demonstrated gallium's antimicrobial activity against non-uropathogenic strains of *E. coli*. Gallium-protoporphyrin IX exerted antimicrobial activity against two strains of *E. coli* in iron-restricted media with minimum inhibitory concentrations of less than 0.5 µg/mL (0.7 nmol/mL), but this effect was absent when the bacteria were cultured under anaerobic conditions (Stojiljkovic et al., 1999). In another investigation, addition of 9.1 nmol/mL gallium nitrate to the iron-restricted growth medium inhibited *E. coli* growth while stimulating iron uptake (Hubbard et al., 1986). Gallium's antimicrobial activity was reduced as the iron concentration of the medium increased, suggesting that gallium competitively inhibits iron uptake and/or metabolism (Hubbard et al., 1986). The observation that gallium nitrate does not inhibit the growth of *E. coli* strains lacking TonB suggests that iron uptake is a key antimicrobial target for gallium compounds (Stojiljkovic et al., 1999).

1.5.5.3. ***Pseudomonas aeruginosa***

Growth of planktonic *Pseudomonas aeruginosa* in vitro is inhibited by gallium nitrate at concentrations as low as 1 µM, with little difference in effects when concentrations increase from 5 to 10 µM (Kaneko et al., 2007). This effect is diminished in the presence of iron. Gallium nitrate concentrations as low as 0.5 µM inhibit biofilm formation in vitro, while 100-1000 µM was required to kill *P. aeruginosa* in established biofilms (Kaneko et al., 2007). The minimum inhibitory concentration of desferrioxamine-gallium against a laboratory strain of *P. aeruginosa* was 32 µM, but biofilm formation was inhibited with concentrations as low as 1 µM. In contrast, 1000 µM was required to kill *P. aeruginosa* in biofilms (Banin et al., 2008).

Gallium compounds also inhibit *P. aeruginosa* in a mouse model of burn infections. At 24 hours post-infection, no bacteria were cultured from the burn wounds of mice that were treated with gallium maltolate (100 mg/kg injected subcutaneously at the burn site) at the time of infection (DeLeon et al., 2009). The probability of post-infection survival is greater in mice treated with gallium maltolate than with gallium nitrate when equivalent doses on a gallium bases are injected subcutaneously (DeLeon et al., 2009).

As gallium readily binds to the pyoverdins elaborated by *P. aeruginosa*, siderophore-mediated uptake may contribute to gallium's antimicrobial activity (Wasielewski et al., 2008). This is supported by the greater antimicrobial activity of desferrioxamine-gallium against *P. aeruginosa* in a rabbit keratitis model relative to gallium chloride (Banin et al., 2008). The inhibitory effect of iron on gallium's antimicrobial activity suggests an interaction between gallium and iron metabolic pathways (Kaneko et al., 2007).

1.5.5.4. ***Burkholderia cepacia*** **complex**

Bacteria in the *Burkholderia* genus were historically classified as *Pseudomonas* spp., and include the causative agents of glanders (an immediately notifiable disease of horses) and melioidosis, *B. pseudomallei* and *B. mallei*, respectively. *B. cepacia* complex is associated with opportunistic lung infections in cystic fibrosis patients, and isolates are frequently resistant to multiple conventional antimicrobial drugs. The minimum inhibitory concentration of gallium nitrate for clinical *B. cepacia* complex isolates in iron-free media was 250 μM, but this effect was absent in the presence of iron (Peeters et al., 2008).

1.5.5.5. ***Rhodococcus equi***

Gallium maltolate has been investigated as a potential therapy for *Rhodococcus equi* pneumonia in foals. Minimum inhibitory concentrations for 98 virulent *R. equi* strains isolated from foals ranged from 0.279-1.115 µg/mL, which corresponds to 4-16 µM (Coleman et al., 2010). Gallium nitrate also inhibits *R. equi* growth in vitro. Similar to observations with *P. aeruginosa*, the antimicrobial activity of gallium compounds against *R. equi* is diminished in the presence of iron (Harrington et al., 2006).

Following intragastric administration of gallium maltolate to foals, the peak serum gallium concentration was approximately 15 µM, suggesting that serum concentrations would exceed the MIC for substantial periods in vivo (Martens et al., 2007). The clinical efficacy of gallium maltolate against *R. equi* has not been reported, although it may reduce bacterial loads in a mouse infection model (Harrington et al., 2006).

1.5.5.6. ***Staphylococcus* spp.**

Minimum inhibitory concentrations of gallium maltolate against a small collection of clinical *Staphylococcus aureus* ranged from 375 – 1500 µg/mL (corresponding to 845 to 3317 µM) in an iron-restricted medium (Baldoni et al., 2010). In the same study, *Staphylococcus epidermidis* were more sensitive to gallium maltolate, with MICs ranging from 211 to 422 µM. In time-kill studies for methicillin-resistant and methicillin-susceptible *S. aureus* and *S. epidermidis* (4 strains in total), bactericidal activity was observed only for gallium maltolate against *S. epidermidis* at concentrations at or above 10 times the MIC (Baldoni et al., 2010).

1.5.5.7. *Mycobacterium avium* and *Mycobacterium tuberculosis*

The growth of extracellular *Mycobacterium avium* and *Mycobacterium tuberculosis* in vitro was reduced by 50% when gallium nitrate was added to the iron-restricted medium at 1.25 – 2.5 μM (Olakanmi et al., 2000). While gallium inhibits iron uptake by mycobacteria, bacteria can overcome the antimicrobial effects of gallium in the presence of excess iron (Olakanmi et al., 2000).

1.5.5.8. *Francisella tularensis*

The Gram-negative bacterium *Francisella tularensis* establishes intracellular infections in macrophages, neutrophils and a variety of other cell types (Chong and Celli, 2010). It causes the potentially fatal multi-systemic infection tularemia and has been incorporated into biological weapons, leading to an interest in therapeutic alternatives to conventional antimicrobials for military use (Dennis et al., 2001; Foley and Nieto, 2010; Olakanmi et al., 2010). Gallium-transferrin inhibits *F. tularensis* growth in human macrophages in vitro at 10 μM (gallium basis), with an 80% reduction in growth rate at 100 μM (Olakanmi et al., 2010).

1.5.6. Gallium maltolate

Gallium maltolate has been promoted as a potential therapeutic agent for a wide variety of medical conditions ranging from bacterial infections to cancer. Numerous patents have been filed by Lawrence R. Bernstein covering these applications (Bernstein, 1993a; Bernstein, 1993b; Bernstein, 2001; Bernstein, 2002; Bernstein, 2007; Bucalo et al., 2007; Bernstein, 2008c; Bernstein, 2008b; Bernstein, 2008a; Bernstein, 2009).

Gallium maltolate is of particular interest because oral administration produces blood gallium concentrations in the range required for pharmacological activity in vitro (Srinivas et al., 2002; Martens et al., 2007). The potential for oral administration is not common to all gallium compounds, as most gallium salts form very poorly soluble gallium hydroxide upon dissolution in aqueous media (Jackson and Byrne, 1996; Bernstein, 1998). Furthermore, preliminary evidence suggests that it can be administered safely. Adverse effects were not noted following administration of gallium maltolate to humans at up to 500 mg, mice at up to 50 mg/kg and horses up to 40 mg/kg during preliminary pharmacokinetic and safety studies (Bernstein et al., 2000; Harrington et al., 2006; Martens et al., 2007; Martens et al., 2010). In a phase I clinical trial, gallium maltolate was well-tolerated in human patients following oral administration (Srinivas et al., 2002).

1.5.6.1. **Structure and characteristics**

Gallium maltolate consists of one atom of trivalent gallium coordinated with three maltol molecules (Figure 1.2.). It is formed upon combination of gallium nitrate and maltol in aqueous solution with subsequent pH adjustment to 7.0 (Bernstein et al., 2000). Washing and solvent evaporation yield a pale yellow powder with a faint sweet aroma.

Gallium maltolate is slightly soluble in water, with a saturated solution containing 10.7 mg/mL at 25°C (Bernstein et al., 2000). Its molecular weight of 445.03 g/mol approaches the upper limit of the range where gastrointestinal absorption is likely (Petit et al., 2012). With nine potential hydrogen bond acceptors and an octanol-water partition coefficient (a measure of lipophilicity commonly termed “LogP”; the logarithm of the ratio of drug concentrations in octanol and in

water after the drug is dissolved in an octanol and water mixture with subsequent separation of solvent layers) of 0.41, it is a reasonable candidate for gastrointestinal absorption according to Lipinski's Rule of Five (Krämer, 1999; Bernstein et al., 2000; Petit et al., 2012). This rule, based on characteristics observed in a database of over 2,000 molecules, predicts poor absorption for compounds possessing the following properties: molecular weight exceeding 500 g/mol, five or more hydrogen bond donors, ten or more hydrogen bond acceptors, and octanol-water partition coefficient of five or greater (Lipinski et al., 1997).

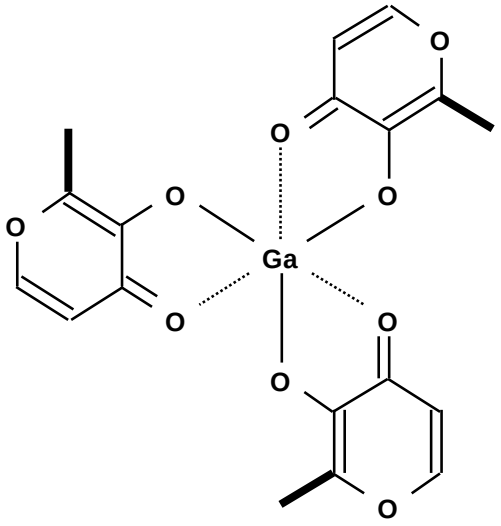

Figure 1.2. Gallium maltolate

1.5.6.2. **Pharmacokinetics**

Preliminary investigations of gallium maltolate pharmacokinetics have been conducted in dogs, humans and horses. In each case, serum or plasma gallium concentrations were used as surrogate

measures for gallium maltolate concentrations. Gallium is incorporated into a variety of compounds in blood following intravenous administration of various salts (Jackson and Byrne, 1996). As the pharmacologically active form of gallium in vivo is unknown, total gallium concentrations are reported without identification of specific gallium complexes. Pharmacokinetic parameter estimates from selected species are summarized in Table1.2.

Species (number of subjects)	Dose & route	Study duration	$C_{max,\ serum}$ (µg/mL)	T_{max}^{*} (h)	Terminal $t_{1/2}^{*}$ (h)	Reference
Dog (2)	9.6 mg/kg orally	48 h	1.47 (21.1 nmol/mL)	3.1	10.4	(Bernstein et al., 2000)
Human (3)	100 mg orally	17 d	0.115 (1.65 nmol/mL)	7.8	34.9	(Bernstein et al., 2000)
Human (3)	200 mg orally	17 d	0.306 (4.39 nmol/mL)	6.3	36.4	(Bernstein et al., 2000)
Human (3)	300 mg orally	17 d	0.566 (8.12 nmol/mL)	4.3	39.9	(Bernstein et al., 2000)
Human (3)	500 mg orally	17 d	0.569 (8.16 nmol/mL)	6.4	37.8	(Bernstein et al., 2000)
Mice infected with *Rhodococcus equi* (3)	10 mg/kg daily for 10 days, gavage	Single time point, 2 h after final dose	110.5 (1.58×10^3 nmol/mL)	-	-	(Harrington et al., 2006)
Mice infected with *Rhodococcus equi* (3)	50 mg/kg daily for 10 days, gavage	Single time point, 2 h after final dose	559.3 (8.02×10^3 nmol/mL)	-	-	(Harrington et al., 2006)
Neonatal foals (6)	20 mg/kg (in distilled water) intragastric	48 h	1.08 (15.5 nmol/mL)	4.3	26.6	(Martens et al., 2007)
Neonatal foals (6)	20 mg/kg (methylcellulose formulation) orally	96 h	0.90 (12.9 nmol/mL)	4	32.8	(Chaffin et al., 2010)
Neonatal foals (6)	40 mg/kg (methylcellulose formulation) orally	96 h	1.8 (25.8 nmol/mL)	4	32.4	(Chaffin et al., 2010)
Horses (6)	20 mg/kg intragastric	120 h	0.28 (4.02 nmol/mL)	3.09	48.8	(Arnold et al., 2010)

Table 1.2. Summary of pharmacokinetic parameter estimates for gallium following oral or intragastric administration of gallium maltolate to selected species

Maximum concentrations (C_{max}) were measured in serum

*T_{max} denotes time to maximum concentration; $t_{1/2}$ denotes half-life.

1.5.6.2.2. **Dogs**

Intestinal absorption of gallium is enhanced when it is administered as gallium maltolate rather than gallium nitrate. Following intraduodenal gallium maltolate administration to beagles, the area under the serum gallium concentration vs. time curve was nearly seven-fold greater than when the same dose (gallium basis) of gallium nitrate was administered by the same route (Bernstein et al., 2000). While maltol chelation increases serum gallium exposure after enteral administration, approximately half of the elemental gallium fails to appear in systemic circulation. Specific gallium complexes in serum were not identified, precluding any inference about absorption of gallium maltolate per se. However, the area under the serum gallium concentration vs. time curve following intravenous administration of gallium nitrate was nearly double that observed with intraduodenal gallium maltolate administration (Bernstein et al., 2000). This suggests that roughly half of the gallium administered as a gallium solution intraduodenally arrives in systemic circulation, but does not provide any insight into any potential transformations of gallium maltolate between the intestinal lumen and peripheral venous blood.

The terminal half-life of gallium in serum following oral administration of gallium maltolate to dogs was estimated at approximately 10 hours (Bernstein et al., 2000). However, this estimate may be subject to bias due to the inclusion of only two dogs in the study and the use of a two-compartment model when data were only available at four times after the maximum concentration was achieved.

1.5.6.2.4. **Humans**

When gallium maltolate was administered orally to human volunteers at 100 mg, 200 mg, 300 mg, and 500 mg (three people per group), the terminal half-life ranged from 104 -115 hours. The 95% confidence intervals for dose-normalized area under the serum concentration vs. time curve overlapped substantially, suggesting that if non-linear pharmacokinetic phenomena occurred they were obscured by the large interindividual variability (Bernstein et al., 2000). Maximum serum concentrations were achieved within 8 hours at all doses. The maximum concentrations following the 300 mg and 500 mg dose were achieved at 4.3 and 6.4 hours, respectively, and were indistinguishable when alpha was set to 0.05 (Bernstein et al., 2000). In the absence of any difference in terminal half-life, this suggests that absorption processes may be saturable.

1.5.6.2.5. **Horses**

Administration of gallium maltolate in distilled water at 10 mg/kg by nasogastric tube to foals resulted in peak gallium concentrations of approximately 1 µg/mL with a terminal half-life of 26.6 hours (Martens et al., 2007). The reliability of the parameter estimates was limited by the relatively short study duration of 48 hours. Oral administration of a methylcellulose-based preparation at 20 mg/kg and 40 mg/kg yielded peak gallium concentrations of 0.9 µg/mL and 1.75 µg/mL, respectively (Chaffin et al., 2010). The terminal half-life was estimated at 32.8 and 32.4 hours at the lower and higher doses (Chaffin et al., 2010). The relative bioavailability of gallium maltolate in the methylcellulose preparation was approximately 50% compared with gallium maltolate in distilled water, but the overlap of the 95% confidence intervals for the $AUC_{0-\infty}$ suggests that this apparent difference may be an artifact of interindividual variability

(Martens et al., 2007; Chaffin et al., 2010). The pharmacokinetics of gallium following administration of gallium maltolate to adult horses have not been evaluated.

1.6. **Synchrotron-based analytical techniques**

Conventional pharmacokinetic analysis of antimicrobial drugs within tissues is performed using tissue homogenization techniques. This approach does not, however, distinguish between intracellular and extracellular location of the drug. Analytical electron microscopy techniques allow the identification and mapping of individual elements, but are unsuitable for distinguishing specific compounds. Synchrotron-based analytical techniques such as hard x-ray microprobe analysis and scanning and transmission x-ray microscopy provide information on both location and chemical speciation of selected elements within a sample. Errors associated with homogenization can be avoided as both methods can be used for tissue sections. Although synchrotron techniques have been applied to environmental science, materials science and physiology experiments, they had not been used to evaluate the distribution and chemistry of an antimicrobial drug prior to the completion of the experiments described in this dissertation.

1.6.1. **Synchrotron description**

Synchrotrons are electron accelerators where bunches of electrons are accelerated to near light-speed and maintained under high vacuum in a ring-like structure where they circulate continuously (Watson and Perlman, 1978; Petibois and Cestelli Guidi, 2008). Each time that the electrons are re-directed around the turns of the storage ring, they emit a very intense and broad spectrum of radiation ranging from the far infra-red through the visible spectrum to hard (high energy) x-rays. Early synchrotron research was principally concerned with sub-atomic particle

behaviour, but the utility of the emitted radiation for studying the chemistry and structure of diverse materials has led to development of synchrotron light sources (Watson and Perlman, 1978; Lombi and Susini, 2009). These facilities are designed to direct and focus the emitted radiation, which is delivered through beamlines containing optical devices such as mirrors and monochromators to further focus the radiation and to select the desired energies.

Synchrotron light sources use electrons emitted from an electron gun into a high-vacuum system where they are accelerated to near-relativistic speed using a linear accelerator and a booster ring (Kamitsubo, 1998; Zhou et al., 2000; Dallin et al., 2003; Carter, 2011). Still under vacuum, the electrons are magnetically guided into a polygonal storage ring. A series of large electromagnets are used to focus and direct the electron beam around the ring. The process of directing the electrons around the ring causes acceleration in a horizontal plane toward the ring centre. Electrons traveling near light speed emit polychromatic (broad spectrum) radiation in a forward direction and upon horizontal acceleration, generate a polarized, intense photon beam oriented tangentially to the curve of the storage ring (Watson and Perlman, 1978). The combined characteristics of this photon beam, namely, intensity, polarization and tunability (i.e., the beam is polychromatic), are essential for numerous analytical techniques and are not replicated by any clinical or laboratory radiation source (Aksenov et al., 2006; Lombi and Susini, 2009).

1.6.2. **X-ray interaction with matter**

Photons approaching matter can behave in any combination of three ways depending on the incident photon energy and sample characteristics:

1. They can be transmitted through the material with no interaction,

2. They can collide with atoms in the material and be scattered elastically or inelastically (Compton scattering), or
3. They can be absorbed by atoms within the sample, initiating a cascade of events.

Photon scattering patterns are measured and interpreted to study crystal structures in x-ray diffraction techniques such as protein crystallography. Elastic and inelastic scattering are sources of noise in techniques that use photon absorption measurements. As an example, conventional diagnostic radiography uses differences in x-ray absorption by various tissue types to produce image contrast. Although x-ray absorption is the critical phenomenon for successful imaging, it is accompanied by x-ray scattering which limits contrast and causes inadvertent radiation exposure to workers.

Upon x-ray absorption, energy is transferred to core electrons, which are then ejected from their respective atoms into the continuum. To maintain atomic stability, an electron from a higher orbital rapidly migrates to fill the core-hole. The energy lost by this electron as it drops from higher to lower orbital can produce one of two results:

1. The energy is released as x-rays of a characteristic energy. The specific energy of the fluorescent x-rays is determined by the binding energy difference between the original and final orbital of the migrating electron. The binding energies are determined by nuclear structure and thus fluorescent x-ray energy values are characteristic for the particular element.

2. Electron migration to fill the core-hole can initiate the Auger process where the excess energy is transferred to another electron from the higher orbital, which is ejected into the continuum. Auger electrons have kinetic energy characteristic for each element at a given incident photon energy. Auger electron kinetic energy is measured in x-ray photoelectron spectroscopy experiments. As electron emission from a given sample is proportional to the concentration of the element of interest and the intensity of the incident radiation, currents generated by Auger processes (typically labelled as "total electron yield") can be used as measures of x-ray absorption. An important limitation of this approach is that the ejected electrons can only travel relatively short distances (dependent on the element in question), restricting analysis to the surface of the sample.

X-ray absorption can be quantified by measuring the intensity of fluorescent radiation or by electron yield. However, Auger electron emission and x-ray fluorescence emission are competing processes. While both phenomena are observed for each element, typically one is predominant at any given absorption edge. Auger processes generally predominate at lower energies, with x-ray fluorescence predominant at higher energies (2001). Both x-ray fluorescence and total electron yield are proportional to x-ray absorption, which is determined by sample thickness (path length), elemental concentration and incident photon energy according to Beer's law.

1.6.3. **X-ray absorption spectroscopy (XAS)**

An x-ray absorption spectrum is generated by plotting x-ray absorption vs. incident x-ray energy for a particular sample. X-ray absorption can be measured as x-ray fluorescence, Auger electron

yield, or as a function of x-ray transmission through the sample. As incident photon energy approaches the "edge" or binding energy of a particular orbital shell, x-ray absorption increases sharply. This marked change in absorption is referred to as an "edge jump," and is a key feature in x-ray absorption spectra. Smaller fluctuations in x-ray absorption in the near-edge range of energies are observed when excited core electrons are not ejected from the atom, but are promoted to higher orbitals (bound states). These fluctuations in the near-edge spectra (x-ray absorption near-edge spectra, or XANES) can provide information about higher electron orbitals, including oxidation states for elements such as iron (Wilke et al., 2001). Oscillations observed at incident energies above the near-edge region are considered in extended x-ray absorption fine structure spectroscopy (EXAFS), and are produced when electrons ejected from the atom of interest interact with electrons from surrounding atoms. The frequency and magnitude of these oscillations reflect the distance to and number of neighbouring electrons, which are interpreted as bond lengths and atomic numbers for adjacent atoms (Aksenov et al., 2006).

1.6.4. **Synchrotron x-ray fluorescence imaging**

Hard x-ray microprobe techniques use x-ray fluorescence measurements, typically from an energy-dispersive detector, following sample irradiation with a 1-5 μm beam to map elemental distributions within cells and tissues. The incident x-ray energy is selected above the absorption edge for the orbital and element of interest. Fluorescent x-ray intensity is then plotted against fluorescent x-ray energy. The elemental origin of the spectral features is determined by comparing the fluorescent x-ray energy of the peak to characteristic elemental fluorescence emission energies. The sample is moved through the beam to allow data collection over an array of points to generate a map of elemental distribution. When regions of interest are identified,

XAS is used as a complimentary technique to generate chemical information from specific points on the sample without the need to move the sample to a different beamline.

1.6.5. **Scanning and transmission x-ray microscopy**

Scanning and transmission x-ray microscopy (STXM) uses soft x-rays from a synchrotron source to conduct spatially-resolved XANES on a nanometre scale. This technique has been used to evaluate the distribution of trace elements in microbial biofilms and to evaluate carbon and nitrogen structures in tissue sections (Loo et al., 2001; Toner et al., 2005; Dynes et al., 2006).

During analysis, x-rays of a selected energy are focused to a small (10-50 nm) point using a Fresnel zone plate, which determines the maximum spatial resolution for the particular equipment configuration (Hitchcock et al., 2008). The sample is placed exactly at the focus of the beam, and transmitted x-rays are detected. X-ray absorption spectra are thus collected across a matrix of points in the selected regions of the sample, allowing chemical mapping of samples based on elements, chemical species, and local concentrations for compounds of interest (Dynes et al., 2006). Although STXM has not been used to evaluate drug distribution in target tissues, the combination of high spectral resolution and nanometre-scale spatial resolution is highly desirable for this application.

Chapter 2. Objectives and hypotheses

The overall objective of this project was to determine the suitability of orally administered gallium maltolate as a potential new therapy for treating urinary tract infections caused by uropathogenic *Escherichia coli*. Six specific objectives and their associated hypotheses and purposes are stated below.

Objective 1: To assemble a library of gallium $L_{2,3}$ –edge and K-edge XANES spectra for gallium reference compounds.

Hypothesis: Gallium compounds are distinguishable by their X-ray absorption near edge spectra at the gallium $L_{2,3}$ edges and at the gallium K-edge.

Objective 2: To select a method of sample preparation and subsequently determine the suitability of STXM for localizing and characterizing gallium in transitional epithelial cells in bladder sections from mice treated with gallium maltolate.

Purposes:

To identify at least one method of sample preparation for producing tissue sections suitable for STXM analysis.

To determine whether iron and zinc are detectable by STXM in bladder sections from healthy mice.

Objective 3: To use hard x-ray microprobe analysis to investigate gallium distribution and its relationship to iron distribution in the bladder mucosa following oral administration of gallium maltolate.

Hypotheses:

Gallium Kα x-ray fluorescence and gallium K-edge x-ray absorption spectroscopy features will be detectable in the bladder mucosa from mice infected with uropathogenic *E. coli* and treated with gallium maltolate.

Gallium and iron will be identically distributed in the bladder mucosa from mice infected with uropathogenic *E. coli* and treated with gallium maltolate.

Objective 4: To describe the pharmacodynamics of gallium maltolate against UPEC in vitro.

Purposes:

To measure minimum inhibitory concentrations of gallium maltolate for selected uropathogenic *E. coli* isolates.

To investigate the relationship between increasing concentrations of gallium maltolate, duration of exposure, and bacterial killing or growth inhibition.

To classify gallium maltolate as bacteriostatic or bactericidal, and as a time-dependent or concentration-dependent antimicrobial drug.

Objective 5: To evaluate the pharmacokinetics of orally administered gallium maltolate in mice and to characterize the effect of urinary tract infection on gallium pharmacokinetics.

Hypothesis: Gallium exposure is greater in bladder, blood and kidney from infected mice than in tissues from healthy mice.

Objective 6: To evaluate the efficacy of orally administered gallium maltolate for reducing tissue bacterial loads in a mouse cystitis model.

Hypothesis: *E. coli* will be cultured from bladders from a smaller proportion of gallium maltolate-treated mice than from untreated control mice.

Chapter 3. Investigation of soft x-ray absorption spectroscopy for evaluating gallium complexes in biological samples

Relationship of this study to the dissertation:

Scanning and transmission x-ray microscopy, an imaging technique based on spatially-resolved soft x-ray absorption spectroscopy, provides the greatest spatial resolution available among all of the synchrotron-based x-ray micro-imaging techniques and could be valuable for localizing and speciating gallium in animal tissue samples. Little information was available on the sensitivity of the soft x-ray absorption spectroscopy for low concentrations of gallium or on its ability to distinguish between different gallium compounds, yet this information was critical for determining the suitability of STXM for investigating gallium distribution and chemistry in tissues from animals treated with gallium maltolate. To address the first objective of this dissertation, the assembly of a library of gallium $L_{2,3}$ –edge x-ray absorption spectra, we collected spectra from a series of gallium compounds including gallium maltolate. We also collected spectra at the gallium $L_{2,3}$ –edges in thin film samples containing low concentrations of gallium. Results of these experiments suggested that STXM may be suitable for examining tissue samples and were used to justify the experiments in Chapter 4 where methods of sample preparation were evaluated.

3.1. **Abstract**

Soft x-ray absorption techniques were used to determine their suitability for investigating the distribution and chemical speciation of gallium in biological samples. X-ray absorption near edge spectroscopy of five gallium reference compounds revealed evident Ga $L_{2,3}$ peaks with distinct spectral features. The Ga L_3 peak was identifiable in thin polymer films containing gallium concentrations as low as 1.30×10^{-4} mol/g.

3.2. **Introduction**

Uropathogenic strains of *Escherichia coli* (UPEC) are the most commonly isolated bacteria from urinary tract infections in humans and dogs, and failure to cure these infections can result in serious and potentially fatal complications (Zhanel et al., 2006; Ball et al., 2008a). Increasing antimicrobial resistance among UPEC has created an urgent need for a new approach to treatment (Zhanel et al., 2006; Ball et al., 2008a). Gallium exerts antimicrobial activity by disrupting bacterial iron metabolism, accumulates in infected tissues, and has activity against some intracellular bacteria (Bernstein, 1998; Olakanmi et al., 2000). These characteristics have created interest in the use of gallium compounds as novel antimicrobial therapy for UPEC infections.

As UPEC can establish an intracellular infection in bladder epithelial cells, successful treatment depends on gallium's arrival at and uptake by the bacteria within these cells (Kau et al., 2005). Soft x-ray scanning and transmission x-ray microscopy (STXM) is well-suited for investigating this process due to its high chemical sensitivity with spatial resolution of less than 50 nm (Dynes et al., 2006). However, little information is available about gallium $L_{2,3}$ x-ray absorption near-edge spectroscopy (XANES), particularly for organic gallium complexes. This study is a

preliminary investigation to determine the suitability of soft x-ray absorption techniques for detecting and distinguishing organic gallium complexes. A series of gallium (III) reference spectra were collected, and the sensitivity of this technique was demonstrated by the evident Ga L_3 peak from polymer thin films with gallium concentrations as low as 1.30×10^{-4} mol/g.

3.3. **Methods**

3.3.1. **Chemicals**

Gallium (III) nitrate ($Ga(NO_3)_3$), gallium (III) oxide (Ga_2O_3), tris (dimethylamido) gallium (III) (GaD_3), tris (8-hydroxyquinolinato) gallium (III) (GaQ_3), poly (methylmethacrylate) (PMMA) and N,N'-bis(3-methylphenyl)-N,N'-diphenylbenzidine (TPD) were purchased from Sigma-Aldrich. Gallium (III) maltolate (GaM) was provided by L.R. Bernstein. All compounds were used as received.

3.3.2. **Sample preparation**

Pure powders were mounted on carbon tape. For thin film fabrication, varying quantities of polymers and GaQ_3 were combined as described in Table 3.1, with the 8.74×10^{-5} mol/g as the lowest concentration of gallium. These mixtures were dissolved in dichloromethane and spin-coated on silicon substrate at 2,000 rpm to produce thin films with a homogeneous distribution of the gallium.

Sample	GaQ_3* (mg)	PMMA* (mg)	TPD* (mg)	Ga concentration (mol/g)
1	5.52	9.91	10.15	4.30×10^{-4}
2	2.40	0	9.80	3.92×10^{-4}
3	1.60	0	9.80	2.79×10^{-4}
4	1.38	10.19	9.50	1.30×10^{-4}
5	0.98	21.36	0	8.74×10^{-5}

Table 3.1. Composition of thin polymer films used to estimate gallium detection limits for x-ray absorption spectroscopy at the Ga $L_{2,3}$ edges
*GaQ_3, tris (8-hydroxyquinolinato) gallium (III); PMMA, poly (methylmethacrylate); TPD, N, N'-bis(3-methylphenyl)-N,N'-diphenylbenzidine

3.3.3. **Data collection**

Total electron yield data were collected at the Ga $L_{2,3}$ edge for the powder samples and at the Ga L_3 edge for the thin polymer films. Data were collected on the High Resolution Spherical Grating Monochromator 11ID-1 (SGM) beamline at the Canadian Light Source (CLS), using the high energy grating (Regier et al., 2007).

3.4. **Results**

3.4.1. **X-ray absorption near-edge spectra at the gallium $L_{2,3}$ edges in reference compounds**

Figure 4.1 shows the Ga $L_{2,3}$ XANES spectra of five gallium compounds. The Ga L_3 edge around 1120 eV was clearly identifiable for all compounds, as was the L_2 edge around 1147 eV. Shifts in the L_2 and L_3 peak positions, along with differing spectral features between these peaks and their satellites, distinguish the spectra of the reference compounds.

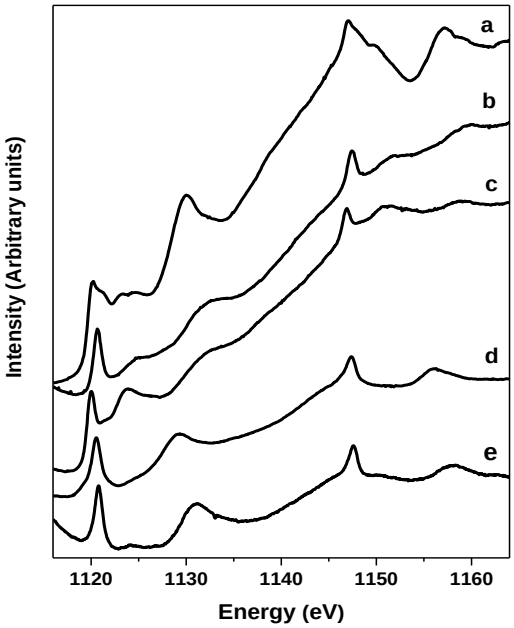

Figure 3.1. Ga $L_{2,3}$ edge XANES spectra of selected gallium compounds
Letters above the spectra indicate the compound evaluated: a, Ga_2O_3; b, $Ga(NO_3)_3$; c, GaD_3; d,GaQ_3; e, GaM.

3.4.2. **X-ray absorption near-edge spectra at the gallium $L_{2,3}$ edges in thin polymer films**

Figure 4.2 shows that the Ga L_3 peaks are evident in samples containing low gallium concentrations. The peak at 1120 eV was distinguishable in thin polymer films with gallium concentrations as low as 1.30×10^{-4} mol/g, and the peak at 1129 eV was clearly distinguishable at gallium concentrations as low as 2.79×10^{-4} mol/g.

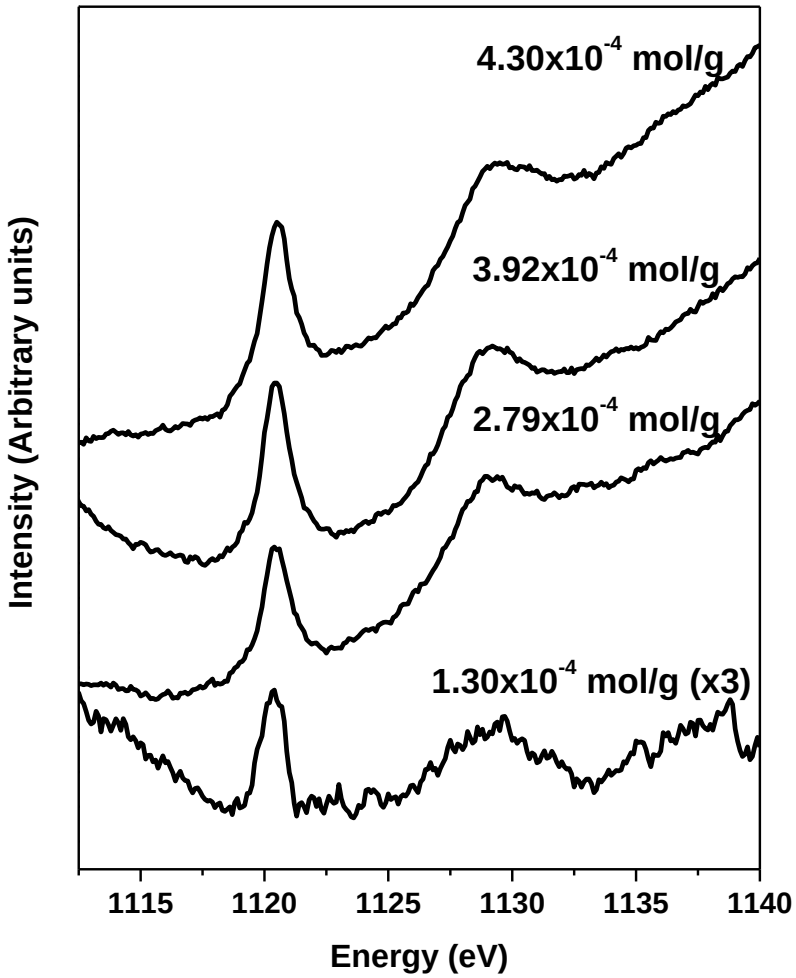

Figure 3.2. X-ray absorption at the Ga $L_{2,3}$ edges by varying concentrations of GaQ_3 embedded in polymer thin films

Gallium concentrations are indicated above each spectrum.

3.5. **Discussion**

The Ga_2O_3 results showed good agreement with published spectra (Shimizu et al., 1996; Zhou et al., 2007b). The Ga_2O_3 spectrum has characteristic features of both octahedral α-Ga_2O_3 and tetrahedral β-Ga_2O_3 (Shimizu et al., 1996; Zhou et al., 2007b). Apart from GaD_3, the other compounds have spectra consistent with gallium in its octahedral α form. The GaD_3 spectrum

has features consistent with both α and β forms, however, GaD_3 is highly reactive and may have decomposed prior to analysis. The results from the analysis of reference compounds clearly show that Ga $L_{2,3}$ XANES is suitable for distinguishing and analyzing organic gallium compounds. Furthermore, Ga $L_{2,3}$ spectra are likely also distinguishable in biological samples, where the gallium may exist in multiple protein-bound and salt forms (Bernstein, 1998).

The detection of gallium at low concentrations in polymer thin films suggests that the total electron yield signal at the Ga $L_{2,3}$ edges has sufficient intensity to allow analysis even in dilute samples. Both total electron yield and x-ray fluorescence yield are proportional to the concentration of the element of interest in a sample, but the relative intensity of these signals differs between elements. At the gallium $L_{2,3}$ edges, the total electron yield is approximately two orders of magnitude greater than the fluorescence yield (Krause, 1979). Consequently, the utility of x-ray fluorescence measurements for Ga $L_{2,3}$ XANES is likely to be more restricted in very dilute samples.

3.6. **Conclusion**

Near-edge x-ray absorption spectroscopy at the Ga $L_{2,3}$ edges can be used to distinguish between organic gallium compounds. As the Ga L_3 peak was observed in dilute samples, this spectral feature is a good candidate for localizing gallium in biological samples using soft x-ray microscopy techniques.

Chapter 4. Preparation of mouse bladder sections for analysis by scanning and transmission x-ray microscopy

Relationship of this study to the dissertation:

The second objective of this dissertation was to identify a method for sample preparation and to determine the suitability of STXM for localizing and speciating gallium in urothelial cells in bladder sections. Having demonstrated in Chapter 3 that gallium compounds can be distinguished using x-ray absorption spectroscopy at the gallium $L_{2,3}$ edges, and that gallium is detectable by this method at low concentrations, we proceeded to evaluate methods of tissue preparation for scanning and transmission x-ray microscopy. Of the three methods evaluated, only fixing with subsequent embedding in LR White resin produced samples suitable for analysis. As iron and zinc exist in tissues at concentrations equal to or greater than those anticipated following gallium maltolate administration, these elements were used as markers to determine the ability of STXM to localize trace elements. As iron and zinc were not reliably detected in any of the tissue sections, it was concluded that STXM was not likely suited for localizing and speciating gallium in animal tissues and that other methods should be investigated to accomplish this. These results led to the investigations described in Chapter 5.

4.1. **Abstract**

Synchrotron scanning and transmission x-ray microscopy (STXM) is used to localize and speciate elements of interest in a variety of samples, and may be useful for investigating the distribution of metal-based drugs within target cells. To determine a suitable method of sample preparation for future studies of gallium and iron distribution, bladders from three healthy mice were prepared for STXM using three different embedding techniques. Fixed tissues were embedded in glycol methacrylate, LR White resin, or trimethylolpropane triglycidal ether- 4,4'-methylenebis (2-methylcyclohexylamine) resin (TTE resin). Of the three methods evaluated, only samples embedded in LR White resin maintained tissue architecture and withstood sectioning at 100 nm and 500 nm. These samples were analyzed at the Canadian Light Source using the scanning and transmission x-ray microscope on beamline 10ID-1 (SM). X-ray absorption measurements at the carbon K-edge allowed identification of anatomic features, but iron was not detected even in regions known to contain erythrocytes. Near-edge spectroscopy revealed changes in carbon chemistry subsequent to sample irradiation for iron mapping and spectroscopy. Methods other than STXM should be investigated for evaluating the distribution and chemistry of iron and gallium in mammalian tissues.

4.2. **Introduction**

Gallium compounds such as gallium maltolate can be safely administered to numerous mammalian species and may be useful for treating antimicrobial resistant urinary tract infections caused by uropathogenic strains of *Escherichia coli* (UPEC) (Bernstein et al., 2000; Martens et al., 2007). Gallium competes with iron in numerous biological processes and exerts antimicrobial activity against Gram-negative and intracellular bacteria (Olakanmi et al., 2000; Kaneko et al., 2007; Coleman et al., 2010). Synchrotron scanning and transmission x-ray microscopy (STXM) may be a powerful tool for confirming that gallium arrives within urothelial cells (the site of UPEC infection), evaluating its

distribution relative to iron, and characterizing its chemistry in tissue sections. Conventional pharmacokinetic analytical techniques are inadequate for this evaluation, as sample homogenization prevents identification of the drug's specific location within the tissue. Analytical electron microscopy techniques such as transmission electron microscopy – electron energy loss spectroscopy allow the identification and mapping of individual elements, but their lower spectral resolution limits the capacity for chemical characterization (Hitchcock et al., 2008). The strong Ga $L_{2,3}$-edge peaks observed for gallium reference compounds suggest that these features could be used to localize and characterize gallium in urothelial cells using STXM (Ball et al., 2008b).

While numerous sample preparation techniques have been evaluated for electron microscopy, little information is available to indicate which is most suitable for STXM analysis of intracellular metals. Tissue preparation methods must preserve both anatomy and chemistry, produce samples that are compatible with the analytical technique and comply with biosafety requirements. As future experiments will involve evaluation of tissues from mice infected with UPEC, samples must be prepared such that any bacteria are contained. Unlike flash-freezing, fixing produces stable samples that pose little risk to human health, as any bacteria present are inactivated during processing.

Fixed tissues have previously been prepared for STXM by embedding in glycol methacrylate, with anatomic details observed using the nitrogen K-edge for contrast (Loo et al., 2001). The electron microscopy laboratory at McMaster University recommends embedding tissue samples in trimethylolpropane triglycidal ether- 4,4'-methylenebis(2-methylcyclohexylamine) resin (TTE resin) for STXM analysis (A. Hitchcock, personal communication 2008). This method has not previously been evaluated for embedding tissue samples, which are more commonly embedded in LR White resin, a proprietary polyhydroxy aromatic acrylic resin. To determine which of these three methods are best suited for analysis of intracellular gallium and iron, mouse bladder tissue was fixed and embedded in

each of the three materials. Sample suitability for analysis was evaluated based on preservation of anatomy, capacity for ultra-thin sectioning, and on maps of iron, zinc and carbon distribution acquired using the STXM at the SM (10ID-1) beamline at the Canadian Light Source.

4.3. **Methods**

4.3.1. **Mice**

This work was approved by the University of Saskatchewan's Animal Research Ethics Board, and adhered to the Canadian Council on Animal Care guidelines for humane animal use. Three 8-10 week old female C57BL/6 mice were euthanized with isoflurane. Bladders were harvested, divided and immersed in ice-cold phosphate-buffered glutaraldehyde-paraformaldehyde immediately following euthanasia.

4.3.2. **Chemicals**

Trimethylolpropane triglycidal ether, and 4,4'-methylenebis(2-methylcyclohexylamine) (MMHA) were obtained from Sigma-Aldrich. LR White reagents and JB-4 (glycol methacrylate) were obtained from Electron Microscopy Sciences (Hatfield PA, USA).

4.3.4. **Sample preparation**

Tissues were fixed in phosphate-buffered paraformaldehyde-glutaraldehyde at 4°C for 3 hours following collection, rinsed in phosphate buffer and subsequently dehydrated in ascending concentrations of ethanol. Bladder tissue from each mouse was then embedded in each of the three media types. Trimethylolpropane triglycidal ether and MMHA were combined in equal volumes and immediately poured into molds containing tissue samples to prepare the TTE-embedded samples. Resin blocks were cured at 60°C for 7.5 hours. For glycol methacrylate and LR White embedding, reagents were prepared according to manufacturers' directions and samples were infiltrated with resin overnight at 4°C and at -10°C, respectively. Following infiltration, glycol methacrylate samples were transferred to airtight capsules and allowed to polymerize at room temperature. Samples in LR White were exposed to ultraviolet light at -4°C for polymerization.

Embedded samples were sectioned at 100 nm, 300 nm and at 500 nm and mounted on copper transmission electron microscopy (TEM) grids without adhesive. Adjacent sections were stained with methylene blue and mounted on glass slides for confirming sample integrity by visible light microscopy.

4.3.5. **Scanning and transmission x-ray microscopy**

Maps of carbon, iron and zinc distribution were acquired along with x-ray absorption stack maps (series of spectra) were collected using the STXM at the SM (10ID-1) beamline at the Canadian Light Source (Kaznatcheev et al., 2007). Regions of interest were identified by light microscopy and then located in the STXM using the row and column markers on the TEM grid.

X-ray absorption at the carbon K-edge, specifically the difference between signals at 280.0 eV and 288.6 eV, was used to identify anatomic features. X-ray absorption spectra at the carbon K-edge and at the iron

and zinc $L_{2,3}$ edges were collected for stack map analysis over regions containing urothelial cells and erythrocytes. Integration times ranged from 1 to 2 ms, and step sizes ranged from 30 to 50 nm. The I_0 spectra were collected from a 1.5 µm x 1.5 µm blank space included in each region specified for stack map analysis.

4.3.6. **Data analysis**

Map data were analyzed using Axis2000 (Lawrence et al., 2003). Images of iron distribution were generated using the difference in x-ray absorption between the pre-edge region and above the L_3 edge (700 eV and 710 eV, respectively). Zinc distribution was evaluated based on x-ray absorption at 1025 eV and on the difference in x-ray absorption between the L_3 pre-edge (1015 eV) and the L_2 post-edge region (1050 eV).

Near-edge spectra from the carbon K-edge were collected from sample regions before and after x-ray exposure and were processed using OriginPro 8.5.1 (OriginLab Corporation, Northampton MA) and the XAS data processing software Athena (Ravel and Newville, 2005). Spectra were normalized to I_0, a pre-edge background was subtracted and a polynomial was fitted to the post-edge region. The Athena flattening algorithm was then applied to reduce the slope in the post-edge line.

4.4. **Results**

4.4.1. **Sample preparation**

While all sample preparation techniques produced firm tissue blocks, only samples embedded in LR White resin were suitable for STXM analysis. These samples were well-suited for ultra-thin sectioning and had abundant, easily identifiable urothelial cells. Glycol methacrylate-embedded samples were too soft to maintain their structure during ultra-thin sectioning. Samples embedded in TTE were successfully

sectioned at both thicknesses but tissue structure was severely distorted with loss of superficial urothelial cell integrity.

4.4.2. **Scanning and transmission x-ray microscopy**

X-ray absorption at the carbon K-edge provided contrast for identifying anatomical features in tissues embedded in LR White resin (Figure 4.1). Sample damage was observed as decreased absorption at 288.6 eV in carbon maps following analysis of a region of interest at the iron L_3 edge (Figure 4.2). The iron analysis was conducted using a 1 ms integration time in 40 nm horizontal and vertical steps, exposing the entire region. Comparison of spectra from damaged and non-damaged regions revealed increased peak intensity at 286.9 eV in the areas that had been previously irradiated, with decreased intensity of the peaks at 288.6 eV and 285.4 eV in the damaged regions (Figure 4.3).

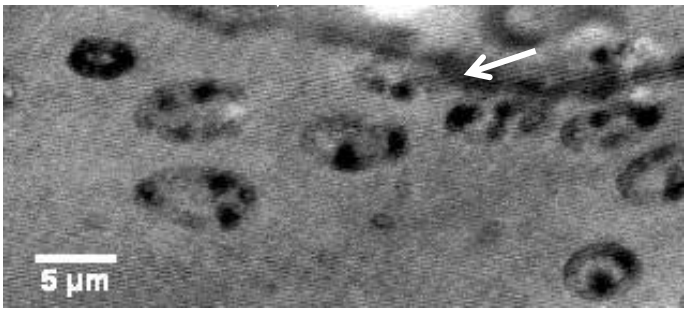

Figure 4.1. Carbon K-edge map showing urothelial nuclei in a 100 nm thick section of mouse bladder tissue embedded in LR White resin
The basement membrane is marked with an arrow.

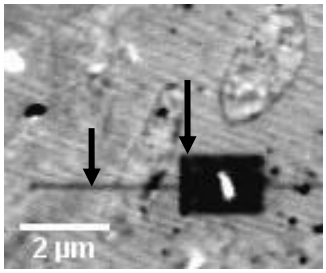

Figure 4.2. Carbon K-edge image of urothelial cells in LR White-embedded mouse bladder tissue sectioned at 100 nm

The arrows indicate regions of sample damage in locations of previous analyses at the iron L_3 edge. The white region in the centre of the radiation damage is a sample contaminant

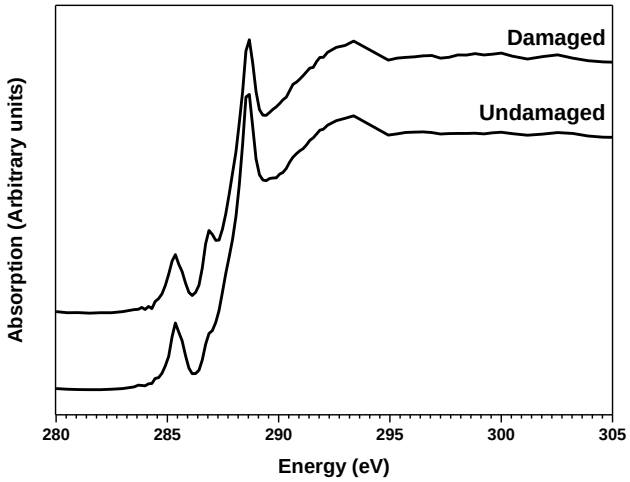

Figure 4.3. Effect of radiation exposure associated with iron analysis on carbon K-edge x-ray absorption spectra from mouse urothelium embedded in LR White resin from radiation-damaged and undamaged regions of the sample.

While sparse regions of increased signal strength were noted in maps of iron distribution, these points were not associated with anatomic features and were deemed artifacts. This interpretation was supported by the failure to detect iron in sample regions known to contain erythrocytes, even in thick (500 nm) sections. Zinc was not detected in any of the sample regions evaluated.

4.5. **Discussion**

Scanning and transmission x-ray microscopy of tissue samples is of interest as an adjunct to conventional pharmacokinetic studies due its high spatial resolution and capacity to speciate elements of interest. While electron microscopy techniques such as transmission electron microscopy electron energy loss spectroscopy (TEM-EELS) can also localize and characterize elements of interest, STXM has substantially greater spectral resolution and causes less sample damage during analysis (Hitchcock et al., 2008). The results of this study demonstrate that STXM analysis can be conducted on tissue embedded in a commonly available medium, using carbon K-edge spectra for contrast to identify anatomic structures.

Identifying anatomic structures by STXM is essential for selecting suitable regions of the sample for analysis and for interpreting results. In this experiment, urothelial nuclei and the basement membrane could be identified in LR White-embedded samples based on x-ray absorption at 288.6 eV. The peak at 288.6 eV is associated with the carboxyl groups of amino acids and is useful for identifying regions of high protein concentration (Kaznacheyev et al., 2002; Solomon et al., 2009). Peak intensity varies with the protein concentration, providing contrast for identifying cellular structures even in the presence of a carbon-based embedding medium.

While features in the near-edge region of carbon K-edge spectra other than the peak at 288.6 eV can indicate the presence of other specific amino acid structures, identification of specific proteins in embedded tissues is likely impractical. Not all amino acids can be distinguished by their carbon K-edge x-ray absorption spectra, and the fixing process denatures and cross-links proteins, introducing artifacts into any analysis of protein structure (Kaznacheyev et al., 2002; Solomon et al., 2009). Along with the carbon in the embedding medium, the abundance and variety of organic compounds within tissue

samples decreases the signal-to-noise ratio for carbon spectra, impeding sensitive analysis of local carbon chemistry and further complicating identification of carbon-based compounds.

In other investigations (reported in part in Chapter 5), zinc and iron were readily detected by x-ray fluorescence imaging and by XANES at their respective K-edges in fixed, paraffin-embedded bladder sections. This suggests that the failure to detect these elements with STXM is not attributable to substantial loss of iron and zinc during the fixing process. The lack of sensitivity for zinc and iron is in part related to the use of the transmitted x-ray intensity to quantify absorption. Unlike x-ray fluorescence imaging with an energy dispersive detector, transmission measurements from STXM cannot isolate the portion of the signal created by a specific element and are influenced by all elements in the sample. The influence of background x-ray absorption on the transmission signal is greater when the elements of interest are present in low concentrations and thus contribute relatively little to the magnitude of x-ray absorption in the sample. As iron concentrations in homogenized mouse bladder observed in other experiments consistently fell below 50 ppm, a low signal-to-noise ratio for this element will be difficult to avoid in the absence of marked accumulation in discrete regions. While the use of an energy-dispersive detector to monitor x-ray fluorescence may improve the signal-to-noise ratio by limiting the influence of x-ray absorption by other elements, the low fluorescence yields from the iron and zinc L-edges will still limit the sensitivity for these elements. The x-ray absorption cross section for gallium at its L_3-edge is lower than those for iron and zinc at their respective L_3-edges, which suggests that sensitivity for gallium will limited compared with iron and zinc. Sensitivity for gallium is likely also limited by low fluorescence yields at the gallium L-edges. As gallium concentrations in tissues are markedly lower than iron concentrations, it is unlikely that gallium will be detectable by STXM unless it is extremely concentrated in discrete foci.

While STXM is not a promising technique for investigating the intracellular distribution of gallium in the urothelium, it may have other applications for studying more abundant elements and those with greater absorption cross-sections in tissue sections. The ability to use samples embedded in LR White resin will facilitate future experiments where fixing and embedding are required to satisfy requirements for sample preservation and biosafety risk management. As radiation damage was observed after intense exposure for iron analysis, the effects of analysis on sample chemistry must be carefully considered during the planning and data analysis stages of future investigations. Pilot experiments using frozen tissues could help to elucidate the effects of fixing and embedding on elemental distribution and chemistry, facilitating further refinement of sample preparation methods.

4.6. **Conclusion**

Fixed tissue embedded in LR White resin can withstand the ultrathin sectioning required for STXM analysis while maintaining anatomic features. Embedding with glycol methacrylate and TTE does not produce suitable samples. X-ray absorption at the carbon K-edge, specifically at 288.6 eV, can be used to identify anatomic features in LR White-embedded tissues. Radiation damage is evident in the carbon spectra in previously analyzed regions, potentially limiting the value of spectra collected from these areas. Further investigation is required to characterize this effect. The failure to detect iron and zinc in tissue samples suggests that STXM will not be useful for investigating the intracellular distribution and chemistry of gallium.

Chapter 5. Hard x-ray microprobe analysis of gallium and iron in bladder mucosa

Relationship of this study to the dissertation:

The second objective of this dissertation was to use hard x-ray microprobe analysis to investigate gallium distribution and its relationship to iron distribution in the bladder mucosa following oral administration of gallium maltolate. The results described in Chapter 4 predicted that scanning and transmission x-ray microscopy would not be suitable for evaluating gallium distribution in tissue samples. Consequently, hard x-ray microprobe analysis was used to confirm gallium's arrival at the bladder mucosa following oral administration of gallium maltolate to mice in addition to addressing the objective stated above. All of these objectives were achieved, marking a successful first application of synchrotron-based micro imaging to antimicrobial pharmacokinetic studies. Combined with the antimicrobial activity demonstrated in Chapter 6, the results reported in this chapter were taken as justification to proceed with the animal model efficacy and pharmacokinetic trials described in Chapters 7 and 8.

5.1. **Abstract**

A mouse model of cystitis caused by uropathogenic *Escherichia coli* was used to study the distribution of gallium in bladder tissue following oral administration of gallium maltolate during urinary tract infection. The median concentration of gallium in homogenized bladder tissue from infected mice was 0.0277 μmol/g after daily administration of gallium maltolate for 5 days. Synchrotron x-ray fluorescence imaging and x-ray absorption spectroscopy of bladder sections confirmed that gallium arrived at the transitional epithelium, a potential site of uropathogenic *E. coli* infection. Gallium and iron were similarly but not identically distributed in the tissues, suggesting that at least some distribution mechanisms are not common between the two elements. The results of this study indicate that gallium maltolate may be a suitable candidate for further development as a novel antimicrobial therapy for urinary tract infections caused by uropathogenic *E. coli*.

5.2. **Introduction**

Urinary tract infections (UTIs) are common in humans and dogs, and most of these infections are caused by uropathogenic strains of *Escherichia coli* (UPEC) (Laupland et al., 2007; Ball et al., 2008a). In addition to patient discomfort and economic burdens from treatment costs and lost work time, failure to cure these infections can lead to serious complications including pyelonephritis and septicaemia (Foxman, 2003). Antimicrobial resistance in UPEC complicates therapy and is of concern for both canine and human patients because these pathogens may be zoonotic (Low et al., 1988; Kurazono et al., 2003; Johnson and Clabots, 2006). Increasing prevalence of antimicrobial resistance among UPEC from human and canine patients has created a need for a new approach to treatment (Gupta et al., 1999; Karlowsky et al., 2002; Ball et al., 2008a; Nys et al., 2008).

Uropathogenic strains of *E. coli* are distinguished by their ability to invade and persist in the urinary tract (Wiles et al., 2008). By invading the transitional epithelial cells, UPEC are able to evade many host defences and can persist in the urinary tract despite the presence of bactericidal concentrations of antimicrobial drugs in urine (Schilling et al., 2002; Blango and Mulvey, 2010). The virulence of UPEC is associated with genes coding for siderophores and siderophore receptors, suggesting that siderophore iron uptake pathways are essential for UPEC survival in the urinary tract (Emody et al., 2003; Wiles et al., 2008). Compounds which arrive at the transitional epithelium and interfere with bacterial iron metabolism may therefore be suitable alternatives to traditional antimicrobial therapy.

The element gallium, as gallium (III), is similar in size and behaviour to iron (III) (Bernstein, 1998). Unlike iron (III), gallium (III) is not known to undergo reduction under physiological conditions (Bernstein, 1998). Gallium binds readily to transferrin, and its transport in mammalian tissues is thought to depend on transferrin receptor pathways (Weiner, 1996). The similarities between gallium and iron also affect bacterial systems. In vitro, gallium binds to *E. coli* siderophores and exerts antimicrobial activity against Gram negative and intracellular pathogens by disrupting iron metabolism (Emery, 1986; Olakanmi et al., 2000; Kaneko et al., 2007). The salts gallium citrate and gallium nitrate are used in human medicine for medical imaging and treating hypercalcemia of malignancy, respectively, but they must be administered intravenously due to negligible oral bioavailability. Gallium maltolate, a complex of gallium (III) with three maltol groups, is of particular interest as a potential UTI therapy as it can be administered orally (Bernstein et al., 2000).

While gallium distribution has been described in a limited number of tissues, its distribution in the urinary bladder is unknown (Berry et al., 1984; Weiner, 1996). Confirmation of gallium distribution to

the transitional epithelium following oral administration of gallium maltolate will support further investigation of gallium maltolate as a new antimicrobial therapy for UTIs caused by UPEC.

Metal detection by analytical methods such as inductively coupled plasma-mass spectrometry require tissue homogenization, possibly with centrifugal separation or fine dissection to achieve a sample suitable for introducing into the instrument. Hard x-ray microprobe analysis is a synchrotron-based analytical technique which includes synchrotron x-ray fluorescence (XRF) imaging and x-ray absorption spectroscopy (XAS). Synchrotrons are electron accelerators which generate intense, focused x-rays that can be used to probe the electron structure of atoms within a variety of sample types, yielding valuable information about the distribution and chemical characteristics of elements within the sample. Elements of interest in intact samples can be localized on a micron scale using XRF imaging and XAS can be used to speciate the elements of interest in regions of interest in the sample (Palmer et al., 2006; Rao et al., 2009). Hard x-ray microprobe analysis has been used to evaluate the distribution of elements in a variety of biological samples including cardiac muscle, macrophages, and neurons (Ishihara et al., 2002; Wagner et al., 2005; Palmer et al., 2006). As tissue homogenization is not required for analysis, these methods are well-suited for investigating the distribution of metal-based drugs within tissues.

The objectives of this study were to use a well-characterized mouse model of UPEC cystitis, XRF imaging and XAS to confirm the arrival of gallium in the bladder mucosa after oral administration of gallium maltolate (Mulvey et al., 1998). The relationship of gallium and iron distribution was also investigated to gain insight into potential mechanisms for gallium distribution in the bladder.

5.4. **Methods**

5.4.1. **Escherichia coli**

The uropathogenic *E. coli* strain used for the infection model was originally isolated from a canine clinical urinary tract infection at the Western College of Veterinary Medicine. The isolate was sub-cultured on TSA agar with 5% sheep blood (Becton, Dickenson and Company, Sparks, MD) prior to preparation of the inoculum.

To confirm the persistence of infection in the control mice, kidney and bladder samples were plated on MacConkey II agar (BD Canada, Missisauga ON) and on trypticase soy agar with 5% sheep blood (BD Canada, Missisauga ON) and incubated at 37˚C for 18-24 hours. Identification was based on colony type and morphology, Gram staining characteristics and growth on MacConkey II agar.

5.4.2. **Gallium maltolate solution**

Gallium maltolate solutions were prepared immediately prior to administration. Gallium maltolate (provided by Lawrence Bernstein) was added to ultrapure water and mixed by vortexing. The solution was then placed in an ultrasonic water bath at 37 ℃ for approximately 20 minutes until no crystals were visible in the solution

5.4.3. **Mice**

This work was approved by the University of Saskatchewan's Animal Research Ethics Board, and adhered to the Canadian Council on Animal Care guidelines for humane animal use. Mice were maintained with tap water and a commercial mouse ration containing 270 ppm iron (Laboratory Rodent Diet 5001, PMI LabDiet, St. Louis, MO, USA) ad libitum prior to and during the experiments. Six, 8-10 week-old female C56BL/6 mice were anesthetized with isoflurane and infected transurethrally with 10^8

colony forming units of a canine clinical uropathogenic *Escherichia coli* isolate (M2B, isolated at the Western College of Veterinary Medicine Bacteriology Laboratory) in a volume of 50 µL as previously described (Mulvey et al., 1998). Treatments were started 48 hours after infection. Three mice received gallium maltolate (provided by Lawrence Bernstein) in distilled water at 200 mg/kg by gavage once daily for five days (treatment group). The remaining three mice each received distilled water by gavage once daily for five days (control group). Two mice in the treatment group died suddenly during handling approximately 24 hours following the last treatment, shortly before the remaining mice were euthanized for sampling. Gross necropsy findings included enteritis in one mouse and mild icterus in the other. Euthanasia of the remaining mice was accomplished by isoflurane exposure and tissues were harvested aseptically from all mice.

5.4.4. **Quantification of tissue gallium concentration by inductively coupled plasma-mass spectrometry**

One third of each bladder from the treated mice was submitted to the Prairie Diagnostic Services Toxicology Laboratory to quantify gallium concentrations in tissue homogenate by inductively coupled plasma-mass spectrometry. These samples were frozen immediately after collection and stored at -20°C until analysis.

5.4.5. **Sample preparation for hard x-ray microprobe analysis**

Formalin fixed, paraffin-embedded tissue from each mouse was sectioned at 20 µm and mounted on high-purity quartz slides (SPI Supplies, West Chester PA). Adjacent sections cut at 5-7 µm and stained with hematoxylin and eosin were used for light microscopy to confirm map locations.

5.4.7. **Data collection**

X-ray fluorescence maps and x-ray absorption spectra were collected using the Pacific Northwest Consortium/X-ray Science Division (PNC/XSD 20 ID) beamline at the Advanced Photon Source located at Argonne National Laboratory (Heald et al., 2007). Formalin fixed, paraffin-embedded tissue from each mouse was sectioned at 20 μm and mounted on high-purity quartz slides (SPI Supplies, West Chester PA). Adjacent sections cut at 5-7 μm and stained with hematoxylin and eosin were used for light microscopy to confirm map locations. For XRF and XAS, incident energy was selected with a double crystal Si(111) monochromator, with the second crystal detuned by 10% for harmonic rejection. Gallium metal foil was used for energy calibration prior to and during data collection. Kirkpatrick-Baez mirrors were used to focus the beam to 5 μm by 5 μm. X-ray fluorescence data were collected at 11 keV with 10 s integration time and 5 μm horizontal and vertical steps. A minimum area of 20,000 μm^2 was mapped for each sample. Gallium, iron, and zinc Kα fluorescence was monitored using a 7-element germanium detector (Canberra Industries Inc., Meriden CT) positioned at 45˚ to the sample and at 90˚ to the incident beam. X-ray absorption spectra at the Ga K-edge were collected from each sample at regions with the strongest Ga signal using 0.5 eV steps and integration time of 5 s. At least two spectra were collected at each region.

5.4.8. **Data analysis**

Gallium and iron XRF data were processed using ImageJ software (Abràmoff et al., 2004). Due to the proximity of the gallium Kα and zinc Kα emission energy ranges, gallium data was corrected for the influence of the zinc signal prior to correlation analysis. Counts for gallium Kα emission were collected between 9.04 keV and 9.28 keV, and counts for zinc Kα emission were collected between 8.36 keV and 8.92 keV. Detector resolution was approximately 200 eV over the range of these emission ranges. Assuming that the emission energy had a Gaussian distribution about the tabulated energy for the

emission line, counts from the zinc signal falling in the gallium Kα count window were estimated and then subtracted from the counts recorded in the gallium Kα window. Iron signals and zinc-corrected gallium signals were normalized to incident beam intensity (I_0) prior to plotting element distribution maps. Spearman's correlation was used to evaluate the relationship between I_0-normalized corrected counts in the gallium Kα emission range and the I_0-normalized in the iron Kα emission range at each pixel from XRF maps. This analysis was conducted with a commercial statistical software package (Stata/IC 10.1 for Windows, StataCorp, College Station TX).

Near-edge spectra collected at the gallium K-edge from the regions of strongest gallium fluorescence signal each region were processed using OriginPro 8.5 (OriginLab Corporation, Northampton MA) and the XAS data processing software Athena (Ravel and Newville, 2005). Spectra were normalized to I_0 and energy values were calibrated using data simultaneously collected from gallium foil. After spectra were averaged, a pre-edge background was subtracted and a polynomial was fitted to the post-edge region. The Athena flattening algorithm was then applied to reduce the slope in the post-edge line.

5.5. **Results**

5.5.1. **Microbiology**

Bacterial growth consistent with *E. coli* was observed from the bladders from all control mice. No bacterial growth was observed from the bladders from mice treated with gallium maltolate. There was no bacterial growth from the kidneys of any mice, indicating that the infection model was limited to cystitis.

5.5.3. **Gallium distribution in bladder sections**

The median gallium concentration in homogenized tissue samples was 0.0277 µmol/g (Table 5.1, data from three mice). X-ray fluorescence at the gallium K-edge was detected in tissue samples from all treated mice. X-ray absorption spectra were collected at the gallium K-edge from the regions with the strongest gallium Kα signal from each mouse (Figure 5.1). The sharp increase in x-ray fluorescence around 10.37 keV is characteristic for gallium, and confirmed the presence of this element in the mapped regions from the treated mice. The inflection point identified on the first derivative plot of the spectra was located at 10.374 keV for all treated mice. The XRF maps revealed a non-homogeneous distribution of gallium within the mucosa (Figure 5.2 and Figure 5.3). Regions of strong fluorescence in the Ga Kα window were not observed in tissues from the control mice. In treated mice, gallium distribution was similar but not identical to iron distribution (Table 5.1, Figure 5.3, Figure 5.4, and Figure 5.5).

Mouse	Gallium concentration (µmol/g)	Iron concentration (µmol/g)	Spearman's rho (p-value)
A	0.0273	2.46	0.60 (<0.0001)
B	0.0334	1.97	0.86 (<0.0001)
C	0.0277	1.39	0.74 (<0.0001)

Table 5.1. Gallium and iron concentrations in homogenized bladder and Spearman's rho for gallium and iron counts in XRF maps obtained from bladder sections from mice with urinary tract infections following gallium maltolate administration by gavage at 200 mg/kg once daily for 5 days

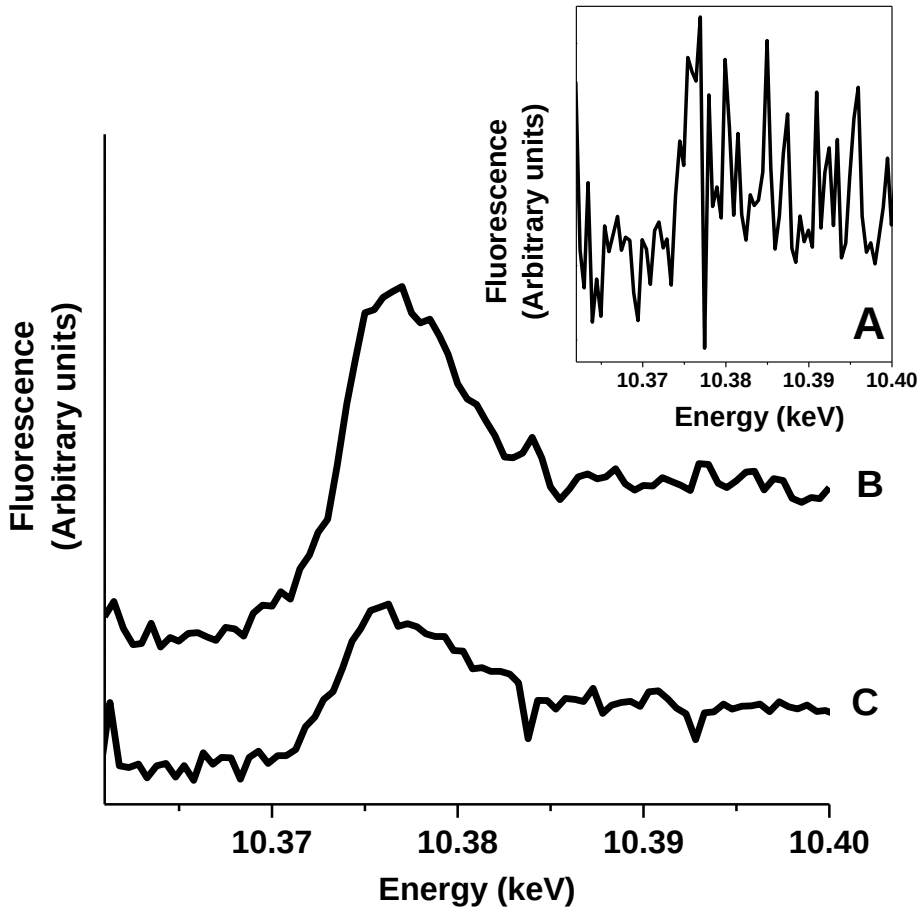

Figure 5.1. Gallium K-edge X-ray absorption spectra from regions of strong gallium fluorescence in bladder tissue from three mice with urinary tract infections treated with gallium maltolate by gavage at 200 mg/kg daily for five days
Letters beside the spectra indicate individual mice. The inset for mouse A uses an expanded y-axis scale to facilitate observation of the small edge jump at the gallium K-edge in this sample.

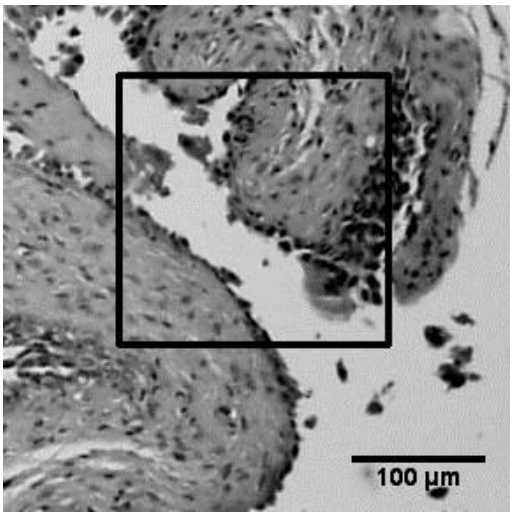

Figure 5.2. Hematoxylin and eosin-stained section of bladder tissue from infected mouse C treated with gallium maltolate by gavage at 200 mg/kg daily for five days, indicating the sample region examined using x-ray fluorescence microscopy

The region represented in Figure 5.3 and Figure 5.4 is outlined.

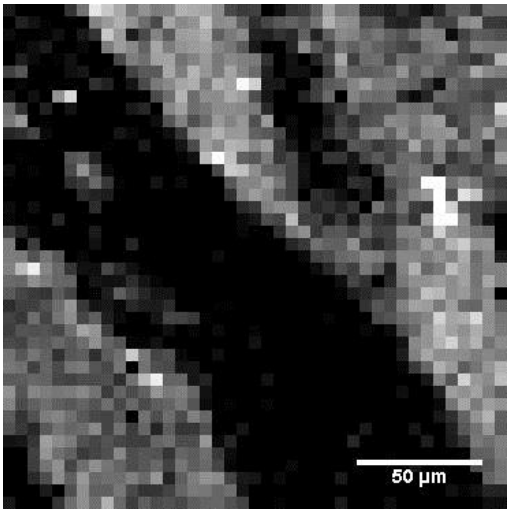

Figure 5.3. Synchrotron x-ray fluorescence map of gallium distribution in a bladder tissue section from infected mouse C treated with gallium maltolate by gavage at 200 mg/kg daily for five days

This map was collected from the region shown in Figure 5.2. Relative fluorescence signal intensity at each pixel is indicated by a colour gradient where white represents strong signals (indicating high local gallium concentration) and black represents a weak signal. The region of weak signals extending from the upper left corner to the lower right corner corresponds to the bladder lumen.

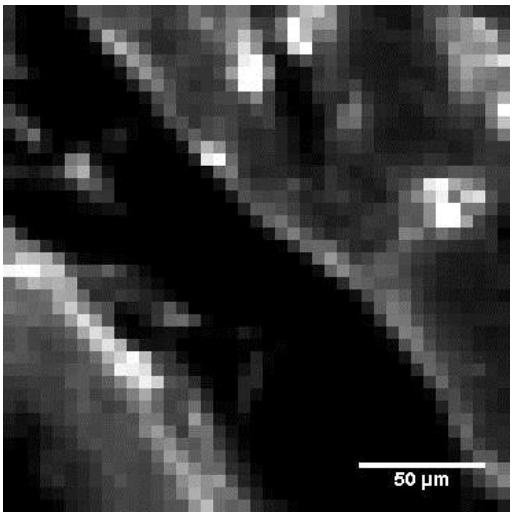

Figure 5.4. Synchrotron x-ray fluorescence map of iron distribution in a bladder tissue section from infected mouse C treated with gallium maltolate by gavage at 200 mg/kg daily for five days

This map was collected simultaneously with the one shown in Figure 5.3, at the same location. Relative fluorescence signal intensity at each pixel is indicated by a colour gradient where white represents strong signals (indicating high local iron concentration) and black represents a weak signal.

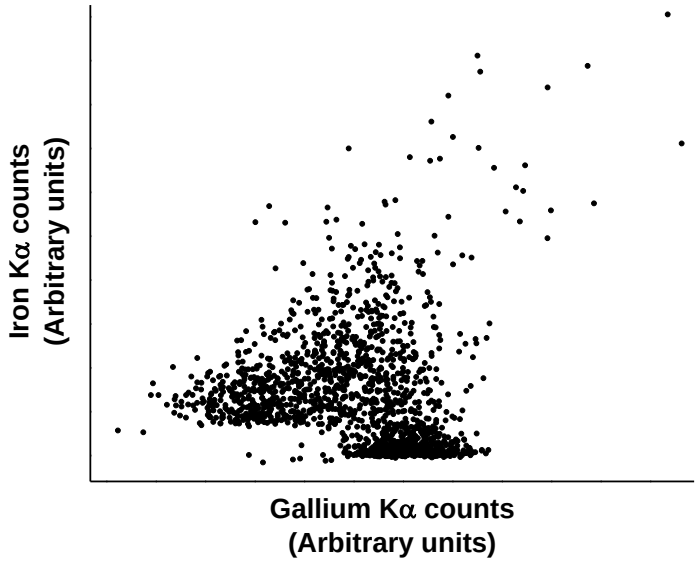

Figure 5.5. Scatter plot of iron counts vs. gallium counts at each pixel in the x-ray fluorescence maps collected from infected mouse C treated with gallium maltolate by gavage at 200 mg/kg daily for five days
Spearman's rho for this data set is 0.74

5.6. **Discussion**

These results are consistent with previous studies which demonstrated absorption of gallium after oral administration of gallium maltolate (Bernstein et al., 2000; Harrington et al., 2006). The mean gallium concentration in homogenized bladder samples from treated mice were approximately five times the serum concentrations reported after oral administration of 50 mg/kg (one quarter of the dose used in the present study) (Harrington et al., 2006). The mean tissue concentration in this study exceeds the concentrations required to inhibit growth of *Pseudomonas aeruginosa* and *Mycobacterium tuberculosis* in vitro, suggesting that oral administration of gallium maltolate can produce potentially clinically relevant gallium concentrations in homogenized bladder tissue (Olakanmi et al., 2000; Kaneko et al., 2007). Further

characterization of the antimicrobial activity of gallium maltolate against UPEC including determination of minimum inhibitory concentrations will be important to better predict its potential clinical utility for treating urinary tract infections caused by UPEC.

Gallium concentrations in homogenized tissue samples are useful to rule out gallium compounds as potential therapeutic agents, since if no gallium is detectable in the sample, it is unlikely that it achieves relevant concentrations in any part of the tissue. As homogenized samples contain all tissue layers, researchers cannot distinguish gallium within the target region of the sample from gallium in other regions of the sample. Hard x-ray microprobe results confirm that gallium reaches the bladder mucosa after gallium maltolate administration and thus meets one of the basic requirements of an antimicrobial compound: it arrives at the site of infection.

Gallium distribution has previously been ascribed in large part to iron transport mechanisms, particularly transferrin-mediated pathways (Bernstein, 1998). Gallium and iron share numerous chemical characteristics such as ionic radius and valence states, and these similarities contribute to similarities in their interactions with other atoms and molecules (Bernstein, 1998). In the present study, the Spearman's rho values of less than 0.9 between iron and gallium signals from treated mice suggest that in the bladder, gallium is partially distributed via mechanisms that do not involve iron. Observations in bone marrow, liver, spleen, and tumour tissues have similarly indicated that gallium and iron are not identically distributed in tissues (Weiner, 1996). The positive values obtained for Spearman's rho suggest that inhibition of one metal's distribution by the other is not a large component of the relationship between gallium and iron in the bladder. This is consistent with a common high-capacity transport system coupled with additional specific

pathways to account for the differences in distribution. The common distribution pathway may include transferrin and transferrin receptors as previously described, while the greater aqueous solubility of gallium compared to iron at physiological pH may explain differences in distribution of non-protein bound gallium and iron (Weiner, 1996).

Iron transport in mammalian tissues is heavily dependent on transferrin and its receptors, and on transporters from solute carrier family 11, notably SLC11A2 (divalent metal transporter-1) and SLC11A3 (ferroportin) (Gunshin et al., 2005; Wang and Pantopoulos, 2011). Iron uptake via transferrin receptors involves endocytosis, release from transferrin, reduction, and subsequent transport of ferrous iron out of the vesicles by SLC11A2 (MacKenzie et al., 2008). While SLC11A2 will accept a variety of divalent cations as substrates, ferric iron must be reduced to its ferrous form before it can be transported (Wang and Pantopoulos, 2011). It is unlikely that gallium, present as a trivalent cation unable to be reduced under physiological conditions, would be efficiently transported by SLC11A2 or SLC11A3. Characterization of the transport mechanisms for gallium will be essential for predicting gallium distribution within other tissue types and for identifying potential drug-drug or drug-nutrient interactions that could lead to clinically significant alterations in pharmacokinetics. Additional hard x-ray microprobe studies may provide critical insight into gallium transport mechanism by revealing intracellular distribution and chemistry.

To the authors' knowledge, this is the first application of synchrotron-based techniques to the identification of antimicrobial distribution within tissues. The simultaneous mapping of multiple elements of interest by synchrotron XRF imaging provides information not only about single

element distribution, but also about the distributional relationships between elements. This capability is useful at the level of tissues, as was accomplished in this experiment, and improvements in spatial resolution should make synchrotron XRF imaging an even more useful method for tracking elemental distribution within biological samples. In this study, we used spatial resolution of 5 μm, which is suitable for mapping elements in tissues and allows analysis of larger regions of the sample in the limited available instrument access time. However, spatial resolution of less than 100 nm have been reported, with speculation that 30 nm resolution should soon be possible (Matsuyama et al., 2009). Accompanied by method refinements to ensure correct identification of cellular elements, this spatial resolution should allow characterization of intracellular elemental distribution without the need to disrupt tissue architecture.

The utility of XAS in hard x-ray microprobe analysis of tissues extends beyond confirming the presence of a specific element. The spectra collected in this study, particularly those from mice b and c, are of sufficient quality to suggest that gallium speciation is possible in these samples. The edge energy inflection point approximately 7 eV above the tabulated electron binding energy for the gallium K-edge is similar to previously reported observations for Ga_2O_3 and for $Ga(NO_3)_3$ (Meitzner et al., 1993; Faro et al., 2008). While these spectroscopy results are preliminary, they demonstrate that near-edge x-ray absorption spectroscopy is possible and that extended x-ray absorption fine structure spectroscopy (EXAFS) may be possible at the gallium K-edge in tissue samples despite the low gallium concentrations observed during treatment. Additional XAS studies of gallium at the site of infection will allow refinement of in vitro antimicrobial susceptibility testing strategies by providing the necessary information to more closely reproduce the chemistry of the site of infection.

Along with the negative bladder cultures from the control mice, positive bladder cultures from all of the control mice suggest that gallium maltolate administration leads to antimicrobial activity in the bladder tissues. While only a small number of mice were included in this experiment, these results are consistent with findings by other research groups that gallium maltolate administration reduces bacterial loads in tissues (Harrington et al., 2006; DeLeon et al., 2009). Along with in vitro pharmacodynamic investigations, further study with larger groups of animals is required to more accurately characterize the antimicrobial activity of gallium maltolate in tissues. In addition to this, the unexpected death of two gallium maltolate-treated mice in the present study should prompt toxicological investigations of this compound. While enteritis and icterus are not classical signs of gallium toxicity, we cannot exclude the potential of toxicity with certainty (Collery et al., 2002). This is particularly true where little toxicology data are available for comparison and where very small groups of animals were involved. Toxicological characterization of gallium maltolate will be essential for determining whether this compound should be further considered as a candidate for clinical use as an antimicrobial therapy.

The distribution characteristics of gallium in the urinary bladder following oral administration of gallium maltolate suggest that this compound may be a suitable candidate for further development as an antimicrobial therapy for UTIs caused by UPEC. This is further supported by its apparent antimicrobial efficacy in a small group of mice, but further efficacy studies using larger groups will be necessary to confirm this observation. Toxicology investigations are indicated to establish whether gallium maltolate may exert unacceptable toxic effects at

potentially therapeutic doses. Elucidation of the major uptake and transport mechanisms for gallium will be essential for predicting potential drug-nutrient and drug-drug interactions, as the behaviour of iron does not accurately reflect the behaviour of gallium. As XRF imaging and in-situ XAS techniques evolve to provide spatial resolution in the 30 nm range, studies of the intracellular distribution and chemistry of gallium should aid to direct investigations of the mechanisms of gallium transport and uptake.

5.7. **Conclusion**

Following oral administration of gallium maltolate to mice with urinary tract infections, gallium arrives at the urothelium and is distributed similarly but not identically to iron. Based on the differences in distribution, gallium is likely partially distributed in the bladder by mechanisms that do not involve iron. Gallium's distribution in the bladder is favourable for treating infections caused by UPEC as it arrives at the putative site of infection.

The results of this experiment also demonstrate that XRF can be used to localize exogenous trace elements in mammalian tissues. The quality of the gallium and iron x-ray absorption spectra suggest that elements of interest can likely be speciated using XANES in situ.

Chapter 6. In vitro pharmacodynamics of gallium maltolate against uropathogenic *Escherichia coli*

Relationship of this study to the dissertation:

A new antimicrobial drug candidate must exert bacteriostatic or bactericidal activity against the target pathogen if additional studies, particularly those using animals, are to be justified. This chapter addresses the fourth objective of this dissertation, to describe the antimicrobial activity of gallium maltolate against uropathogenic *E. coli*. Isolates from human and canine clinical urinary tract infections were exposed to gallium maltolate in vitro in conventional susceptibility testing, and time-kill studies were conducted for a subset of these isolates. These experiments demonstrate that gallium maltolate exerts bacteriostatic antimicrobial activity against multiple strains of uropathogenic *E. coli* in a time-dependent manner.

6.1. **Abstract**

Gallium compounds such as gallium maltolate exert antimicrobial activity against a variety of Gram negative pathogens in vitro, and are of interest as potential treatments for urinary tract infections caused by antimicrobial-resistant uropathogenic *Escherichia coli* (UPEC). Minimum inhibitory concentrations and time-kill studies were used to characterize the antimicrobial activity of gallium maltolate against UPEC in vitro. Minimum inhibitory concentrations of gallium maltolate for six canine clinical UPEC isolates and for three type strains isolated from humans, UTI89, American Type Culture Collection (ATCC) 700336 (J96) and ATCC 700928 (CFT073) ranged from 0.144 µmol/mL to >9.20 µmol/mL, with a median value of 1.15 µmol/mL. Time-kill studies conducted on four of the canine clinical isolates and two of the type strains indicated that gallium maltolate exerts primarily bacteriostatic, time-dependent antimicrobial effects against UPEC. Cross-resistance between gallium maltolate and conventional antimicrobials may be uncommon as susceptibility to conventional antimicrobials was a poor predictor of gallium maltolate susceptibility. Microbial capacity to produce siderophores and their receptors was not predictive of gallium maltolate susceptibility in the type strains, suggesting that antimicrobial activity at least partly results from interference with metabolic processes other than siderophore-mediated iron uptake. Further investigation of gallium concentrations and chemistry at the site of infection will be critical for optimizing susceptibility testing methods and for predicting whether clinically relevant antimicrobial activity is likely in vivo.

6.2. **Introduction**

Urinary tract infections are common in humans and dogs, affecting over 90% of women, 10% of men, and 14% of dogs in their lifetimes (Ling, 1984; Foxman and Brown, 2003). As the most common cause of urinary tract infections, uropathogenic strains of *Escherichia coli* are responsible for a large disease burden (Zhanel et al., 2005; Ball et al., 2008a). Left untreated or in the case of treatment failure, these infections can lead to renal failure, septicemia and death. The similarities between human and canine UPEC isolates, along with epidemiological evidence, suggest that these infections may be zoonotic (Johnson et al., 2003; Johnson and Clabots, 2006). Increasing prevalence of antimicrobial resistance among UPEC isolated from human and canine sources has created a need for novel approaches to antimicrobial therapy (Ball et al., 2008a; Johnson et al., 2009a; Karlowsky et al., 2011).

Gallium compounds interfere with bacterial iron metabolism and have been investigated as potential new antimicrobial therapies for infections caused by Gram negative and intracellular pathogens including *Pseudomonas aeruginosa, Francisella tularensis, Mycobacterium tuberculosis* and *Rhodococcus equi* (Olakanmi et al., 2000; Kaneko et al., 2007; Banin et al., 2008; DeLeon et al., 2009; Coleman et al., 2010; Olakanmi et al., 2010). Gallium causes similar effects in non-uropathogenic strains of *E. coli* (Emery, 1986; Hubbard et al., 1986). Gallium (III) is similar to iron (III) in size and chemical behaviour, and is thought to exert antimicrobial activity by substituting for iron in essential bacterial enzymes that ordinarily contain iron. Gallium can bind to siderophores from the hydroxyamate, peptide and catecholate families, and these iron transport systems which serve as virulence factors in UPEC may also contribute to gallium uptake (Emery, 1986; Banin et al., 2008; Wasielewski et al., 2008; Wiles et al., 2008).

As no currently available antimicrobials target bacterial iron metabolism, extensive cross-resistance between gallium compounds and conventional antimicrobials is not expected. Consequently, gallium compounds such as gallium maltolate may be well-suited for treating multidrug-resistant infections in addition to routine cases.

To investigate whether gallium maltolate may be suitable for further evaluation as a novel antimicrobial therapy for urinary tract infections caused by UPEC, its antimicrobial activity was investigated in vitro. Three UPEC type strains originally isolated from human urinary tract infections and six canine clinical UPEC isolates were characterized by their minimum inhibitory concentrations (MIC) for conventional antimicrobials. Minimum inhibitory concentrations for gallium maltolate were then determined for each isolate. Time-kill studies were conducted for two of the type strains and for four of the canine clinical isolates to further characterize gallium maltolate's antimicrobial activity.

6.3. **Methods**

6.3.1. **Escherichia coli isolates**

A convenience sample of six *E. coli* strains isolated from canine clinical urinary tract infections at the Western College of Veterinary Medicine (K01, K02, K03, K07, K08, M2B) were selected for the study along with three type strains originally isolated from human patients, ATCC 700336 (J96), ATCC 700928 (CFT073) and UTI89 (obtained from M. Mulvey, University of Utah). Isolates were stored at -80°C in litmus milk, and sub-cultured on TSA agar with 5% sheep blood prior to testing.

6.3.2. **Media**

Trypticase soy agar with 5% sheep blood, Mueller-Hinton II agar, MacConkey II agar (Becton, Dickenson and Company, Sparks, MD, USA), and RPMI 1640 with L-glutamine (Lonza, Walkersville, MD, USA) were used as received. Cation-adjusted Mueller-Hinton II broth (Becton, Dickenson and Company, Sparks, MD) was prepared according to manufacturer's directions.

Samples of RPMI and Mueller-Hinton broth used for MIC and time-kill studies were submitted to the Prairie Diagnostic Services Toxicology Laboratory for measurement of gallium and iron concentrations by inductively coupled plasma-mass spectrometry.

6.3.3. **Measurement of minimum inhibitory concentrations for conventional antimicrobials**

The minimum inhibitory concentrations (MICs) of nine antimicrobials, trimethoprim-sulfamethoxazole, tetracycline, gentamicin, ceftriaxone, cephalothin, chloramphenicol, ciprofloxacin, ampicillin and amoxicillin-clavulanic acid were determined using plastic strips containing pre-defined antimicrobial concentrations for all nine isolates (E-tests, AB Biomérieux, Solna, Sweden). Following inoculation of Mueller-Hinton II agar plates and placement of E-test strips, cultures were incubated at 35°C and interpreted after 18-24 hours in accordance with manufacturer and Clinical and Laboratory Standards Institute (CLSI) guidelines (Biomerieux, 2008; CLSI, 2008). *Escherichia coli* ATCC 25922, *Staphylococcus aureus* ATCC 29213 and *Enterococcus faecalis* ATCC 29212 were used for quality control (CLSI, 2008).

6.3.5. **Measurement of minimum inhibitory concentrations for gallium maltolate**

Minimum inhibitory concentrations for gallium maltolate were determined by the broth microdilution method. Gallium maltolate was used as received from L. Bernstein**.** Minimum inhibitory concentrations were determined in both cation-adjusted Mueller Hinton II broth and RPMI 1640 with L-glutamine, using gallium maltolate in doubling dilutions ranging from 0.562 nmol/mL through 9.20 µmol/mL. A MacFarland 0.5 suspension of the test organism was made in sterile, deionized water (Trek Diagnostics, Cleveland, OH, USA), and 25 µL of this suspension was added to 5 ml of broth containing gallium maltolate for a final concentration of approximately 5 x 10^5 CFU/mL as per CLSI guidelines (CLSI, 1999; CLSI, 2006). Media were incubated at 35°C and visually inspected after 18-24 hours. The presence of turbidity or bacterial pellets was considered evidence of growth, and the MIC was defined as the lowest concentration where growth was inhibited.

6.3.6. **Time-kill studies**

Bacterial growth/kill curves were generated in RPMI for four of the canine clinical UPEC isolates and for two of the type strains (K01, K03, K07, M2B, UTI89 and ATCC 700336). A bacterial growth curve was obtained using RPMI with no additives. Antimicrobial activity was assessed in 20 mL of RPMI with an initial bacterial concentration of 5 x 10^5 CFU/mL and containing gallium maltolate at three multiples of the organism's MIC. Five organisms were exposed to gallium maltolate concentrations of 0.5 MIC, MIC and to 10 MIC. The sixth isolate was exposed to concentrations of 0.5 MIC, MIC and 2 MIC as the solubility limit of gallium maltolate precluded evaluation at higher MIC multiples. Cultures were incubated at 35°C for the duration of the experiment. Colony counts were determined immediately following inoculation

and at 4, 8, 12, 24, 48 and 72 hours post-inoculation. Bacterial concentrations were calculated from colony counts on TSA blood agar plates inoculated in triplicate with broth dilutions ranging from 10^{-1} to 10^{-8}. Calculations were made using counts from plates containing between 20 and 200 colonies following overnight incubation at 35°C.

6.3.7. **Data analysis**

The area between the bacterial growth curve and the kill curves (ABBC) served as a measure of antimicrobial activity and was calculated by subtracting the area under the inhibition curve (i.e., obtained from cultures containing gallium maltolate) from the area under the bacterial growth curve (i.e., cultured without gallium maltolate) for the same bacterial strain. This calculation was repeated to generate ABBC values for each multiple of the MIC using OriginPro 8.5.1 (OriginLab Corporation, Northampton MA, USA) (Firsov et al., 1997). To account for inter-strain differences in growth curves and allow comparison of ABBC values between strains, raw ABBC values were normalized to the area under the control curve. The relationship between gallium maltolate MIC multiple and normalized ABBC was evaluated using the Friedman test. Data were grouped by isolate and gallium maltolate dilution factors were entered as categorical variables.

6.4. **Results**

6.4.1. **Susceptibility to conventional antimicrobials**

The MICs for all isolates fell in the 'susceptible' range defined by CLSI (Document M7-MIC) for trimethoprim/sulfamethoxazole, tetracycline, gentamicin, ceftriaxone, chloramphenicol, and amoxicillin/clavulanic acid (Table 6.1.). Three isolates, K03, M2B, and ATCC 700928 exhibited

intermediate susceptibility to cephalothin. Ciprofloxacin resistance was observed in K03, and ampicillin resistance was observed in M2B. Minimum inhibitory concentrations for the quality control strains of *E. coli* (ATCC), *E. faecalis* (ATCC), and *S. aureus* (ATCC) were within the ranges specified by ATCC.

	Minimum inhibitory concentration (susceptibility category in parentheses for conventional antimicrobials)									
Isolate	**Trimethoprim/ sulfamethoxazole µg/mL**	**Tetracycline µg/mL**	**Gentamicin µg/mL**	**Ceftriaxone µg/mL**	**Cephalothin µg/mL**	**Chloramphenicol µg/mL**	**Ciprofloxacin µg/mL**	**Ampicillin µg/mL**	**Amoxicillin/ clavulanic acid µg/mL**	**Gallium maltolate µmol/mL**
K01	0.094 (S)	2 (S)	0.5 (S)	0.047 (S)	8 (S)	4 (S)	0.12 (S)	3 (S)	3 (S)	0.288
K02	0.125 (S)	2 (S)	0.75 (S)	0.064 (S)	8 (S)	6 (S)	0.016 (S)	4 (S)	4 (S)	2.30
K03	0.125 (S)	3 (S)	0.75 (S)	0.047 (S)	12 (I)	4 (S)	>32 (R)	4 (S)	3 (S)	0.288
K07	0.064 (S)	2 (S)	0.75 (S)	0.032 (S)	8 (S)	8 (S)	0.016 (S)	3 (S)	3 (S)	0.144
K08	0.064 (S)	1.5 (S)	1 (S)	0.064 (S)	8 (S)	4 (S)	0.016 (S)	4 (S)	4 (S)	>9.20
M2B	0.064 (S)	3 (S)	0.5 (S)	0.032 (S)	12 (I)	6 (S)	0.016 (S)	>256 (R)	4 (S)	1.15
UTI89	0.064 (S)	1.5 (S)	1 (S)	0.032 (S)	6 (S)	3 (S)	0.016 (S)	3 (S)	3 (S)	>9.20
ATCC 700336 (J96)	0.125 (S)	1.5 (S)	1 (S)	0.064 (S)	8 (S)	4 (S)	0.023 (S)	4 (S)	3 (S)	1.15
ATCC 700928 (CFT073)	0.094 (S)	2 (S)	1 (S)	0.064 (S)	12 (I)	4 (S)	0.023 (S)	4 (S)	4 (S)	>9.20
Median	**0.094**	**2**	**0.75**	**0.047**	**8**	**4**	**0.016**	**4**	**3**	**1.15**

Table 6.1. Minimum inhibitory concentrations of conventional antimicrobials and gallium maltolate for nine canine and human UPEC isolates

Gallium maltolate MICs were determined by broth dilution in RPMI 1640; all other MICs were determined using E-tests. Susceptibility categories are indicated in parentheses for antimicrobials with CLSI susceptibility testing interpretation guidelines.

6.4.2. **Minimum inhibitory concentrations for gallium maltolate**

The concentrations of iron and gallium in Mueller-Hinton broth prior to any addition of gallium maltolate exceeded the concentrations measured in RPMI by greater than threefold (Table 6.2.). The MICs of gallium maltolate in Mueller-Hinton broth exceeded the highest concentration evaluated (9.20 µmol/mL) for all isolates. In RPMI, gallium maltolate MICs ranged from 0.144 µmol/mL to >9.20 µmol/mL (Table 6.1.). The MICs for the conventional susceptibility testing quality control strains *Enterococcus faecalis* (ATCC 29212), *Staphylococcus aureus* (ATCC 29213) and *E. coli* (ATCC 25922) were 0.144 µmol/mL, 0.288 µmol/mL and >9.20 µmol/mL, respectively.

Elemental concentration	Cation-adjusted Mueller-Hinton II	RPMI 1640 with L-Glutamine
Gallium	0.0304 nmol/mL	<LLOQ*
Iron	4.39 nmol/mL	1.23 nmol/mL

Table 6.2. Gallium and iron concentrations measured by inductively coupled plasma-mass spectrometry in media used for determining minimum inhibitory concentrations of gallium maltolate against uropathogenic *E. coli*

*Lower limit of quantification (LLOQ) for gallium was 0.387 pmol/mL

6.4.3. **Effect of exposure time and gallium maltolate concentration on antimicrobial activity**

Bacterial counts vs. time for six isolates are shown in Figure 6.1. One isolate with MIC>9.20 µmol/mL was observed at gallium maltolate concentrations of 4.60 µmol/mL, 9.20 µmol/mL and 18.4 µmol/mL as it was impractical to evaluate growth/kill curves at greater MIC multiples.

The ABBC increased with gallium concentrations for all isolates except ATCC 700336 and M2B, but this trend was not statistically significant (p=0.3711). A 3 $\log_{10}$ reduction in bacterial concentrations was achieved within the first 24 hours for only one isolate at 10 MIC (Table 6.3). Two isolates exhibited greater than 3 $\log_{10}$ reductions in bacterial concentrations at 10 MIC at 72 hours, and a third isolate approached a 3 $\log_{10}$ decrease at 72 hours.

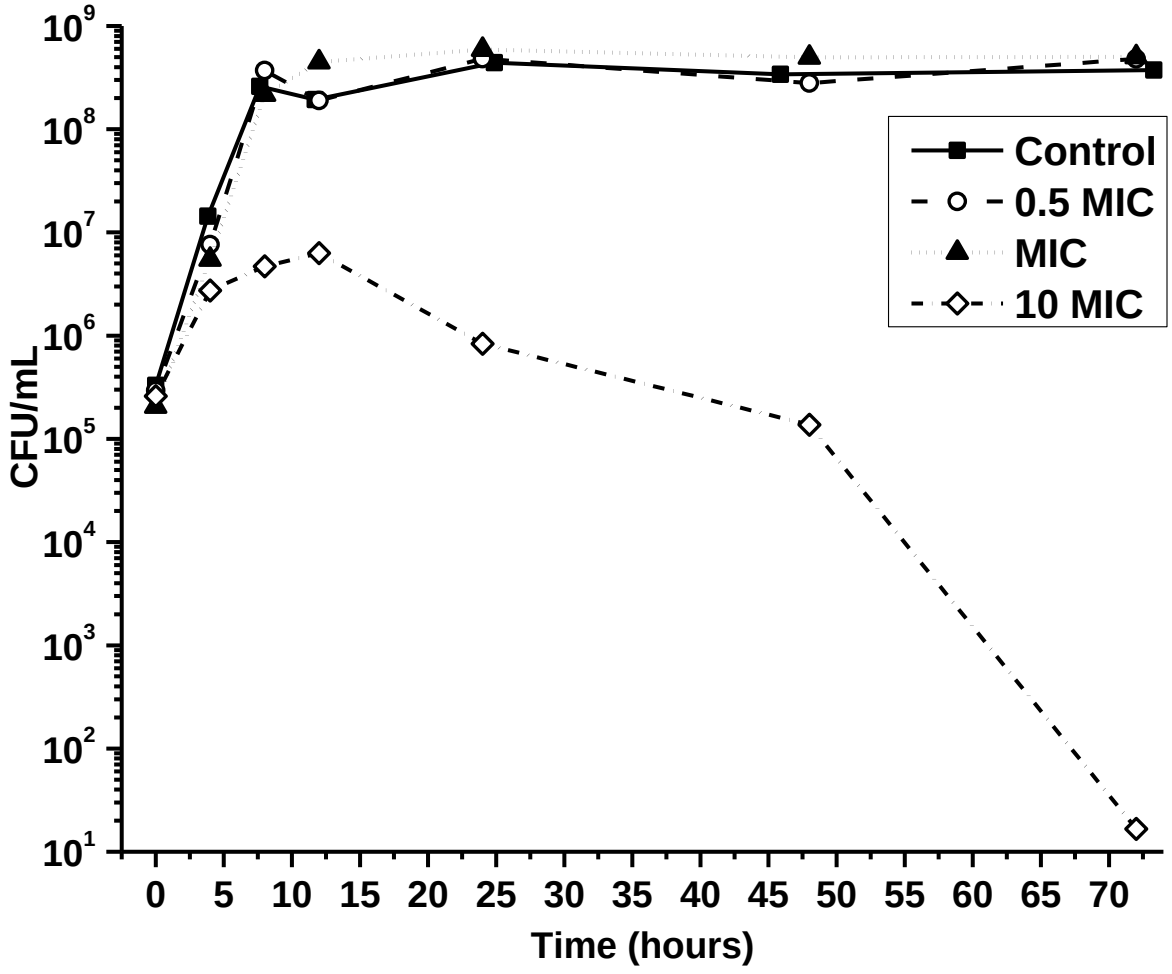

Figure 6.1. Bacterial concentration vs. time for UPEC isolate K01cultured in RPMI 1640 in the presence of increasing concentrations of gallium maltolate
Gallium maltolate MIC for this isolate was 0.288 µmol/mL.

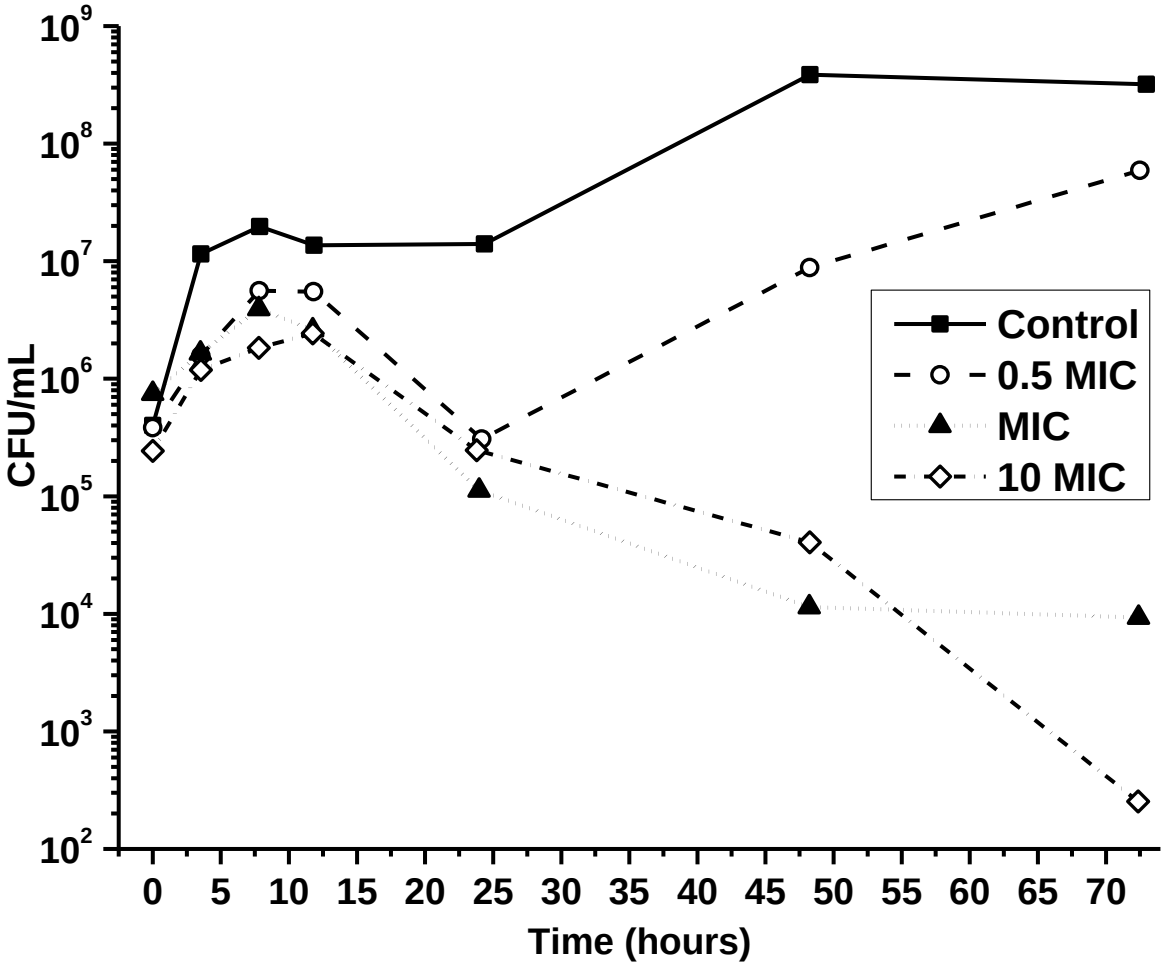

Figure 6.2. Bacterial concentration vs. time for UPEC isolate K03 cultured in RPMI 1640 in the presence of increasing concentrations of gallium maltolate
Gallium maltolate MIC for this isolate was 0.288 µmol/mL.

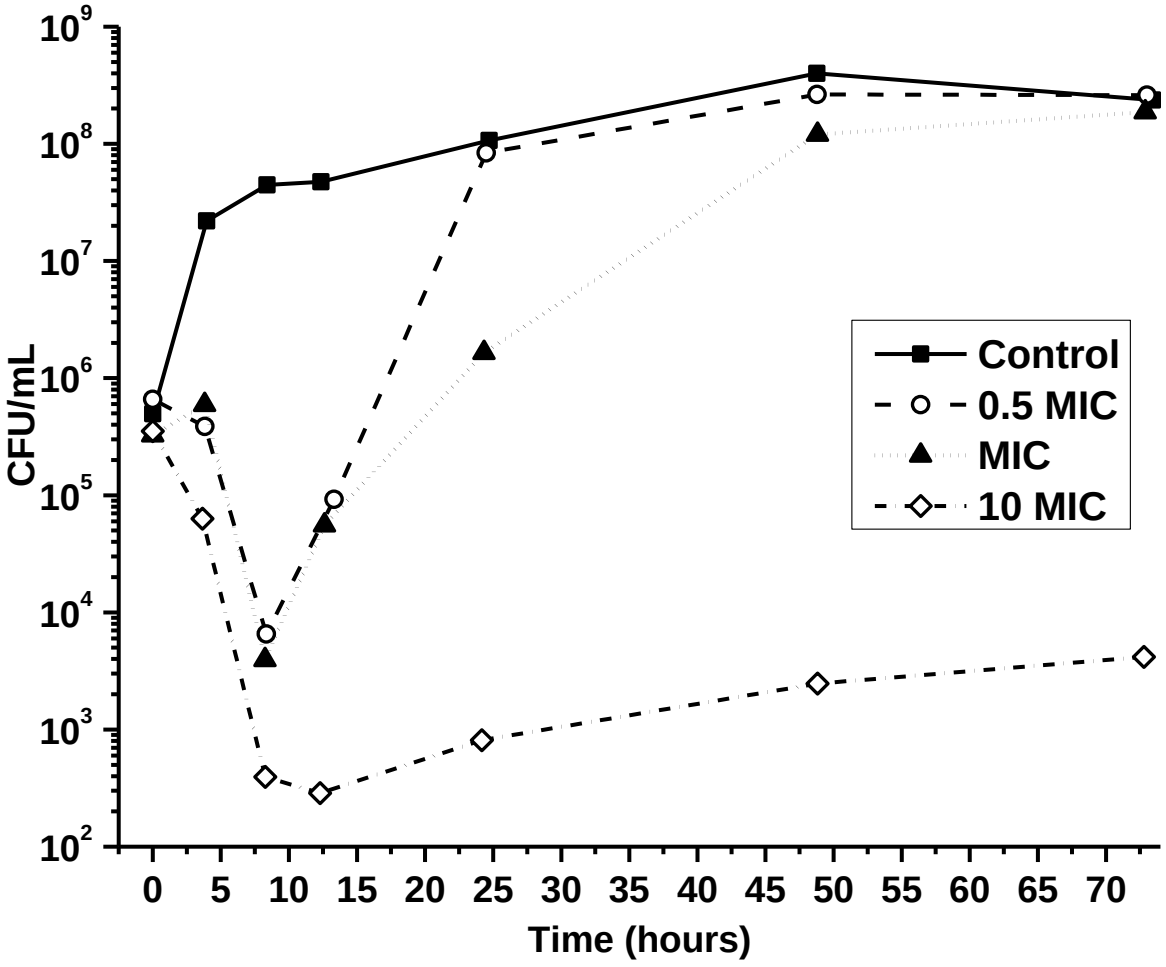

Figure 6.3. Bacterial concentration vs. time for UPEC isolate K07 cultured in RPMI 1640 in the presence of increasing concentrations of gallium maltolate
Gallium maltolate MIC for this isolate was 0.144 µmol/mL.

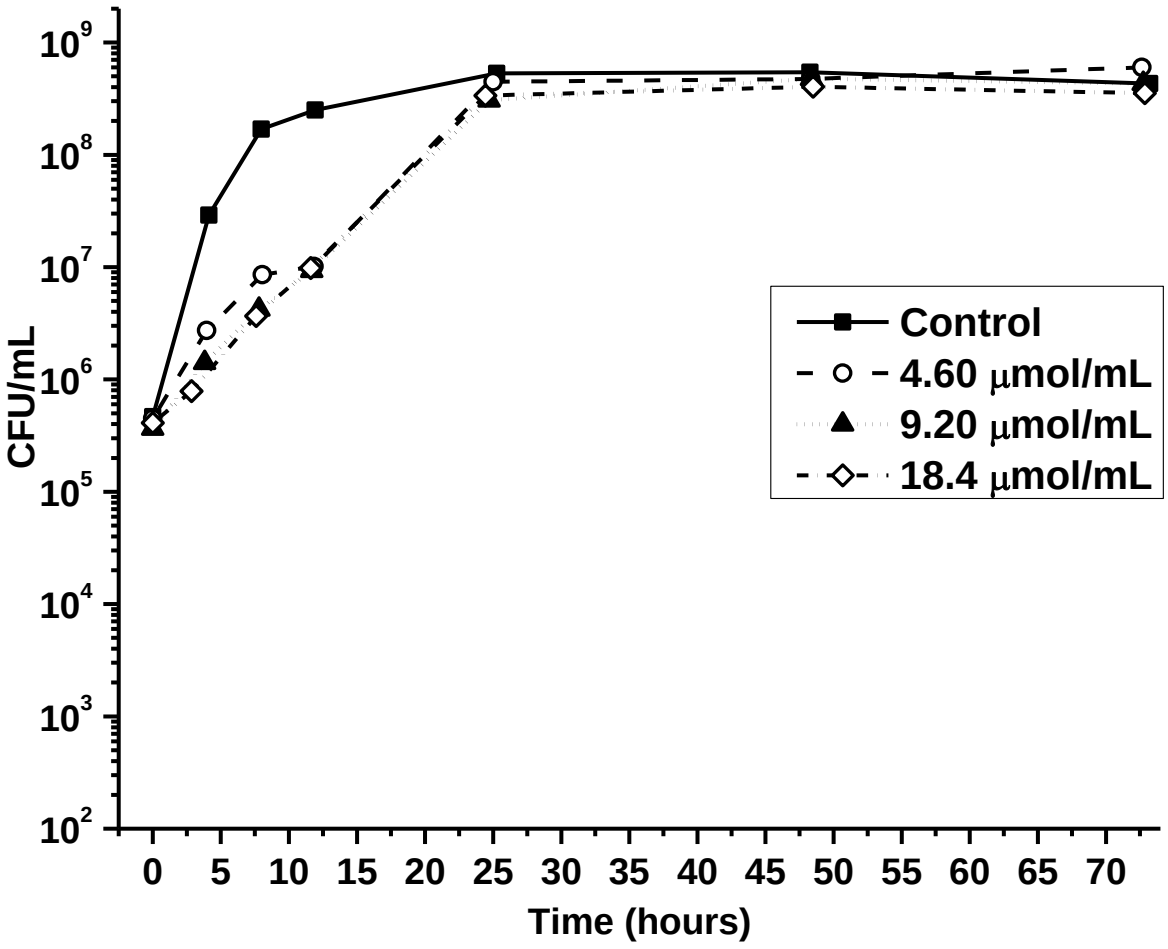

Figure 6.4. Bacterial concentration vs. time for UPEC isolate UTI89 cultured in RPMI 1640 in the presence of increasing concentrations of gallium maltolate

Gallium maltolate MIC for this isolate was >9.20 μmol/mL.

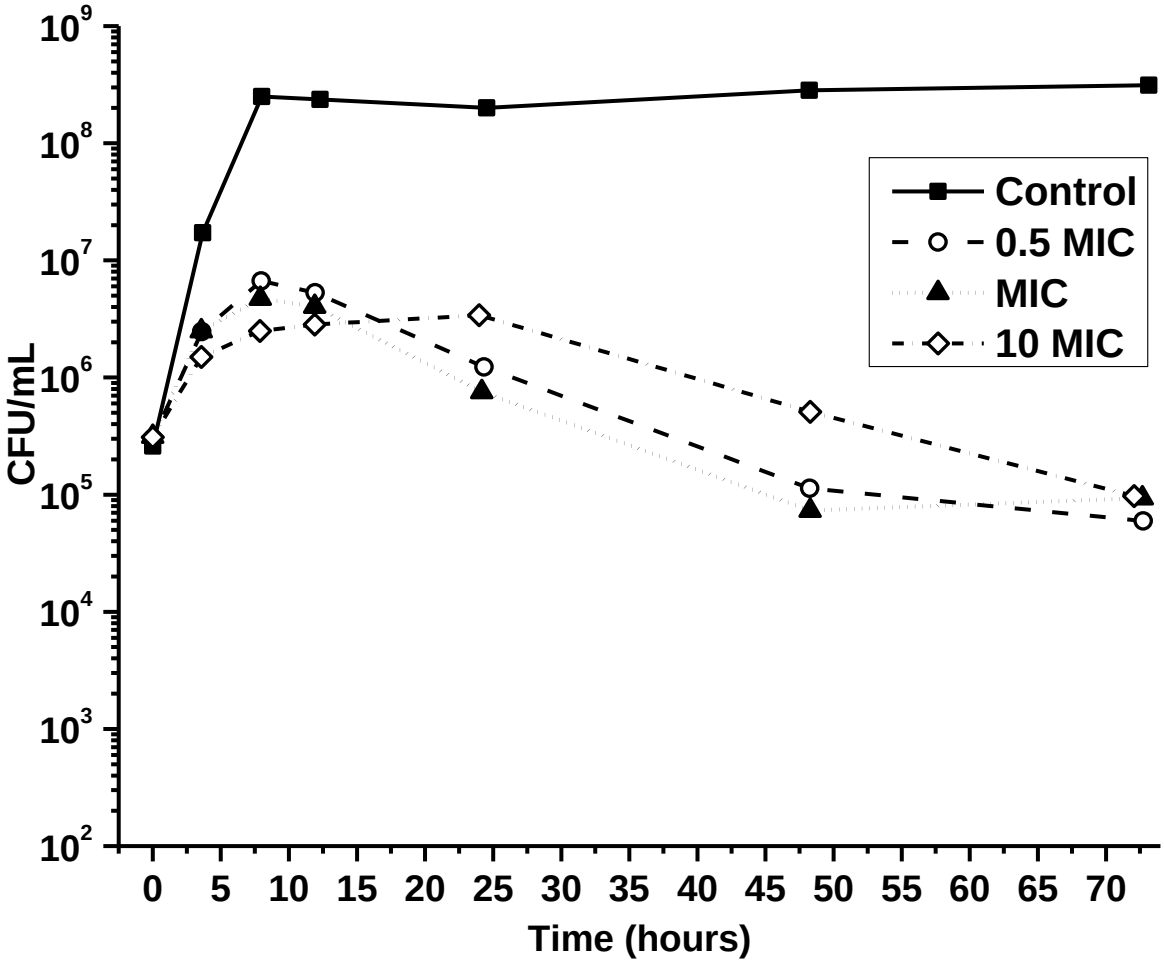

Figure 6.5. Bacterial concentration vs. time for UPEC isolate ATCC 700336 cultured in RPMI 1640 in the presence of increasing concentrations of gallium maltolate

Gallium maltolate MIC for this isolate was 1.15 µmol/mL.

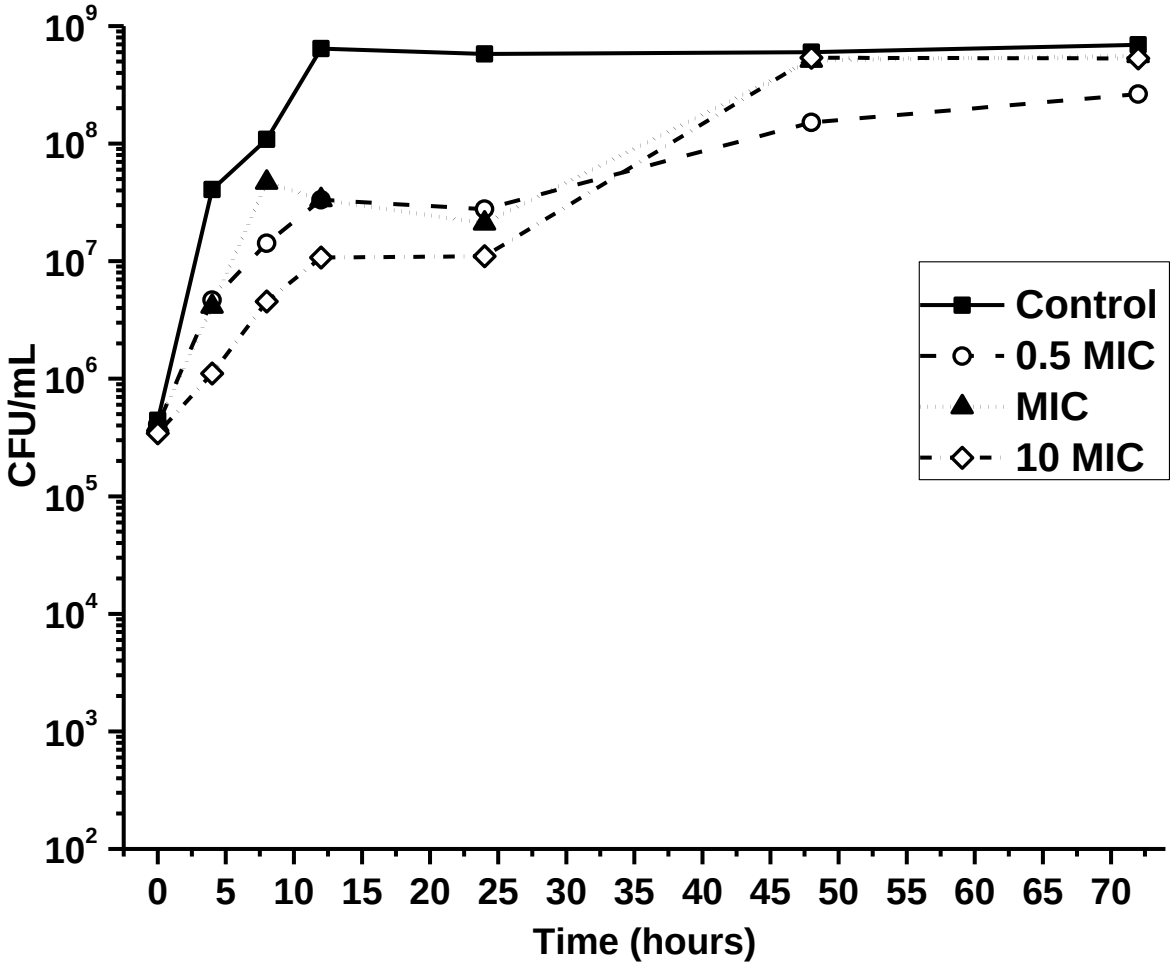

Figure 6.6. Bacterial concentration vs. time for UPEC isolate M2B cultured in RPMI 1640 in the presence of increasing concentrations of gallium maltolate

Gallium maltolate MIC for this isolate was 1.15 µmol/mL.

Isolate	MIC multiple	Maximum decrease in bacterial concentration (log CFU/mL)	Time to minimum bacterial concentration (h)	Change in log CFU/mL at 24h
K01	Control	n.d.*	-	3.12
	0.5	n.d.	-	3.22
	1	n.d.	-	3.46
	10	-4.19	72	0.506
K03	Control	n.d.	-	1.54
	0.5	-0.097	24	-0.097
	1	-1.90	72	-0.823
	10	-2.98	72	0.006
K07	Control	n.d.	-	2.33
	0.5	-2	8	2.1
	1	-1.92	8	0.703
	10	-3.09	12	-2.64
UTI89	Control	n.d.	-	3.06
	0.5	n.d.	-	3
	1	n.d.	-	2.92
	2	n.d.	-	2.91
ATCC 700336	Control	n.d.	-	2.89
	0.5	-0.701	72	0.613
	1	-0.631	48	0.381
	10	-0.503	72	1.04
M2B	Control	n.d.	-	3.12
	0.5	n.d.	-	1.83
	1	n.d.	-	1.72
	10	n.d.	-	1.51

Table 6.3. Effect of gallium maltolate exposure on bacterial concentrations after 24 hours and at the time of maximal population decrease for six UPEC isolates cultured in RPMI 1640

* n.d. signifies that no bacterial concentrations lower than the initial value were observed.

6.5. **Discussion**

Gallium maltolate exerts antimicrobial activity against UPEC in vitro, satisfying a major criterion for its development as a novel therapy for urinary tract infections. An important feature of gallium maltolate as a novel potential antimicrobial therapy is that its hypothesized mechanism of action is different from other antimicrobials currently in clinical use. Gallium inhibits the growth of *Pseudomonas aeruginosa*, *Francisella tularensis* and of *Mycobacterium avium* complex by inhibiting iron uptake, and is hypothesized to have similar effects in *Staphylococcus aureus* and *Rhodococcus equi* (Olakanmi et al., 2000; Kaneko et al., 2007; Baldoni et al., 2010; Coleman et al., 2010; Olakanmi et al., 2010). Other effects of gallium exposure on bacterial iron metabolism vary between species. Gallium exposure leads to superoxide dismutase inhibition in *F. tularensis* (Olakanmi et al., 2010). In *P. aeruginosa*, gallium exposure induces pyochelin gene expression and suppresses *pvdS* gene-controlled pathways including the synthesis of pyoverdine and its receptor (Kaneko et al., 2007). Gallium nitrate inhibits the growth of *E. coli* K12 under iron-restricted conditions and likely causes this effect by interfering with iron metabolism, but the precise mechanism is unknown (Hubbard et al., 1986).

As the primary mechanisms of action of currently available antimicrobials do not alter bacterial iron metabolism, cross-resistance between gallium compounds and conventional antimicrobials is likely rare. In this study, three isolates that were highly resistant to gallium maltolate were not classified as resistant to any of the other antimicrobial drugs evaluated, yet isolates that were classified as resistant to ciprofloxacin or ampicillin had relatively low gallium maltolate MICs. This supports the hypothesis that cross-resistance is uncommon between gallium maltolate and

conventional antimicrobials, and is consistent with the hypothesized difference in mechanism of action. As the growth of some strains was not inhibited even at high gallium maltolate concentrations, susceptibility testing will be necessary to identify infections amenable to gallium maltolate treatment in a clinical setting.

Siderophore systems contribute to gallium uptake, as enterobactin will bind gallium and the enterobactin-gallium complex is taken up by *E. coli* in vitro (Ecker et al., 1986; Emery, 1986). This process occurs at a slower rate than enterobactin-iron uptake, but it likely contributes to the moderate growth inhibition observed when *E. coli* K12 is exposed to gallium nitrate (Ecker et al., 1986). Despite the potential role of siderophores in gallium uptake, the presence of multiple siderophore systems is not a good predictor of gallium maltolate susceptibility. The effects of gallium maltolate on three well-characterized UPEC strains isolated from humans, ATCC 700336, ATCC700928 and UTI89 varied substantially, yet all three possess enterobactin, yersiniabactin and salmochelin pathways (Henderson et al., 2009). In addition to these mechanisms, ATCC 700928 and UTI89 can acquire iron via aerobactin and its receptor while ATCC 700336 (the most susceptible of these three strains) does not possess this pathway. Hence, differences in aerobactin transport capacity do not account for the differences observed in gallium maltolate susceptibility. This result suggests that gallium maltolate's antimicrobial activity at least partially arises from interference with metabolic processes other than siderophore-mediated iron uptake.

The antimicrobial activity of gallium maltolate was markedly affected by the culture medium. Although Mueller-Hinton broth is widely used for antimicrobial susceptibility testing, little

information is available about its trace element composition. The iron concentration in this batch of Mueller-Hinton broth was over three times that observed in RPMI, and may have contributed to the apparent absence of antimicrobial activity for any of these isolates in Mueller-Hinton broth. In non-uropathogenic strains of *E. coli*, high iron concentrations abolish the antimicrobial effect of gallium (Hubbard et al., 1986). This is not surprising, as gallium competes with iron for bacterial uptake in multiple bacterial species including non-uropathogenic *E. coli* (Olakanmi et al., 2000). Because of the substantial effect of medium composition on antimicrobial activity in vitro, optimization of susceptibility testing for gallium maltolate will require further characterization of gallium and iron at the site of infection. Furthermore, gallium binds readily to transferrin and other mammalian proteins that accumulate at sites of infection (Harris and Pecoraro, 1983; Groessl et al., 2009). As the potency of gallium-protein complexes is not likely identical to that of gallium maltolate, this phenomenon may also contribute to discrepancies between observations in vitro and in vivo (Kaneko et al., 2007).

For clinical use, antimicrobials are commonly classified as bactericidal or bacteriostatic depending on the magnitude of the antimicrobial effect after 24 hours of exposure. As even the highest concentrations of gallium maltolate failed to produce a 3 $\log_{10}$ reduction in bacterial numbers in all but one isolate within the first 24 hours, its activity can be classified as primarily bacteriostatic (Finberg et al., 2004). Single-point measures such as time to a specific reduction in bacterial numbers allow comparison between isolates, but cannot take into account bacterial re-growth or prolonged growth inhibition, both of which can be clinically important (Firsov et al., 1997). Among the six isolates studied here, there were instances of bacterial growth followed by a delayed decline in bacterial numbers, early and prolonged killing, and marked early killing

followed by re-growth. With the exception of K01, the growth of all isolates was inhibited in the first 24 hours following exposure to gallium maltolate at any concentration. Area-based measures extract information from all the data points collected and can account for strain-specific growth characteristics, re-growth and duration of effect. The ABBC meets these criteria and can be used to summarize and compare data from multiple isolates when the data collection period is constant (Firsov et al., 1997).

To assist clinicians in establishing dosing regimens, antimicrobial activity is often classified as time-dependent or concentration-dependent based on time-kill data. Because this information is typically available only from a limited number of bacterial isolates and not for clinical strains isolated at diagnostic laboratories, clinicians must rely on published data. Using information obtained from multiple isolates may increase the likelihood that the selected dosing regimen achieves therapeutic success, and quantitative measures of antimicrobial activity such as ABBC facilitate this process. While the activity of all antimicrobial compounds is time- and concentration-dependent to some extent, our inability to demonstrate a statistically significant effect of MIC multiplier on ABBC in this experiment suggests that gallium maltolate's antimicrobial activity is primarily time-dependent.

The gallium maltolate MICs observed for UPEC in this study are markedly greater than gallium concentrations observed in plasma from dogs, horses and humans, suggesting that concentrations in vivo may be insufficient to produce clinically useful antimicrobial effects (Bernstein et al., 2000; Arnold et al., 2010; Chaffin et al., 2010). However, gallium is used in medical imaging because it accumulates at sites of inflammation, which indicates that tissue concentrations can

significantly exceed blood gallium concentrations (Tsan, 1985; Weiner, 1996). The distribution of gallium within target tissues and transitional epithelial cells during infection may produce local gallium concentrations in the ranges of the MICs measured in this study. It is also possible that bacterial susceptibility to gallium exposure in vivo differs substantially from in vitro observations. While the MIC is one of the most commonly used antimicrobial pharmacodynamic metrics, it may be a poor predictor of activity against UPEC in vivo because the UPEC proteome differs substantially between in vitro and in vivo conditions (Reigstad et al., 2007).

The long half-lives observed for gallium in dogs, horses and people are well-suited for clinical use of the time-dependent, bacteriostatic antimicrobial gallium maltolate (Bernstein et al., 2000; Martens et al., 2007; Arnold et al., 2010). Further investigation of the distribution of gallium within target tissues and cells is indicated to better predict the potential utility of gallium maltolate as a novel therapy for urinary tract infections. In addition, conventional pharmacokinetic studies and characterization of its mechanism of antimicrobial action will be useful to predict the potential for emerging resistance and to optimize the clinical use of gallium maltolate.

6.6. **Conclusion**

Gallium maltolate exerts antimicrobial activity against this collection of UPEC in vitro in a primarily bacteriostatic, time-dependent manner and thus may be useful for treating urinary tract infections caused by UPEC. While the MICs measured in this study exceed plasma concentrations of gallium observed in horses, dogs and humans following gallium maltolate

administration, further research is required to characterize the relationship between gallium concentration and antimicrobial activity in vivo.

Chapter 7. Pharmacokinetics of gallium after oral administration of gallium maltolate to mice with and without urinary tract infections

Relationship of this study to the dissertation:

The results described in Chapters 5 and 6, namely, that gallium arrives at the bladder mucosa following oral administration of gallium maltolate and that gallium maltolate exerts antimicrobial activity against uropathogenic *E. coli*, suggest that this compound could potentially be a clinically useful antimicrobial therapy for urinary tract infections. Characterizing the pharmacokinetics of gallium maltolate in the presence and absence of urinary tract infection can identify whether dosing regimens must be adjusted during infection to avoid treatment failure or toxicity. Pharmacokinetic parameter estimates are also useful for selecting dosing regimens for efficacy trials in animal models, particularly when minimum inhibitory concentration data are available (as in Chapter 6). In the case of gallium maltolate, the results reported in this chapter indicated that peak whole blood and tissue gallium concentrations were substantially lower than the minimum inhibitory concentrations observed for uropathogenic *E. coli* in vitro. This led to the decision to use a higher dose for the efficacy trials in Chapter 8.

7.1. **Abstract**

Uropathogenic strains of *Escherichia coli* are the most common cause of urinary tract infections in dogs and humans. The increasing prevalence of antimicrobial resistance among these pathogens has created a need for new antimicrobial therapies. Gallium maltolate is of particular interest, as it exerts antimicrobial activity against uropathogenic *E. coli* in vitro and because its putative mechanism of action differs from those of all conventional antimicrobials. The pharmacokinetics of orally administered gallium maltolate were investigated in healthy mice and in a murine model of urinary tract infection caused by uropathogenic *E. coli*. Following administration of a single dose of gallium maltolate at 100 mg/kg, gallium exposures were greatest in kidney, followed by bladder and blood. Gallium exposure in the bladder was significantly greater in infected mice relative to healthy mice. The terminal first-order rate constant in the bladder was smaller in infected mice relative to healthy mice, with a correspondingly greater half-life (80.0 and 46.4 hours, respectively). This difference approached statistical significance. Maximum blood gallium concentration and time of maximum concentration were not influenced by infection status. While there was a trend toward longer terminal half-lives and decreased oral clearance in blood from infected mice, no statistically significant differences in pharmacokinetic parameter estimates were observed in blood or kidney samples. Although the long terminal half-life of gallium is well-suited to its time-dependent antimicrobial activity against uropathogenic *E. coli*, none of the tissues achieved gallium concentrations equal to or greater than the minimum inhibitory concentrations observed in vitro. Therapeutic efficacy is anticipated only if in vivo conditions differ substantially from laboratory conditions used to measure minimum inhibitory concentrations. Should this occur, dosing

regimens must be designed to rapidly achieve therapeutic gallium concentrations while avoiding excessive accumulation and potential toxicity.

7.2. **Introduction**

Uropathogenic strains of *Escherichia coli* (UPEC) are the most common cause of urinary tract infections in humans and dogs (Zhanel et al., 2006; Ball et al., 2008a; Karlowsky et al., 2011). The ability of these pathogens to invade urothelial cells and evade many conventional antimicrobials and the increasing prevalence of antimicrobial resistance restrict the treatment options available (Schilling et al., 2002; Mysorekar and Hultgren, 2006; Blango and Mulvey, 2010). Gallium compounds such as gallium maltolate may be useful as potential new therapeutic agents as they disrupt bacterial iron metabolism in a variety of bacterial species and exert antimicrobial activity against UPEC in vitro (Chapter 3) (Olakanmi et al., 2000; DeLeon et al., 2009; Baldoni et al., 2010; Olakanmi et al., 2010).

Gallium accumulates at sites of inflammation, and this feature is exploited when gallium radioisotopes are used as contrast agents for medical imaging (Tsan, 1985; Yeh et al., 2011). This characteristic may also produce elevated gallium concentrations in the urinary tract during therapy, potentially contributing to antimicrobial efficacy in vivo. It may also alter systemic pharmacokinetics during infection, potentially leading to longer half-lives and accumulation upon multiple dosing. If gallium concentrations in blood or sensitive tissues are affected, dosing regimens based on data from healthy individuals may place diseased patients at risk of toxicity.

The pharmacokinetics of gallium in the urinary tract and the effect of urinary tract infection on gallium pharmacokinetics are unknown but will be key determinants of the clinical utility of gallium maltolate as an antimicrobial therapy. The mouse model of urinary tract infection is well-suited for investigating the effect of disease on gallium pharmacokinetics, as the pathogenesis of UPEC infection in mice is similar to that observed in humans (Mulvey et al., 1998; Rosen et al., 2007). Furthermore, the model has been used to investigate the effects of conventional antimicrobial therapy on urothelial UPEC infection (Blango and Mulvey, 2010). The objectives of this study were to characterize the pharmacokinetics of gallium in the urinary tract following oral administration of gallium maltolate to mice, and to determine the effect of urinary tract infection on gallium pharmacokinetics in blood and in the urinary tract. A mouse model of urinary tract infection using a type strain of UPEC (J96, ATCC 700336) was used to investigate the latter (Melkerson-Watson et al., 2000).

7.3. **Methods**

7.3.1. **Escherichia coli**

Uropathogenic *E. coli* ATCC 700336 was sub-cultured on TSA agar with 5% sheep blood (Becton, Dickenson and Company, Sparks, MD) prior to suspension in physiologic saline solution for intravesical infusion.

7.3.2. **Gallium maltolate solution**

Gallium maltolate solutions were prepared immediately prior to administration as described in 6.3.2.

7.3.3. **Mice**

This work was approved by the University of Saskatchewan's Animal Research Ethics Board, and adhered to the Canadian Council on Animal Care guidelines for humane animal use. Mice were maintained with tap water and a commercial mouse ration containing 270 ppm iron (Laboratory Rodent Diet 5001, PMI LabDiet, St. Louis, MO, USA) ad libitum prior to and during the experiments. Female, 8-10 week old C57BL/6 mice were randomly allocated into two groups of 60. All mice were weighed and anesthetized with isoflurane for ear punching 48 hours prior to administration of gallium maltolate. Mice in the "infected" group were infected with ATCC 700336 as described in 6.3.3. Gallium maltolate was administered by gavage at 100 mg/kg.

7.3.4. **Sampling**

Tissues were collected in a destructive sampling scheme at 2, 4, 8, 12, 24 hours after dosing, and at 2, 3, 5, 7, 10, and 15 days after dosing. Five mice from each group were euthanized with isoflurane at each sampling point except for three points where only four mice were available due to mortality losses.

Whole blood, bladder and kidney samples from each mouse were stored at -20°C and submitted to the Prairie Diagnostic Services Toxicology laboratory (University of Saskatchewan, Saskatoon, SK) for analysis. Gallium concentrations were measured using inductively coupled plasma-mass spectrometry according to a procedure validated in rabbit blood with lower limit of quantification 0.387 pmol/mL.

7.3.5. **Data analysis**

Data were pooled for non-compartmental analysis in WinNonLin 5.3 using the "sparse sampling" option. Where gallium concentrations were quantifiable in at least two animals sampled at any time point, concentrations less than the lower limit of quantification were estimated using Ganser and Hewett's method for β-substitution (Ganser and Hewett, 2010). If fewer than two mice had quantifiable gallium concentrations at a particular time point, concentrations below the lower limit of quantification were assigned a value of zero.

A commercial statistical software package (Stata/IC 10.1 for Windows, StataCorp, College Station, TX, USA) was used for hypothesis testing and non-linear regression analysis. Area under the curve estimates for infected and healthy mice were tested for equality according to Bailer's method, using the contrast

$$AUC_{\text{tissue, infected mice}} - AUC_{\text{tissue, healthy mice}} = 0 \text{ (Bailer, 1988).}$$

Maximum gallium concentrations were compared with the Mann-Whitney test. Terminal first-order rate constant were estimated by fitting an exponential decay model to the terminal portion of the time vs. concentration curve by non-linear least squares regression. The contribution of infection status to the model fit was evaluated using a t-test for a coefficient indicating infection status:

$$C_t = C_0 e^{-(\lambda z + \text{status} * \text{coefficient})t} \quad (7.1)$$

where C_t indicates gallium concentration in the selected matrix at time t, C_0 indicates the gallium concentration measured at the first time point included in the analysis (72 hours for blood and kidney; 48 hours for bladder), "status" is a dummy variable indicating infection status (a value of 1 was assigned for infected animals and 0 for healthy animals), and "coefficient" was the

parameter estimated to adjust for potential differences in the terminal rate constant (λ_z) between infected and healthy mice.

7.4. **Results**

Three infected mice developed pyelonephritis and septicemia within 24 hours of infection (prior to gallium maltolate administration) and were withdrawn from the study. Consequently, data were available for only four infected mice at 4 hours, 8 hours and 10 days post-treatment. Pyelonephritis and septicemia were diagnosed based on gross necropsy lesions and positive cultures for *E. coli* in liver, spleen and kidney.

Plots of gallium concentration vs. time and pharmacokinetic parameter estimates in blood, kidney and bladder are presented in figures and tables 7.1, 7.2, and 7.3 respectively. Gallium was not detected in samples collected immediately prior to administration of gallium maltolate. By two hours post-dose, gallium was detected in all tissues. Maximum gallium concentrations in whole blood were achieved by 4 hours post-dose in both groups (Figure 7.1 and Table 7.1). Peak concentrations in tissue samples occurred at or after the time of maximum concentrations in whole blood (Figures and Tables 7.2 and 7.3). Gallium persisted in blood, bladder and kidney from both groups at 15 days post-dose (Figures and Tables 7.1 to 7.3).

Maximum gallium concentrations in whole blood, kidney and bladder did not differ between healthy and infected mice (Figure 7.1 and Tables 7.1, 7.2, and 7.3). Gallium exposure was greatest in kidney, followed by bladder and then blood. The $AUC_{0\text{-}360}$ values in whole blood and kidney were not significantly different between healthy and infected mice (Figures 7.1, 7.2 and

Tables 7.1 and 7.2). In contrast, $AUC_{0\text{-}360}$ in bladder was increased by roughly two-fold in infected mice.

The estimated first order terminal rate constants for all tissues were greater in healthy mice compared with infected mice, with a corresponding difference in terminal half-life (Figures 7.1, 7.2 and 7.3). These effects were not statistically significant, although the difference approached significance in bladder. Although maximum gallium concentrations in bladder tissue occurred later in infected mice than in healthy mice, the concentrations were not significantly different between the two groups. Gallium exposure (represented by $AUC_{0\text{-}360}$) did not differ between healthy and infected mice in the kidney, but was significantly greater in bladder among infected mice.

	Healthy	Infected	p-value
T_{max} (h)	4	4	
C_{max} (nmol·mL^{-1})	4.46 (2.75 – 6.18)	4.80 (2.53 – 7.06)	>0.999
AUC_{0-360} (h·nmol·mL^{-1})	94.63 (78.18 – 111.08)	117.51 (82.63 – 152.39)	0.2449
$AUC_{0-\infty}$ (h·nmol·mL^{-1})	95.45	120.86	
% of $AUC_{0-\infty}$ extrapolated	1.24	4.22	
Cl/F (L·h^{-1}·kg^{-1})	15.03	11.87	
MRT (h)	36.2	45.0	
V_{ss}/F (L·kg^{-1})	916.2	849.6	
λ_z (h^{-1})	0.0170	0.0106	0.065
$t_{1/2(z)}$ (h)	40.9	65.2	

Table 7.1. Pharmacokinetic parameter estimates for gallium in whole blood from destructive sampling of 52 mice with urinary tract infections and 55 mice without urinary tract infections following administration of gallium maltolate by gavage at 100 mg/kg
Values in parentheses indicate 95% confidence intervals.

	Healthy	Infected	p-value
T_{max} (h)	4	8	
C_{max} (nmol·g^{-1})	2.81 (1.93 – 3.70)	3.98 (1.24 – 6.73)	>0.999
AUC_{0-360} (h·nmol·g^{-1})	239.33 (186.48 – 292.19)	526.55 (362.09 – 691.01)	0.0011
λ_z (h^{-1})	0.0149	0.00866	0.054
$t_{1/2(z)}$ (h)	46.4	80.0	

Table 7.2. Pharmacokinetic parameter estimates for gallium in bladder from destructive sampling of 52 mice with urinary tract infections and 55 mice without urinary tract infections following administration of gallium maltolate by gavage at 100 mg/kg
Values in parentheses indicate 95% confidence intervals.

	Healthy	Infected	p-value
T_{max} (h)	12	48	
C_{max} (nmol·g^{-1})	3.32 (1.21 – 5.43)	4.87 (-0.11 – 9.86)	>0.999
AUC_{0-360} (h·nmol·g^{-1})	703.81 (605.99 –801.62)	778.54 (594.36 – 962.72)	0.4824
λ_z (h^{-1})	0.00150	0.00138	0.869
$t_{1/2(z)}$ (h)	462	501	

Table 7.3. Pharmacokinetic parameter estimates for gallium in kidney from destructive sampling of 52 mice with urinary tract infections and 55 mice without urinary tract infections following administration of gallium maltolate by gavage at 100 mg/kg

Values in parentheses indicate 95% confidence intervals.

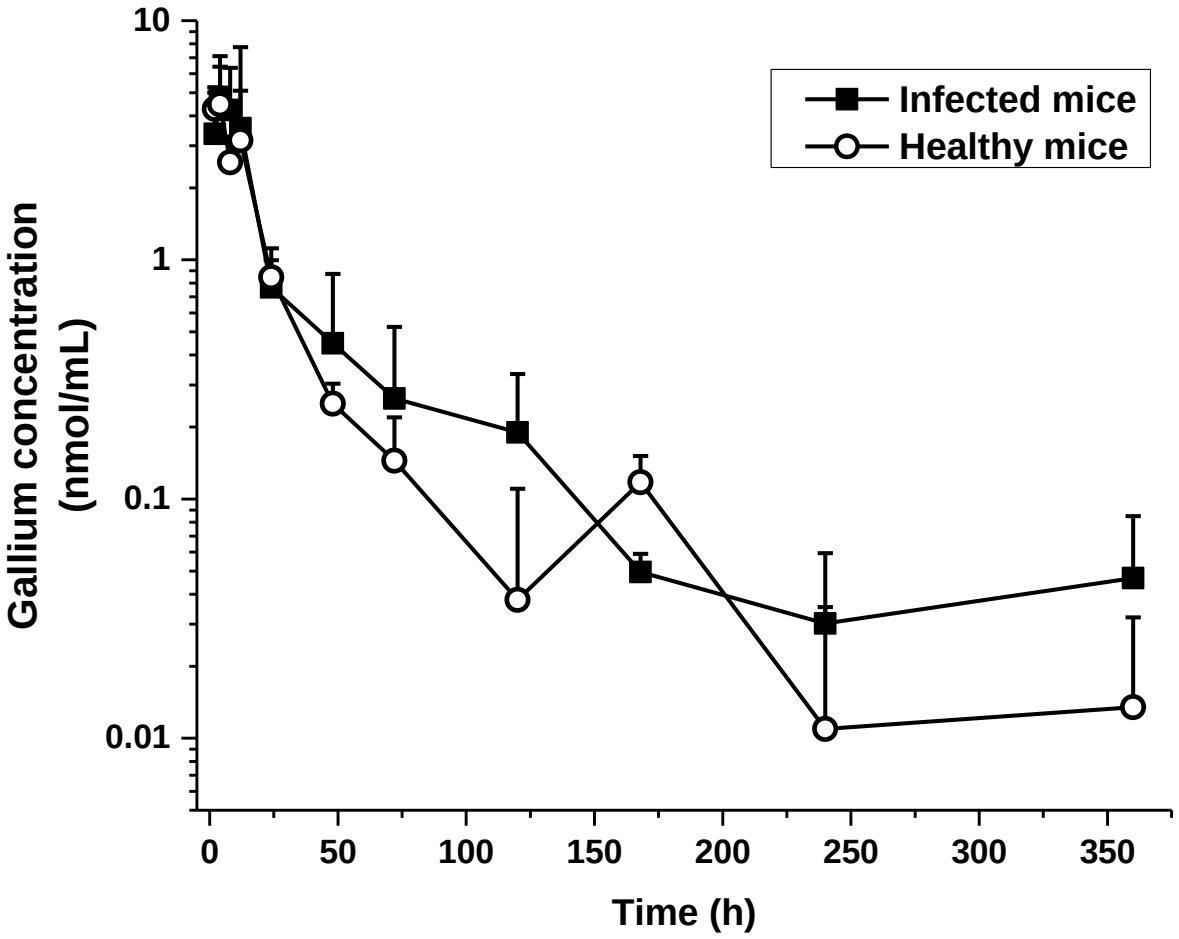

Figure 7.1. Gallium concentration vs. time in whole blood from destructive sampling of 52 mice with urinary tract infections and 55 mice without urinary tract infections following administration of gallium maltolate by gavage at 100 mg/kg

Data points and error bars indicate mean + standard deviation. Five mice from each group were sampled at every time point except for 4, 8 and 10 hours post-dosing where four infected mice and five healthy mice were sampled.

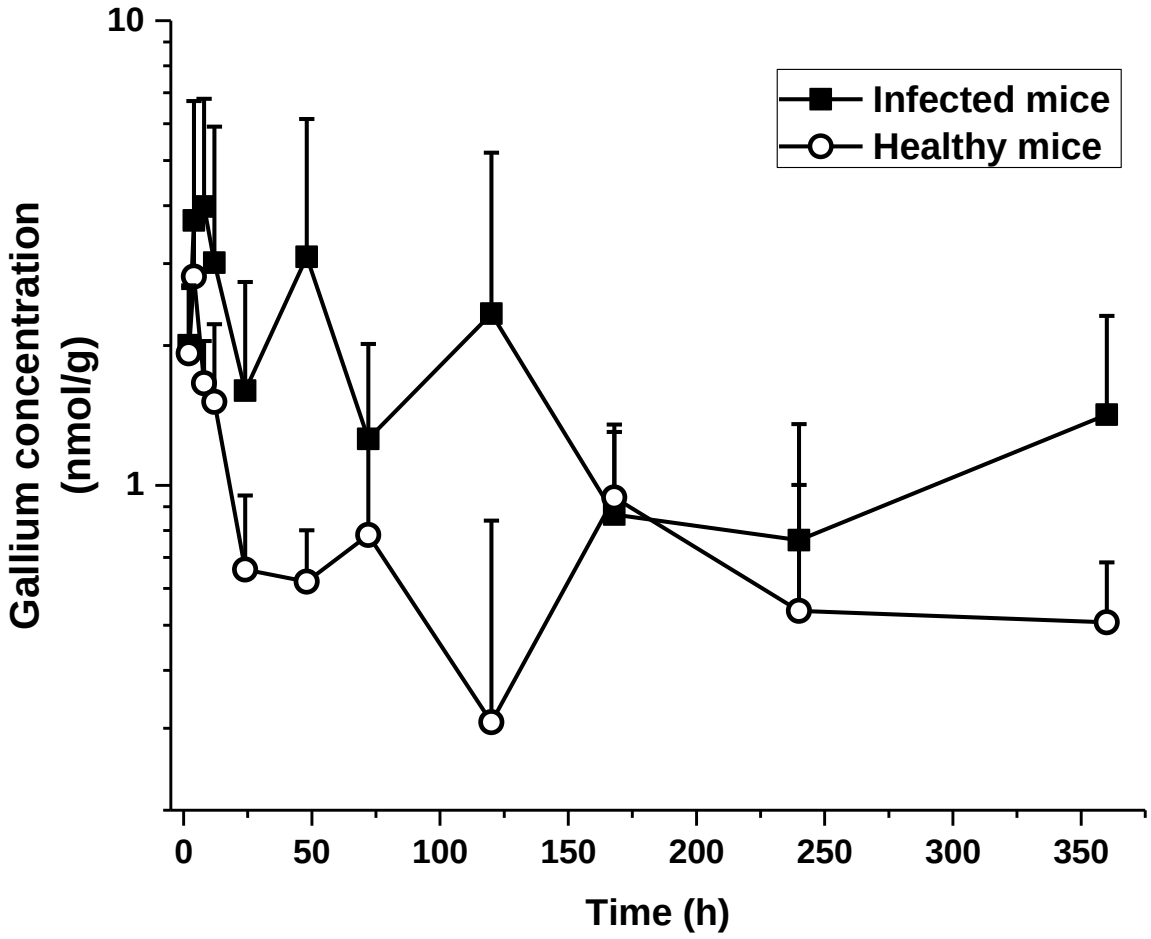

Figure 7.2. Gallium concentration vs. time in homogenized bladder from destructive sampling of 52 mice with urinary tract infections and 55 mice without urinary tract infections following administration of gallium maltolate by gavage at 100 mg/kg

Data points and error bars indicate mean + standard deviation. Five mice from each group were sampled at every time point except for 4, 8 and 10 hours post-dosing where four infected mice and five healthy mice were sampled.

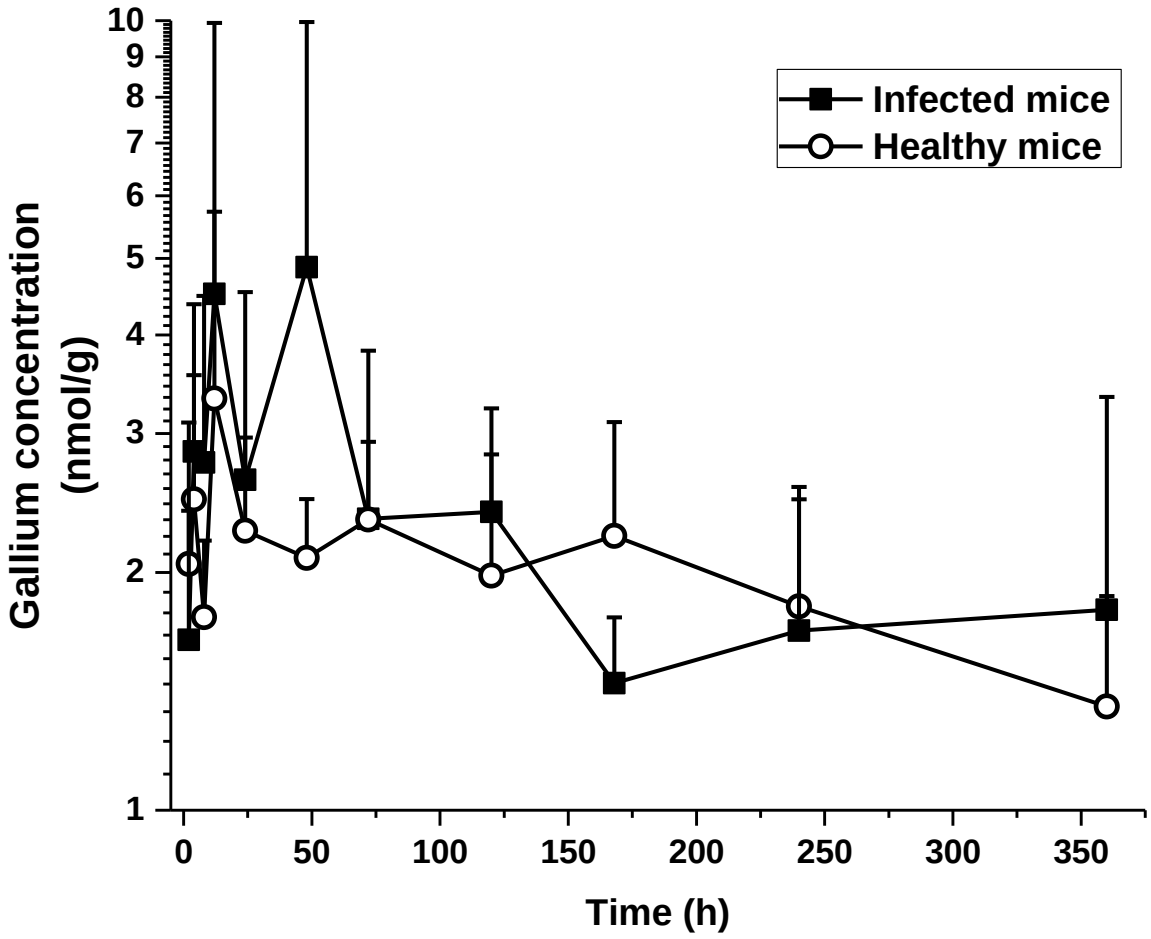

Figure 7.3. Gallium concentration vs. time in homogenized kidney from destructive sampling of 52 mice with urinary tract infections and 55 mice without urinary tract infections following administration of gallium maltolate by gavage at 100 mg/kg

Data points and error bars indicate mean + standard deviation. Five mice from each group were sampled at every time point except for 4, 8 and 10 hours post-dosing where four infected mice and five healthy mice were sampled.

7.5. **Discussion**

Successful antimicrobial therapy requires maintenance of therapeutic concentrations at the site of action for a sufficient period to inhibit bacterial growth or to kill bacterial cells. Combined with pharmacodynamic data, pharmacokinetic parameter estimates are used to design dosing regimens. This process is complicated when disease states influence pharmacokinetics because the parameter estimates are frequently obtained from healthy individuals. Although gallium exposure in the bladder was statistically significantly greater during infection, no statistically significant difference between infected and healthy mice was observed in this study for systemic and renal gallium exposure. This observation is likely related to the very small contribution of the bladder to body tissue mass (Gibaldi and Koup, 1981). This will necessarily influence experimental considerations for investigating toxicity and therapeutic efficacy. Pharmacokinetic data from bladder samples during infection will likely be of higher value for predicting therapeutic outcomes than blood or plasma concentration data. In contrast, systemic toxicity risks related to blood or plasma gallium concentrations may not change substantially during urinary tract infection. The persistence of gallium in the kidney merits particular attention as accumulation may lead to nephrotoxicity, one of the most common adverse effects of gallium administration (Bernstein, 1998; Leyland-Jones, 2004).

As the gastrointestinal transit time in mice is less than 24 hours, the terminal half-life observed for gallium in whole blood in this study is unlikely an artifact of absorption processes (Thornton et al., 2011). The long terminal half-life of gallium in blood combined with slow elimination from bladder and kidney suggests that systemic gallium elimination is limited by gallium re-distribution to blood from tissues. As a long terminal half-life is accompanied by a slow

approach to steady state, dosing regimens must be designed accordingly (Toutain and Bousquet-Melou, 2004c). This may include using a loading dose or limiting accumulation by adjusting dosing intervals or duration of therapy. It is possible that prolonged blood sampling along with very sensitive analytical techniques could reveal an additional elimination phase with a very small elimination rate constant. The clinical relevance of such an elimination phase is limited, as less than 2% of the area under the curve for whole blood from healthy mice is extrapolated using the present data set (Toutain and Bousquet-Melou, 2004c). However, it may be important if gallium accumulates in tissues that are susceptible to gallium toxicity.

The maximum blood gallium concentrations observed in this study differ substantially from findings in other species after administration of gallium maltolate dissolved in distilled water (Bernstein et al., 2000; Harrington et al., 2006; Martens et al., 2007). When gallium maltolate was administered intragastrically to foals at 20 mg/kg, the maximum serum concentration exceeded the maximum blood concentrations observed in the present study by over three-fold (Martens et al., 2007). Considering that gallium is minimally distributed into erythrocytes, the concentration observed in foals exceeds those observed in mice in the present study, despite a five-fold difference in bodyweight-normalized dose (Bernstein, 1998). Oral administration of gallium maltolate to beagle dogs at 10 mg/kg yielded maximum plasma concentrations approximately 1.5 times those observed in serum from foals treated with 20 mg/kg, but this effect may be related to a loss of protein-bound gallium during serum separation (Bernstein et al., 2000). As gallium maltolate was administered orally in every case, the differences in maximum concentrations achieved could have arisen from species differences in bioavailability, protein binding in blood and tissues, or in systemic clearance (Toutain and Bousquet-Melou,

2004d; Toutain and Bousquet-Melou, 2004b; Toutain and Bousquet-Melou, 2004a). This suggests that inter-species scaling based on bodyweight may be inappropriate for gallium maltolate pharmacokinetic parameter estimates.

The lack of effect of infection on C_{max}, T_{max}, AUC_{0-360} and the observed terminal first-order rate constant suggests that bioavailability is also minimally affected by urinary tract infection. However, altered gallium bioavailability due to an interaction with dietary iron may have contributed to the disparity in gallium concentrations in blood and plasma of mice in the present study and in previously published work (Harrington et al., 2006). Previous studies used mice fed iron-restricted diets with less than 25% of the iron concentration of the standard diet used in the present experiment, though in all cases dietary iron concentrations exceeded recommended minimum values (National Research Council Subcommittee on Laboratory Animal Nutrition, 1995; Harrington et al., 2006). Duodenal non-heme iron uptake is transcellular and requires reduction of iron (III) to iron (II) by intraluminal ferroreductases with subsequent transport through SLC11A2 (divalent metal transporter-1) (MacKenzie et al., 2008). As SLC11A2 will not transport iron (III), it is unlikely that it would transport gallium (III) or contribute to a potential iron-gallium interaction (Garrick et al., 2006). Non-specific transport of gallium by heme carrier protein-1 could account for an interaction between dietary heme iron and gallium maltolate, but the affinity of this transporter for gallium compounds is unknown (MacKenzie et al., 2008). As iron deficiency is not anticipated in most ambulatory patients with urinary tract infections, non-iron-deficient mice may provide information that is more relevant to the ultimate clinical application of gallium maltolate. Further investigation to elucidate the mechanism of gallium uptake from the gastrointestinal tract and to characterize the potential for interaction with food,

mineral supplements and other drugs will be critical for optimizing the clinical use of gallium maltolate.

An important limitation of this study is that gallium concentrations were quantified using an inductively coupled plasma-mass spectrometry method that detects elemental gallium. Consequently, the gallium compounds in blood and tissues could not be distinguished or identified and remain unknown. Similar limitations have affected previous investigations of gallium pharmacokinetics following oral administration of gallium maltolate (Bernstein et al., 2000; Martens et al., 2007; Arnold et al., 2010). This limitation has precluded investigation of the pharmacokinetics and bioavailability of gallium maltolate per se (Toutain and Bousquet-Melou, 2004a). However, if gallium compounds formed in vivo after gallium maltolate administration are responsible for pharmacological and toxicological effects, then the true bioavailability of gallium maltolate may be of limited importance. Furthermore, if gallium maltolate is not the predominant form of gallium in vivo, then in vitro susceptibility testing using gallium maltolate is of limited value for predicting therapeutic outcomes. Future research should identify which gallium compounds are present in the body following gallium maltolate administration and lead to investigation of the relevant pharmacokinetic characteristics, particularly bioavailability.

The long terminal half-life of gallium in target tissues and blood is compatible with convenient dosing regimens and well-suited to its time-dependent antimicrobial activity. In spite of these favourable characteristics, the mismatch between gallium concentrations in vivo and minimum inhibitory concentrations suggests that therapeutic outcomes may be disappointing.

Assuming that gallium exhibits linear pharmacokinetics over a wide range of concentrations, it could be impractical to administer sufficiently large doses of gallium maltolate to produce a therapeutic benefit. The lowest minimum inhibitory concentration observed for gallium maltolate against uropathogenic *E. coli* (concentration measured on a gallium basis) exceeds the maximum gallium concentrations in any tissue type by greater than an order of magnitude (Chapter 3). Multiple dosing regimens with daily administration would lead to accumulation, but the long terminal half-life dictates a slow approach to steady state. Consequently, a loading dose with subsequent maintenance doses would be indicated to achieve target concentrations within a reasonable time. This approach assumes that gallium exhibits linear pharmacokinetics over a wide range of doses and concentrations, and that it is practical to deliver the large quantity of gallium maltolate that would be necessary as a loading dose. Under linear conditions, approximately 3.6 g of gallium maltolate per kilogram of bodyweight would be required to achieve bladder gallium concentrations commensurate with the lowest minimum inhibitory concentration observed in vitro (Chapter 3). Considering its solubility limit of 24 μmol/mL, the volume of an aqueous solution for oral administration would be impractical as a single dose (336 mL per kilogram of body weight) (Bernstein et al., 2000). Solid dosage forms or suspensions containing higher concentrations of gallium maltolate could deliver sufficient quantities in a practical volume, but solubility limitations would likely hinder dissolution and bioavailability. Dose magnitude may also be limited by adverse effects at high gallium concentrations. The limited toxicology data available for gallium maltolate precludes any prediction of whether such large doses could be administered safely.

If gallium achieves disproportionately high concentrations in intracellular bacterial communities, concentrations in homogenized bladder may not accurately predict bacterial gallium exposure. Should this be the case, gallium maltolate treatment could yield a therapeutic effect in disease models in spite of achieving relatively low gallium concentrations in homogenized tissues. Furthermore, UPEC metabolism and activity change substantially during infection, such that antimicrobial activity in vitro may be a poor predictor of activity in vivo (Snyder et al., 2004; Blango and Mulvey, 2010). The effects of host physiology may also influence the predictive value of minimum inhibitory concentrations determined in vitro, as the antimicrobial activity of gallium differs depending on the nature of the complex (Stojiljkovic et al., 1999; Olakanmi et al., 2010). If gallium is present at the site of infection in complexes other than gallium maltolate, this may account for unexpected antimicrobial activity in vivo. Along with identification of gallium complexes present in blood and tissues following oral administration of gallium maltolate, pilot studies of antimicrobial efficacy in animal models will be essential to predict the potential clinical utility of gallium maltolate.

7.6. **Conclusion**

Gallium exhibits a long terminal half-life which is well-suited to its time-dependent mechanism of antimicrobial activity. While the peak concentrations achieved in bladder and kidney are lower than in blood, gallium exposure is greater in urinary tract tissues than in blood.

In this study, increased gallium exposure in the bladder during infection was the only statistically significant difference detected between the two groups (infected and healthy mice). While there were trends toward increased terminal half-life in blood and bladder during infection, we were

unable to demonstrate a statistically significant effect. As peak gallium concentrations in the bladder are substantially lower than the minimum inhibitory concentrations for gallium maltolate against UPEC, therapeutic success using doses of 100 mg/kg is only anticipated if in vitro testing conditions do not reflect bacterial and host pathophysiology.

Chapter 8. Efficacy of gallium maltolate as an antimicrobial therapy in a mouse urinary tract infection model

Relationship of this study to the dissertation:

The results reported in Chapters 5, 6, and 7 indicated that gallium maltolate exerts antimicrobial activity against uropathogenic *E. coli*, that gallium arrives at the bladder mucosa following oral administration of gallium maltolate, and that urinary tract infection minimally influences the pharmacokinetics of gallium after oral administration of gallium maltolate. Furthermore, the persistence of gallium in whole blood and tissues is well-suited to its time-dependent antimicrobial activity. Although these characteristics suggested that gallium maltolate may have antimicrobial efficacy in animal models, there was a large gap between the minimum inhibitory concentrations observed in vitro and the maximum gallium concentrations observed in Chapter 7. This left considerable uncertainty about the potential utility of gallium maltolate as an antimicrobial therapy. To address this uncertainty along with the sixth objective of this dissertation, we evaluated the efficacy of orally administered gallium maltolate for reducing tissue bacterial loads in a mouse cystitis model by comparing its effects with those of ciprofloxacin and sham treatments.

8.1. **Abstract**

The novel antimicrobial drug gallium maltolate exerts antimicrobial activity against uropathogenic strains of *Escherichia coli* in vitro. Oral administration leads to gallium accumulation in the bladder mucosa, but concentrations in homogenized tissue are substantially lower than the minimum inhibitory concentrations observed in vitro for gallium maltolate against UPEC. As host-pathogen interactions and infection-specific changes in bacterial metabolism may influence antimicrobial susceptibility in vivo, the efficacy of gallium maltolate for treating UPEC infection was compared to ciprofloxacin and sham treatment in a mouse infection model. Treatments were administered by gavage beginning 48 hours after transurethral UPEC infection, and were administered once daily for five days. Six mice were treated with 200 mg/kg gallium maltolate, six received 20 mg/kg ciprofloxacin, and six received distilled water. Bacteriologic cure rates in bladder and kidney did not differ significantly between the treatment groups, indicating that infection-related changes in host and pathogen physiology may be insufficient to overcome the large gap between in vitro minimum inhibitory concentrations and gallium concentrations in vivo. Based on the results of this study, it seems unlikely that gallium maltolate will be clinically useful for managing urinary tract infections.

8.2. **Introduction**

Uropathogenic strains of *Escherichia coli* (UPEC) are the most common cause of urinary tract infections in humans and dogs (Zhanel et al., 2006; Ball et al., 2008a; Karlowsky et al., 2011). The ability of these pathogens to invade urothelial cells and evade many conventional antimicrobials and the increasing prevalence of antimicrobial resistance restrict the treatment options available (Schilling et al., 2002; Mysorekar and Hultgren, 2006; Blango and Mulvey,

2010). Failure of the antimicrobial to reach the intracellular bacteria may partially explain the inability of in vitro antimicrobial susceptibility testing to predict therapeutic success when the pathogen is susceptible to the selected antimicrobial in vitro (Blango and Mulvey, 2010). Differences in bacterial metabolism between laboratory settings and in host tissues likely also limit the predictive value of in vitro susceptibility testing.

Gallium maltolate may be useful as a new therapeutic agent for UPEC infections as it exerts antimicrobial activity against UPEC in vitro and oral administration leads to gallium accumulation in the bladder mucosa (Chapter 8). In addition, gallium compounds including gallium maltolate disrupt iron metabolism in a variety of bacterial pathogens including *E. coli* (Hubbard et al., 1986; Olakanmi et al., 2000; Harrington et al., 2006; Kaneko et al., 2007; Olakanmi et al., 2010). This is particularly favourable for treating UPEC infections as iron uptake pathways are virulence factors for these bacteria and are upregulated during infection, suggesting that iron metabolism may be a vulnerable target for antimicrobial therapy (Hagan et al., 2010; Garcia et al., 2011). Although the concentrations of gallium achieved in homogenized bladder tissue are substantially lower than the minimum inhibitory concentrations of gallium maltolate (gallium basis) observed for UPEC in vitro, upregulation of iron acquisition may lead to increased gallium susceptibility (Chapters 6 and 7). By evaluating gallium maltolate's efficacy for treating urinary tract infections in an animal model, host effects and bacterial metabolic features unique to infection are incorporated into the analysis. This is of substantial value for determining whether further investigation of its potential clinical utility is warranted. The objective of this study was to determine the antimicrobial efficacy of orally administered gallium

maltolate for treating urothelial infections caused by a type strain of UPEC (J96, ATCC 700336) in a mouse model.

8.3. **Methods**

8.3.1. ***Escherichia coli***

Uropathogenic *E. coli* ATCC 700336 was sub-cultured on TSA agar with 5% sheep blood (Becton, Dickenson and Company, Sparks, MD) prior to suspension in physiologic saline solution for intravesical infusion.

8.3.2. **Antimicrobial solutions**

Gallium maltolate and ciprofloxacin solutions were prepared immediately prior to administration. Gallium maltolate solutions were produced as described in 6.3.2. Ciprofloxacin (pharmaceutical secondary standard grade, obtained from Sigma-Aldrich, St. Louis MO, USA) was dissolved in ultrapure water and treated in the same manner as the gallium maltolate solutions.

8.3.3. **Mice**

This work was approved by the University of Saskatchewan's Animal Research Ethics Board, and adhered to the Canadian Council on Animal Care guidelines for humane animal use. Mice were maintained and infected as described in 7.3.3. Treatments were administered by gavage beginning 48 hours after infection. Mice in the "gallium maltolate" received gallium maltolate at 200 mg/kg, positive controls received ciprofloxacin at 20 mg/kg and negative controls received distilled water. Mice received five treatments at 24 hour intervals.

8.3.4. **Sampling**

Mice were euthanized with isoflurane 24 hours following the last treatment. Bladders and kidneys were harvested aseptically. A focal region of the kidney surface was seared with a flame-heated scalpel blade, and an inoculation loop was inserted through a small incision through the seared region. The loop was twirled, withdrawn, and then used to streak trypticase soy agar with 5% sheep blood and MacConkey agar plates. For bladder cultures, a sterile scalpel and forceps were used to expose the mucosal surface of the bladder, which was then smeared firmly on the surface of trypticase soy agar with 5% sheep blood and MacConkey agar plates. A section of bladder was also placed in peptone water for selective enrichment of Enterobacteriaceae. Colonies were identified as *E. coli* based on colony morphology, Gram staining characteristics and biochemical tests.

8.3.5. **Data analysis**

The relationship between treatment and culture results for kidney and bladder were evaluated using the Kruskal-Wallis test. Bladder tissue was considered culture-positive if *E. coli* were retrieved on primary culture or following enrichment in peptone water.

8.4. **Results**

There was no statistically significant relationship between treatment and the proportion of culture-positive bladder ($p=0.8086$) or kidney samples ($p=0.1194$) (Table 8.1). All positive cultures were observed on primary culture except for two bladders from gallium maltolate-treated mice where *E. coli* was isolated only after enrichment in peptone water. Among the mice

that received gallium maltolate or ciprofloxacin, *E. coli* was cultured from the kidneys of a single mouse in the gallium maltolate group. No *E. coli* were isolated from the kidneys of ciprofloxacin- or gallium maltolate-treated mice with culture-positive bladders. *E. coli* were isolated from the bladders of two of the three negative control mice with culture-positive kidneys.

			Number of mice where *E. coli* was cultured from specified tissue	
Treatment	**Number of mice**	**Mice with *E. coli* recovered from urinary tract post-treatment**	**Bladder**	**Kidney**
Untreated control	6	4	3	3
Gallium maltolate	6	5	4	1
Ciprofloxacin	6	3	3	0

Table 8.1. Microbiological culture results from bladder and kidney harvested from mice infected with ATCC 700336 and subsequently treated by gavage with gallium maltolate at 100 mg/kg, ciprofloxacin at 20 mg/kg, or distilled water once daily for five days

8.5. **Discussion**

Uropathogenic *E. coli* can persist in the urothelium in mouse models despite treatment with apparently suitable antimicrobials and bacterial eradication from the urine (Schilling et al., 2002; Blango and Mulvey, 2010). Antimicrobial susceptibility tests in vitro are also poor predictors of therapeutic outcome in human urinary tract infections (Ferry et al., 1988). Failure to eradicate urothelial bacterial reservoirs may lead to apparently recurrent urinary tract infections (Ejrnaes et al., 2006). Elimination of bacteria from the bladder mucosa rather than from urine alone may

therefore be a more useful pharmacodynamic endpoint for laboratory-based investigation of new therapies for UPEC infections.

In this study, we failed to demonstrate a statistically significant effect of treatment with ciprofloxacin, gallium maltolate or distilled water (sham treatment) on the proportion of mice remaining infected with UPEC. The failure of ciprofloxacin to provide a therapeutic advantage over sham treatment is consistent with the findings of other groups. Notably, antimicrobial therapy generally results in suppression of bacterial numbers in urine despite bacterial persistence in the urothelium (Schilling et al., 2002; Blango and Mulvey, 2010). In addition to potential failure of ciprofloxacin to attain therapeutic concentrations within intracellular bacterial communities, differences in UPEC metabolism between laboratory and host environments may lead to altered antimicrobial susceptibility (Snyder et al., 2004; Hagan et al., 2010). Host responses to infection and inflammation may also influence the therapeutic outcomes by influencing the local physicochemical environment, potentially disrupting antimicrobial distribution or uptake by the bacteria (Nielubowicz and Mobley, 2010). Similar failures of antimicrobial susceptibility in vitro to predict antimicrobial efficacy in animal models are observed for aminoglycosides, cephalosporins, fluoroquinolones, penicillins, potentiated sulfonamides, tetracyclines, nitrofurantoin and fosfomycin (Schilling et al., 2002; Blango and Mulvey, 2010).

As the clinical utility of gallium maltolate depends on antimicrobial efficacy in mammalian patients, in vitro demonstrations of antimicrobial efficacy are useful for identifying drug candidates for further study but are insufficient for determining whether this compound may be a

clinically useful therapeutic agent. Results of pharmacodynamic investigations in animal models thus contribute substantially to the decision to proceed with clinical trials in the target mammalian species. In this small study, gallium maltolate treatment did not produce any statistically significant therapeutic effects compared with ciprofloxacin and sham treatments, suggesting that its utility for managing apparently recurrent infections is limited. Further investigation in larger populations may potentially demonstrate a small effect, but researchers must carefully consider whether small treatment effects are likely to be clinically relevant.

In this study, the prolonged gallium exposure that would have resulted from its long terminal half-life and from repeated administration did not apparently overcome the low ratio of tissue gallium concentration to in vitro minimum inhibitory concentrations, despite the time-dependent nature of gallium's antimicrobial activity. As minimum inhibitory concentrations (gallium basis) observed for nine gallium maltolate-naïve UPEC strains all exceeded the peak gallium concentrations observed in bladder in this animal model by at least an order of magnitude, it is unlikely that different therapeutic effects would be observed for any of these other strains.

8.6. **Conclusion**

This study failed to demonstrate a statistically significant reduction in bacterial populations in the urinary tract between groups of mice infected with a UPEC type strain and subsequently treated with gallium maltolate, ciprofloxacin, or distilled water (sham treatment). The lack of a statistically significant treatment effect for gallium maltolate may be a result of the large gap between minimum inhibitory concentrations and gallium concentrations in target tissues, in which case gallium maltolate may not produce therapeutically useful reductions in urothelial

bacterial populations for other UPEC strains. While the mechanism responsible for the absence of a statistically significant treatment effect was not identified, the results of this experiment suggest that alternatives to gallium maltolate should be sought out as potential new therapeutic agents for urinary tract infections involving the urothelium.

Chapter 9. General discussion

Urinary tract infections present a significant health care and societal burden due to their high prevalence. Emerging antimicrobial resistance can lead to treatment failure with conventional antimicrobials, creating an ever greater disease burden. Development of antimicrobial treatments with novel mechanisms of action offers the potential to treat infections resistant to conventional antimicrobial drugs and ultimately, to improve individual and societal well-being. Ideally, new drug candidates will exert antimicrobial activity through mechanisms different from conventional antimicrobial drugs to reduce the potential for cross-resistance. Unlike currently available antimicrobial drugs, gallium compounds are hypothesized to exert antimicrobial activity by interfering with bacterial iron metabolism, making them of particular interest as potential new therapeutic agents (Baldoni et al., 2010; Coleman et al., 2010).

To address the challenge of identifying novel antimicrobial drug candidates, we adopted a two-pronged approach. By investigating a metal-based drug using synchrotron-based techniques, we had two opportunities to address the growing need for new antimicrobial therapies. In this strategy, demonstrating gallium maltolate as a reasonable drug candidate or demonstrating that synchrotron-based analytical techniques are useful to compliment conventional antimicrobial research methods could be considered successful outcomes. While identifying a novel antimicrobial drug candidate would potentially expedite adoption of clinically useful treatments for antimicrobial-resistant infections, demonstrating the utility of a novel research technique would potentially lead to discovery of a wider variety of new antimicrobial treatments over the longer term.

The initial phase of this work was designed to confirm that gallium maltolate exerts antimicrobial activity against UPEC to ensure that it was a reasonable candidate for further characterization as a novel therapeutic agent. In the experiments described in Chapter 6, gallium maltolate exerted antimicrobial activity against six of nine UPEC isolates in vitro. Although this effect was dependent on the culture medium, there was a nearly three-fold difference in iron concentrations between the media tested. Considering the role of iron-withholding as a host defense mechanism, and the known ability of high iron concentrations to reduce gallium's antimicrobial activity, the antimicrobial activity observed in iron-poor media was considered sufficient support for proceeding with additional investigations (Hubbard et al., 1986). Gallium maltolate's antimicrobial activity was further characterized as bacteriostatic and time-dependent based on time-kill studies using six of the UPEC isolates. As conventional qualitative analysis of time-kill curves was not amenable to summarizing results from multiple isolates, we used an area-based measure, area between the microbial growth and kill curves, to facilitate data compilation and comparison (Firsov et al., 1997). This allowed us to conclude that in the small group of isolates evaluated in our study, the antimicrobial activity observed was primarily time-dependent. The findings reported in Chapter 6 represent a substantial advance in the investigation of gallium compounds for treating urinary tract infections, as no previous data on minimum inhibitory concentrations or time-kill analyses had been previously reported for any gallium compounds against UPEC.

As UPEC establish infections in urothelial cells, it was important to establish that gallium arrived at the true site of infection following oral administration of gallium maltolate. Synchrotron-based analytical techniques were of particular interest as they can localize and speciate elements of

interest (including gallium) in a sample without the need for tissue homogenization. We initially elected to investigate synchrotron-based soft x-ray techniques for evaluating gallium distribution in tissues. Of the synchrotron-based techniques, scanning and transmission x-ray microscopy was of particular interest as it could potentially speciate and localize gallium with nanometre-scale spatial resolution (Dynes et al., 2006; Kaznatcheev et al., 2007). At the time, few gallium compounds had been characterized by x-ray absorption spectroscopy at the gallium $L_{2,3}$ edges in the soft x-ray region (Shimizu et al., 1996; Zhou et al., 2007a). This was in part due to the paucity of synchrotron beamlines with the capability to reliably collect high resolution x-ray absorption spectra in this energy range. The SGM (11ID-1) beamline at the Canadian Light Source is well suited for this analysis, and produced high quality spectra for an assortment of gallium reference compounds as described in Chapter 3 (Regier et al., 2007). These results clearly demonstrated that gallium compounds could be distinguished spectroscopically at the $L_{2,3}$ edges, indicating that in the presence of sufficient concentrations, a variety of gallium compounds could be distinguished within tissue samples using scanning and transmission x-ray microscopy. Additional experiments examining thin polymer films containing gallium compounds at varying concentrations (also described in Chapter 3) revealed that quality spectra could be obtained from relatively low gallium concentrations, suggesting that soft x-ray absorption spectroscopy may be feasible at the low gallium concentrations expected in tissue samples. In addition to supporting ongoing synchrotron analysis of gallium compounds, these results were key in securing research funding and synchrotron facility access for the remainder of the work described in this dissertation.

Proceeding with scanning and transmission x-ray microscopy presented a new challenge: how to prepare animal tissue samples for analysis. Although suggestions were available from experienced STXM users in the materials science area, data for identifying acceptable sample preparations for animal tissues were scarce. Ideally, sample preparation techniques would minimally disturb tissue anatomy and chemistry, ensure that samples were ultimately classified within biohazard risk group one (due to facility restrictions at the time), could be sectioned at 100-500 nm, and could withstand the low pressures required for analysis. Because the technique could eventually be used to evaluate tissues from animals infected with UPEC and subsequently treated with gallium compounds, fixing the samples in formalin was virtually unavoidable if the samples were to remain in biohazard risk group one. Furthermore, cryogenically preserved samples were impractical as it would be nearly impossible to prevent freeze-thaw cycling (with subsequent sample degradation) during the prolonged and potentially repeated analyses typical of the technique. By necessity, the assumption was made that like iron, most gallium within cells would be protein-bound and as such would likely not undergo substantial leaching during the fixing process. This assumption was supported by the common use of special staining of fixed tissue samples to diagnose metal storage disorders, including iron storage disorders, in histopathological examinations.

After attempting to embed fixed mouse bladder samples using two techniques suggested by the experienced STXM users and one conventional technique for preparing tissues for ultra-thin sectioning for electron microscopy, only the latter preserved anatomy and could withstand sectioning at 100 and 500 nm (Chapter 4). As zinc and iron are both present in urothelial cells in protein-bound states, they were used as markers to predict whether gallium would likely be

detectable in urothelial cells using STXM. Neither of these two elements were detectable, leading us to conclude that it was unlikely we would be able to detect gallium within urothelial cells using this method.

Although STXM was not suited to investigate gallium distribution in urothelial cells, hard x-ray microprobe analysis provided new insight into the nature of gallium distribution in tissues in Chapter 5. This work was the first application of synchrotron x-ray fluorescence imaging and in situ x-ray absorption spectroscopy to investigate the distribution of an antimicrobial compound in a target tissue. The simultaneous localization and relative quantification of gallium and iron by x-ray fluorescence micro-imaging of tissue sections was of key importance in demonstrating the distributional relationship between the two elements. Gallium and iron are not identically distributed within tissues, and this relationship does not center on inhibition. This implies that certain iron transportation pathways discriminate between gallium and iron, and that a portion of gallium distribution occurs through pathways that do not readily incorporate iron. Researchers investigating other potential therapeutic applications of gallium compounds must therefore confirm that gallium indeed arrives at the target locations rather than assuming that it will simply follow iron distribution. The non-iron distribution mechanisms for gallium may also be vulnerable to drug-drug or drug-nutrient interactions. While it is possible to make educated guesses about factors that may influence gallium distribution through inhibition or induction of iron transportation pathways, it is impossible to make any prediction of potential interactions with the unidentified non-iron transportation pathways. As these interactions could potentially influence gallium absorption, distribution, metabolism and excretion, they could place patients at risk of toxicity or treatment failure. Elucidation of the principal mechanisms of gallium

distribution should be of high priority if interest in the clinical application of gallium maltolate persists.

In addition to confirming gallium distribution to the bladder mucosa, synchrotron-based analysis of tissues from gallium maltolate-treated mice also yielded x-ray absorption spectra of sufficient quality to allow speciation in future studies. Near-edge x-ray absorption spectra for iron and gallium in 5 micron-wide regions were of good quality despite the small number of scans that could be conducted in the limited time available on the instrument. This suggests that x-ray absorption spectroscopy could be used in future work to identify specific gallium compounds in tissue section, distinguishing between the parent compound, protein-bound gallium, and gallium salts. Similar applications are likely also possible for other trace elements. Determining the forms of gallium present in regions of interest will allow researchers to refine methods for in vitro pharmacodynamic testing, and can provide vital insight into mechanisms of action.

While the experiments in chapters 5 and 6 demonstrated that gallium maltolate exerts antimicrobial activity against UPEC and that oral administration leads to gallium distribution to the bladder mucosa, further investigation was required to characterize the time course of gallium concentrations after oral administration of gallium maltolate. The prolonged terminal half-life of gallium in blood, kidney and bladder following oral administration of gallium maltolate (identified in Chapter 7) are favourable for therapeutic use of a time-dependent antimicrobial drug. In this study, we were unable to find a statistically significant effect of infection on the pharmacokinetics of gallium in blood after oral administration of gallium maltolate. Pronounced interindividual variability in gallium concentrations may have obscured small disease effects

such that a larger study may have demonstrated a statistically significant effect. The relatively small volume of tissue affected may have led to a minimal effect of disease on blood gallium concentrations, making it difficult to demonstrate such an effect within the constraints of common analytical techniques and statistical analysis.

The minimum inhibitory concentrations observed in vitro and reported in Chapter 6 substantially exceed the maximum gallium concentrations in vivo (Chapters 7 and 8), leaving us concerned that this may make therapeutic success unlikely. As a substantial treatment effect (relative to controls) would be necessary for gallium maltolate to be of interest as a clinical antimicrobial therapy, we concluded that a small efficacy trial would allow us to determine whether gallium maltolate was likely to satisfy this criterion prior to proceeding with a larger trial. In the small efficacy trial detailed in Chapter 8, changes in bacterial loads in bladder tissue were not distinguishable between gallium maltolate, sham treatment or ciprofloxacin, which is inefficacious for eradicating intracellular UPEC infections. Although small effects may not have achieved statistical significance, the outcome of this small trial suggests that differences between in vitro minimum inhibitory concentrations and gallium concentrations in target tissues may not have been overcome by the contribution of the host immune response, changes in bacterial metabolism during infection, or localized accumulation of gallium following oral administration of gallium maltolate to mice with urinary tract infections. Unless additional data become available and indicate that much higher doses yield substantially greater gallium concentrations in tissues and can be administered safely, it is difficult to justify further investigation of gallium maltolate as a potential antimicrobial therapy for urinary tract infections caused by UPEC.

Based on the results reported in Chapters 5, 6, 7 and 8, we concluded that gallium maltolate appears to have limited potential clinical application as an antimicrobial therapy for UPEC infections. However, the pharmacokinetic characterization can support other studies of biomedical applications of gallium maltolate, potentially leading to important new developments in therapy for other infections and disease processes.

Despite the disappointingly low potential of gallium maltolate to become a useful antimicrobial therapy for urinary tract infections, we successfully demonstrated that synchrotron-based analytical techniques can contribute to the characterization of antimicrobial drug candidates. The results from synchrotron hard x-ray analyses provide a glimpse of the synchrotron's great potential as a research tool to compliment conventional pharmacokinetic and pharmacodynamic methods. In the context of the ongoing and desperate search for novel therapeutic alternatives for treating infectious diseases and cancer, the ability to localize and characterize metal-based drugs within tissue sections should be a welcome addition to the research arsenal.

Chapter 10. Conclusions and future directions

10.1. **Conclusions**

a. Organic gallium compounds can be distinguished using near-edge x-ray absorption spectroscopy at the Ga $L_{2,3}$ edges (Chapter 3).

b. The Ga L_3 peak could be used as a spectral marker for localizing gallium in biological samples using soft x-ray microscopy techniques (Chapter 3).

c. Unlike samples embedded in glycol methacrylate or in TTE resin, fixed tissue embedded in LR White resin can withstand the ultrathin sectioning required for STXM analysis while maintaining anatomic features. X-ray absorption at the carbon K-edge can be used to identify anatomic features in LR White-embedded tissues, but samples are prone to degradation with repeated analysis at a particular location (Chapter 4).

d. The sensitivity of scanning and transmission x-ray microscopy conducted at the Canadian Light Source SM beamline (10-ID1) was insufficient to detect iron and zinc in mouse tissues, suggesting that it is not likely sufficient to analyze gallium in tissues (Chapter 4).

e. Oral administration of gallium maltolate to mice with urinary tract infections leads to gallium distribution to the urothelium in a manner similar but not identical to iron (Chapter 5).

f. Gallium is likely partially distributed in the bladder by mechanisms that do not involve iron (Chapter 5).

g. Synchrotron x-ray fluorescence imaging can be used to localize exogenous trace elements in mammalian tissues. Elements of interest can likely be speciated using XANES in situ (Chapter 5).

h. Gallium maltolate exerts primarily bacteriostatic, time-dependent antimicrobial activity against selected UPEC in vitro (Chapter 6).

i. Following oral administration of gallium maltolate, peak gallium concentrations in blood exceed those observed in bladder and kidney. In contrast, gallium exposure is greater in bladder and kidney than in blood (Chapter 7).

j. The influence of urinary tract infection on gallium pharmacokinetics in whole blood may be small, based on the lack of statistical significance upon comparing pharmacokinetic parameters from whole blood between infected and healthy mice (Chapter 7).

k. Following oral administration of gallium maltolate at 100 mg/kg, peak gallium concentrations in the bladder are substantially lower than the minimum inhibitory concentrations for gallium maltolate against UPEC (Chapters 6 and 7).

l. No statistically significant difference was detected for reduction of bacterial loads in bladder tissue from mice treated with gallium maltolate, ciprofloxacin, or sham treatment. Orally administered gallium maltolate may not provide a clinically relevant therapeutic advantage over the other treatments evaluated for infections caused by a UPEC type strain in a mouse model (Chapter 8).

m. At the dose ranges investigated, gallium maltolate's clinical utility for treating urinary tract infections caused by UPEC is likely very limited.

10.2. **Future directions**

Although gallium maltolate is a poor candidate for treating urinary tract infections, it exerts antimicrobial activity against control strains of *Enterococcus faecalis* and *Staphylococcus aureus* and may be useful for treating superficial infections where it can be administered topically. Local administration would produce very high gallium concentrations, and with appropriate dressings, these concentrations could be maintained for prolonged periods. The relatively inefficient uptake of gallium from the gastrointestinal tract necessarily leaves substantial quantities of gallium maltolate in the gastrointestinal lumen. Consequently, oral administration is effectively local administration to the gastrointestinal tract and may be useful for treating bacterial gastroenteritis and colitis. An initial survey of pathogen susceptibility to gallium maltolate would help to determine whether further investigation is warranted.

If interest in gallium maltolate as a therapeutic product continues, toxicity evaluation should be a top priority. The upper limits of the dosing ranges cannot be identified until concentration- (or

dose-) toxicity relationships are characterized. The influence of gallium maltolate treatment on a) calcium metabolism, b) erythropoiesis, c) renal function and d) the composition of gastrointestinal bacterial populations should be investigated in animal models and in target species prior to widespread use for any application.

Additional research and method development are warranted to fully exploit the potential of synchrotron-based hard x-ray analytical techniques for pharmacology research. One of the challenges encountered in the present work was identifying anatomic features in the elemental distribution maps. Identifying stains that do not influence x-ray absorption spectra of the metals of interest would allow researchers to use photomicrographs and visual sample inspection to select regions for analysis and align anatomic and elemental distribution maps. The use of metal-labelled antibodies to identify specific cellular structures could provide further confirmation of the anatomic location of the elemental distribution maps. Improved spatial resolution will allow localization and identification of metal-based compounds within cells, although the increased x-ray exposure of the sample must be managed to minimize the risk of generating tissue damage artifacts.

Chapter 11. References

Abdul-Tehrani H, Hudson AJ, Chang Y-S, Timms AR, Hawkins C, Williams JM, Harrison PM, Guest JR, and Andrews SC (1999) Ferritin mutants of *Escherichia coli* are iron deficient and growth impaired, and fur mutants are iron deficient. *J Bacteriol* **181:**1415-1428.

Abràmoff MD, Magalhães PJ, and Ram SJ (2004) Image processing with imageJ. *Biophotonics Int* **11:**36-41.

Akram M, Shahid M, and Khan AU (2007) Etiology and antibiotic resistance patterns of community-acquired urinary tract infections in J N M C Hospital Aligarh, India. *Ann Clin Microbiol Antimicrob* **6:**4.

Aksenov VL, Koval'chuk MV, Kuz'min AY, Purans Y, and Tyutyunnikov SI (2006) Development of methods of EXAFS spectroscopy on synchrotron radiation beams: Review. *Crystallogr Rep* **51:**908-935.

Ali AS, Townes CL, Hall J, and Pickard RS (2009) Maintaining a sterile urinary tract: the role of antimicrobial peptides. *J Urol* **182:**21-28.

Alteri CJ and Mobley HLT (2007) Quantitative profile of the uropathogenic *Escherichia coli* outer membrane proteome during growth in human urine. *Infect Immun* **75:**2679-2688.

Anderson GG, Palermo JJ, Schilling JD, Roth R, Heuser J, and Hultgren SJ (2003) Intracellular bacterial biofilm-like pods in urinary tract infections. *Science* **301:**105-107.

Andrews SC, Robinson AK, and Rodriguez-Quinones F (2003) Bacterial iron homeostasis. *FEMS Microbiol Rev* **27:**215-237.

Anonymous (2008) Commission Staff Working Document Accompanying the Communication from the Commission to the European Parliament and the Council: The Raw Materials Initiative - Meeting Our Critical Needs for Growth and Jobs in Europe. Commission of the European Communities, Brussels.

Apseloff G (1999) Therapeutic uses of gallium nitrate: past, present, and future. *Am J Ther* **6:**327-339.

Arnold C, Chaffin MK, Cohen N, Fajt VR, Taylor RJ, and Bernstein LR (2010) Pharmacokinetics of gallium maltolate after intragastric administration in adult horses. *Am J Vet Res* **71:**1371-1376.

Arslan S, Caksen H, Rastgeldi L, Uner A, Oner AF, and Odabas D (2002) Use of urinary gram stain for detection of urinary tract infection in childhood. *Yale J Biol Med* **75:**73-78.

Bailer AJ (1988) Testing for the equality of area under the curves when using destructive measurement techniques. *J Pharmacokinet Biopharm* **16:**303-309.

Baldoni D, Steinhuber A, Zimmerli W, and Trampuz A (2010) In vitro activity of gallium maltolate against *Staphylococci* in logarithmic, stationary, and biofilm growth phases: comparison of conventional and calorimetric susceptibility testing methods. *Antimicrob Agents Chemother* **54:**157-163.

Ball KR, Rubin JE, Chirino-Trejo M, and Dowling PM (2008a) Antimicrobial resistance and prevalence of canine uropathogens at the Western College of Veterinary Medicine Veterinary Teaching Hospital, 2002-2007. *Can Vet J* **49:**985-990.

Ball KR, Sampieri F, Dowling PM, Chirino-Trejo JM, Bernstein LR, Sham TK, Blyth RIR, and Thompson J (2008b) Preliminary investigation of soft x-ray absorption spectroscopy for evaluating gallium complexes in biological samples. *Nucl Instrum Meth A***:**In press.

Banin E, Berenshtein E, Kitrossky N, Pe'er J, and Chevion M (2000) Gallium-desferrioxamine protects the cat retina against injury after ischemia and reperfusion. *Free Radic Biol Med* **28:**315-323.

Banin E, Lozinski A, Brady KM, Berenshtein E, Butterfield PW, Moshe M, Chevion M, and Greenberg EP (2008) The potential of desferrioxamine-gallium as an anti-*Pseudomonas* therapeutic agent. *Proc Natl Acad Sci USA* **105:**16761-16766.

Banin E, Morad Y, Berenshtein E, Obolensky A, Yahalom C, Goldich J, Adibelli FM, Zuniga G, DeAnda M, Pe'er J, and Chevion M (2003) Injury induced by chemical warfare agents: characterization and treatment of ocular tissues exposed to nitrogen mustard. *Invest Ophthalmol Vis Sci* **44:**2966-2972.

Bartges J (2004) Diagnosis of urinary tract infections. *Vet Clin North Am Small Anim Pract* **34:**923-933.

Baselga J, Kris MG, Scher HI, Phillips M, and Heelan RT (1993) Phase II trial of gallium nitrate in previously treated patients with small cell lung cancer. *Invest New Drugs* **11:**85-86.

Beckel JM and Holstege G (2011) Neuroanatomy of the lower urinary tract. *Handb Exp Pharmacol***:**99-116.

Behnam Azad B, Cho C-F, Lewis JD, and Luyt LG (2012) Synthesis, radiometal labeling and in vitro evaluation of a targeted PPIX derivative. *Appl Radiat Isot* **70:**505-511.

Bernstein L (2009) Gallium compounds and methods of use to treat inflammatory bowel disease, WO2009111681A2, Washington DC: United States Patent and Trademark Office.

Bernstein LR (1993a) Oral pharmaceutical compositions containing gallium complexes of 3-hydroxy-4-pyrones, US5258376A, Washington DC: United States Patent and Trademark Office.

Bernstein LR (1993b) Pharmaceutical compositions of gallium complexes of 3-hydroxy-4-pyrones, WO9309776A1, Washington DC: United States Patent and Trademark Office.

Bernstein LR (1998) Mechanisms of therapeutic activity for gallium. *Pharmacological reviews* **50:**665-682.

Bernstein LR (2001) Gallium complexes of 3-hydroxy-4-pyrones to treat infection by intracellular prokaryotes, DNA viruses and retroviruses, WO2001024799A1, Washington DC: United States Patent and Trademark Office.

Bernstein LR (2002) Gallium complexes of 3-hydroxy-4-pyrones to treat mycobacterial infections, US20020068761A1, Washington DC: United States Patent and Trademark Office.

Bernstein LR (2007) Oral gallium compositions, US20070098815A1, Washington DC: United States Patent and Trademark Office.

Bernstein LR (2008a) Gallium compositions for the treatment of liver cancer and methods of use, WO2008036429A1, Washington DC: United States Patent and Trademark Office.

Bernstein LR (2008b) Local administration of gallium compositions to treat pain, WO2008058210A2, Washington DC: United States Patent and Trademark Office.

Bernstein LR (2008c) Ophthalmic gallium compositions and methods of their use, US20080292726A1, Washington DC: United States Patent and Trademark Office.

Bernstein LR, Tanner T, Godfrey C, and Noll B (2000) Chemistry and pharmacokinetics of gallium maltolate, a compound with high oral gallium bioavailability. *Metal-Based Drugs* **7:**33-47.

Berry JP, Poupon MF, Galle S, and Escaig F (1984) Role of lysosomes in gallium concentration by mammalian tissues. *Biol Cell* **51:**43-51.

Betoulle S, Etienne JC, and Vernet G (2002) Acute immunotoxicity of gallium to carp (*Cyprinus carpio* L.). *Bull Environ Contam Toxicol* **68:**817-823.

Beveridge LA, Davey PG, Phillips G, and McMurdo ME (2011) Optimal management of urinary tract infections in older people. *Clin Interv Aging* **6:**173-180.

Bhat RG, Katy TA, and Place FC (2011) Pediatric urinary tract infections. *Emerg Med Clin North Am* **29:**637-653.

Bidet P, Mahjoub-Messai F, Blanco J, Blanco J, Dehem M, Aujard Y, Bingen E, and Bonacorsi S (2007) Combined multilocus sequence typing and O serogrouping distinguishes *Escherichia coli* subtypes associated with infant urosepsis and/or meningitis. *J Infect Dis* **196:**297-303.

Biomerieux (2008) Etest for antimicrobial susceptibility testing, AB bioMerieux, Solna, Sweden.

Blango MG and Mulvey MA (2010) Persistence of uropathogenic *Escherichia coli* in the face of multiple antibiotics. *Antimicrob Agents Chemother* **54:**1855-1863.

Boczek LA, Rice EW, Johnston B, and Johnson JR (2007) Occurrence of antibiotic-resistant uropathogenic *Escherichia coli* clonal group A in wastewater effluents. *Appl Environ Microbiol* **73:**4180-4184.

Bokil NJ, Totsika M, Carey AJ, Stacey KJ, Hancock V, Saunders BM, Ravasi T, Ulett GC, Schembri MA, and Sweet MJ (2011) Intramacrophage survival of uropathogenic *Escherichia coli*: Differences between diverse clinical isolates and between mouse and human macrophages. *Immunobiology* **216:**1164-1171.

Bower JM, Eto DS, and Mulvey MA (2005) Covert operations of uropathogenic *Escherichia coli* within the urinary tract. *Traffic (Copenhagen, Denmark)* **6:**18-31.

Bubenik LJ, Hosgood GL, Waldron DR, and Snow LA (2007) Frequency of urinary tract infection in catheterized dogs and comparison of bacterial culture and susceptibility testing results for catheterized and noncatheterized dogs with urinary tract infections. *J Am Vet Med Assoc* **231:**893-899.

Bucalo LR, Sreedharan S, Allamneni KP, and Bernstein LR (2007) Treatment and prevention of adverse liver conditions using gallium compounds, US20070128294A1, Washington DC: United States Patent and Trademark Office.

Burns LA and Munson AE (1993) Gallium arsenide selectively inhibits T cell proliferation and alters expression of CD25 (IL-2R/p55). *J Pharmacol Exp Ther* **265:**178-186.

Burns LA, Sikorski EE, Saady JJ, and Munson AE (1991) Evidence for arsenic as the immunosuppressive component of gallium arsenide. *Toxicol Appl Pharmacol* **110:**157-169.

Burns LA, Spriggs TL, Fuchs BA, and Munson AE (1994) Gallium arsenide-induced increase in serum corticosterone is not responsible for suppression of the IgM antibody response. *J Pharmacol Exp Ther* **268:**740-746.

Bush BM (1976) A review of the aetiology and consequences of urinary tract infections in the dog. *Br Vet J* **132:**632-641.

Campion JJ, Chung P, McNamara PJ, Titlow WB, and Evans ME (2005a) Pharmacodynamic modeling of the evolution of levofloxacin resistance in *Staphylococcus aureus*. *Antimicrob Agents Chemother* **49:**2189-2199.

Campion JJ, McNamara PJ, and Evans ME (2005b) Pharmacodynamic modeling of ciprofloxacin resistance in *Staphylococcus aureus*. *Antimicrob Agents Chemother* **49:**209-219.

Carlsson S, Wiklund NP, Engstrand L, Weitzberg E, and Lundberg JON (2001) Effects of pH, nitrite, and ascorbic acid on nonenzymatic nitric oxide generation and bacterial growth in urine. *Nitric Oxide* **5:**580-586.

Carroll KC, Hale DC, Von Boerum DH, Reich GC, Hamilton LT, and Matsen JM (1994) Laboratory evaluation of urinary tract infections in an ambulatory clinic. *Am J Clin Pathol* **101:**100-103.

Carter RG (2011) Acceleration technologies for charged particles: an introduction. *Contemp Phys* **52:**15-41.

Chaffin MK, Fajt V, Martens RJ, Arnold CE, Cohen ND, O'Conor M, Taylor RJ, and Bernstein LR (2010) Pharmacokinetics of an orally administered methylcellulose formulation of gallium maltolate in neonatal foals. *J Vet Pharmacol Ther* **33:**376-382.

Chang AY, Nora Tu Z, Smith JL, Bonomi P, Smith TJ, Wiernik PH, and Blum R (1995) Phase II trial of gallium nitrate, amonafide and teniposide in metastatic non-small cell lung cancer. *Invest New Drugs* **13:**137-141.

Chang R, Greene MT, Chenoweth CE, Kuhn L, Shuman E, Rogers MAM, and Saint S (2011) Epidemiology of hospital-acquired urinary tract–related bloodstream infection at a university hospital. *Infect Control Hosp Epidemiol* **32:**1127-1129.

Chen T-C, Tsai J-P, Huang H-J, Teng C-C, Chien S-J, Kuo H-C, Huang W-S, and Chen C-N (2011) Regulation of cyclooxygenase-2 expression in human bladder epithelial cells infected with type I fimbriated uropathogenic *E. coli*. *Cell Microbiol* **13:**1703-1713.

Chen WC, Tsai KD, Chen CH, Lin MS, Chen CM, Shih CM, and Chen W (2012) Role of gallium-67 scintigraphy in the evaluation of occult sepsis in the medical ICU. *Intern Emerg Med* **7:**53-58.

Chitambar C and Zivkovic Z (1987) Inhibition of hemoglobin production by transferrin-gallium. *Blood* **69:**144-149.

Chitambar CR (2010) Medical applications and toxicities of gallium compounds. *Int J Environ Res Public Health* **7:**2337-2361.

Chitambar CR and Purpi DP (2010) A novel gallium compound synergistically enhances bortezomib-induced apoptosis in mantle cell lymphoma cells. *Leuk Res* **34:**950-953.

Chitambar CR, Purpi DP, Woodliff J, Yang M, and Wereley JP (2007) Development of gallium compounds for treatment of lymphoma: gallium maltolate, a novel hydroxypyrone gallium compound, induces apoptosis and circumvents lymphoma cell resistance to gallium nitrate. *J Pharmacol Exp Ther* **322:**1228-1236.

Chitambar CR and Seligman PA (1986) Effects of different transferrin forms on transferrin receptor expression, iron uptake, and cellular proliferation of human-leukemic HL60 cells

- mechanisms responsible for the specific cytotoxicity of transferrin-gallium. *J Clin Invest* **78:**1538-1546.

Chong A and Celli J (2010) The *Francisella* intracellular life cycle: toward molecular mechanisms of intracellular survival and proliferation. *Front Microbiol* **1:**138.

Chromek M and Brauner A (2008) Antimicrobial mechanisms of the urinary tract. *J Mol Med (Berl)* **86:**37-47.

Chromek M, Slamova Z, Bergman P, Kovacs L, Podracka L, Ehren I, Hokfelt T, Gudmundsson GH, Gallo RL, Agerberth B, and Brauner A (2006) The antimicrobial peptide cathelicidin protects the urinary tract against invasive bacterial infection. *Nat Med* **12:**636-641.

Chu B, Garcia-Herrero A, Johanson T, Krewulak K, Lau C, Peacock R, Slavinskaya Z, and Vogel H (2010) Siderophore uptake in bacteria and the battle for iron with the host; a bird's eye view. *Biometals* **23:**601-611.

Chua AC, Graham RM, Trinder D, and Olynyk JK (2007) The regulation of cellular iron metabolism. *Crit Rev Clin Lab Sci* **44:**413-459.

Chua MS, Bernstein LR, Li R, and So SK (2006) Gallium maltolate is a promising chemotherapeutic agent for the treatment of hepatocellular carcinoma. *Anticancer Res* **26:**1739-1743.

Cicmanec JF, Shank RA, and Evans AT (1985) Overnight concentration of urine: Natural defense mechanism against urinary tract infection. *Urology* **26:**157-159.

Clines GA (2011) Mechanisms and treatment of hypercalcemia of malignancy. *Curr Opin Endocrinol Diabetes Obes* **18:**339-346.

CLSI (1999) Methods for Determining Bactericidal Activity of Antimicrobial Agents. M26-A. Clinical and Laboratory Standards Institute, Wayne, PA, USA.

CLSI (2006) Methods For Dilution Antimicrobial Susceptibility Tests For Bacteria That Grow Aerobically; Approved Standard - Seventh Edition. M7-A7. Clinical and Laboratory Standard Institute,

CLSI (2008) Performance Standards for Antimicrobial Susceptibility Testing. M100-S18. Clinical and Laboratory Standards Institute,

Cohn LA, Gary AT, Fales WH, and Madsen RW (2003) Trends in fluoroquinolone resistance of bacteria isolated from canine urinary tracts. *J Vet Diagn Invest* **15:**338-343.

Coleman M, Kuskie K, Liu M, Chaffin K, Libal M, Giguere S, Bernstein L, and Cohen N (2010) In vitro antimicrobial activity of gallium maltolate against virulent *Rhodococcus equi*. *Vet Microbiol* **146:**175-178.

Collery P, Keppler B, Madoulet C, and Desoize B (2002) Gallium in cancer treatment. *Crit Rev Oncol Hematol* **42:**283-296.

Crawford ED, Saiers JH, Baker LH, Costanzi JH, and Bukowski RM (1991) Gallium nitrate in advanced bladder carcinoma: Southwest oncology group study. *Urology* **38:**355-357.

Cullen IM, Manecksha RP, McCullagh E, Ahmad S, O'Kelly F, Flynn RJ, McDermott T, Murphy P, Grainger R, Fennell JP, and Thornhill JA (2011) The changing pattern of antimicrobial resistance within 42 033 *Escherichia coli* isolates from nosocomial, community and urology patient-specific urinary tract infections, Dublin, 1999-2009. *BJU Int*.

Cvitkovic F, Armand JP, Tubiana-Hulin M, Rossi JF, and Warrell RP, Jr. (2006) Randomized, double-blind, phase II trial of gallium nitrate compared with pamidronate for acute control of cancer-related hypercalcemia. *Cancer J* **12:**47-53.

Dailey HA, Dailey TA, Wu CK, Medlock AE, Rose JP, and Wang KF (2000) Ferrochelatase at the millennium: structures, mechanisms and [2Fe-2S] clusters. *Cell Mol Life Sci* **57:**1909-1926.

Dallin L, Blomqvist I, de Jong M, Lowe D, and Silzer M (2003) The Canadian Light Source, in: *Proceedings of the 2003 Particle Accelerator Conference, Vols 1-5* (Chew J, Lucas P, and Webber S eds), pp 220-223, Ieee, New York.

David LM, Natin D, Walzman M, and Stocker D (1996) Urinary symptoms, sexual intercourse and significant bacteriuria in male patients attending STD clinics. *Genitourin Med* **72:**266-268.

Davidson RE, Chesters CJ, and Reid JD (2009) Metal ion selectivity and substrate inhibition in the metal ion chelation catalyzed by human ferrochelatase. *J Biol Chem* **284:**33795-33799.

de Laeter JR, Boehlke JK, de Bievre P, Hidaka H, Peiser HS, Rosman KJR, and Taylor PDP (2003) Atomic weights of the elements: Review 2000 (IUPAC technical report). *Pure Appl Chem* **75:**683-800.

DeLeon K, Balldin F, Watters C, Hamood A, Griswold J, Sreedharan S, and Rumbaugh KP (2009) Gallium maltolate treatment eradicates *Pseudomonas aeruginosa* infection in thermally injured mice. *Antimicrob Agents Chemother* **53:**1331-1337.

Dennis DT, Inglesby TV, Henderson DA, Bartlett JG, Ascher MS, Eitzen E, Fine AD, Friedlander AM, Hauer J, Layton M, Lillibridge SR, McDade JE, Osterholm MT, O'Toole T, Parker G, Perl TM, Russell PK, and Tonat K (2001) Tularemia as a biological weapon: medical and public health management. *JAMA* **285:**2763-2773.

Deysine M, Robinson R, Rafkin H, Teicher I, Silver L, and Aufses AH, Jr. (1974) Clinical infections detected by 67Ga scanning. *Ann Surg* **180:**897-901.

Dhakal BK and Mulvey MA (2009) Uropathogenic *Escherichia coli* invades host cells via an HDAC6-modulated microtubule-dependent pathway. *J Biol Chem* **284:**446-454.

Dhanji H, Murphy NM, Akhigbe C, Doumith M, Hope R, Livermore DM, and Woodford N (2011) Isolation of fluoroquinolone-resistant O25b:H4-ST131 *Escherichia coli* with CTX-M-14 extended-spectrum β-lactamase from UK river water. *J Antimicrob Chemother* **66:**512-516.

Dolejska M, Frolkova P, Florek M, Jamborova I, Purgertova M, Kutilova I, Cizek A, Guenther S, and Literak I (2011) CTX-M-15-producing *Escherichia coli* clone B2-O25b-ST131 and *Klebsiella* spp. isolates in municipal wastewater treatment plant effluents. *J Antimicrob Chemother* **66:**2784-2790.

dos Santos JC, Weber LP, and Perez LR (2007) Evaluation of urinalysis parameters to predict urinary-tract infection. *Braz J Infect Dis* **11:**479-481.

Drazenovich N, Ling GV, and Foley J (2004) Molecular investigation of *Escherichia coli* strains associated with apparently persistent urinary tract infection in dogs. *J Vet Intern Med* **18:**301-306.

Dreicer R, Propert KJ, Roth BJ, Einhorn LH, and Loehrer PJ (1997) Vinblastine, ifosfamide, and gallium nitrate—an active new regimen in patients with advanced carcinoma of the urothelium. *Cancer* **79:**110-114.

Dunn LL, Rahmanto YS, and Richardson DR (2007) Iron uptake and metabolism in the new millennium. *Trends Cell Biol* **17:**93-100.

Dynes JJ, Tyliszczak T, Araki T, Lawrence JR, Swerhone GD, Leppard GG, and Hitchcock AP (2006) Speciation and quantitative mapping of metal species in microbial biofilms using scanning transmission X-ray microscopy. *Environ Sci Technol* **40:**1556-1565.

Ecker DJ, Matzanke BF, and Raymond KN (1986) Recognition and transport of ferric enterobactin in *Escherichia coli*. *J Bacteriol* **167:**666-673.

Ejrnaes K (2011) Bacterial characteristics of importance for recurrent urinary tract infections caused by *Escherichia coli*. *Dan Med Bull* **58:**B4187.

Ejrnaes K, Sandvang D, Lundgren B, Ferry S, Holm S, Monsen T, Lundholm R, and Frimodt-Moller N (2006) Pulsed-field gel electrophoresis typing of *Escherichia coli* strains from samples collected before and after pivmecillinam or placebo treatment of uncomplicated community-acquired urinary tract infection in women. *J Clin Microbiol* **44:**1776-1781.

El Hage Chahine J-M, Hémadi M, and Ha-Duong N-T (2012) Uptake and release of metal ions by transferrin and interaction with receptor 1. *Biochim Biophys Acta* **1820:**334-347.

Emery T (1986) Exchange of iron by gallium in siderophores. *Biochemistry* **25:**4629-4633.

Emody L, Kerenyi M, and Nagy G (2003) Virulence factors of uropathogenic *Escherichia coli*. *Int J Antimicrob Agents* **22 Suppl 2:**29-33.

Ewers C, Grobbel M, Stamm I, Kopp PA, Diehl I, Semmler T, Fruth A, Beutlich J, Guerra B, Wieler LH, and Guenther S (2010) Emergence of human pandemic O25:H4-ST131 CTX-M-15 extended-spectrum-β-lactamase-producing *Escherichia coli* among companion animals. *J Antimicrob Chemother* **65:**651-660.

Faro AC, Eon JG, Nogueira L, da Silva RF, and Rodrigues VD (2008) XAFS study of H-ZSM5 catalysts modified with gallium. *Catal Today* **133:**913-918.

Feria CP, Correia JD, Machado J, Vidal R, and Goncalves J (2000) Urinary tract infection in dogs. Analysis of 419 urocultures carried out in Portugal. *Adv Exp Med Biol* **485:**301-304.

Ferry S, Burman LG, and Holm SE (1988) Clinical and bacteriological effects of therapy of urinary tract infection in primary health care: Relation to in vitro sensitivity testing. *Scand J Infect Dis* **20:**535-544.

Finberg RW, Moellering RC, Tally FP, Craig WA, Pankey GA, Dellinger EP, West MA, Joshi M, Linden PK, Rolston KV, Rotschafer JC, and Rybak MJ (2004) The importance of bactericidal drugs: future directions in infectious disease. *Clin Infect Dis* **39:**1314-1320.

Firsov AA, Vostrov SN, Shevchenko AA, and Cornaglia G (1997) Parameters of bacterial killing and regrowth kinetics and antimicrobial effect examined in terms of area under the concentration-time curve relationships: action of ciprofloxacin against *Escherichia coli* in an in vitro dynamic model. *Antimicrob Agents Chemother* **41:**1281-1287.

Flora SJS, Kumar P, Kannan GM, and Rai GP (1998) Acute oral gallium arsenide exposure and changes in certain hematological, hepatic, renal and immunological indices at different time intervals in male Wistar rats. *Toxicol Lett* **94:**103-113.

Foley A and French L (2011) Urine clarity inaccurate to rule out urinary tract infection in women. *J Am Board Fam Med* **24:**474-475.

Foley JE and Nieto NC (2010) Tularemia. *Vet Microbiol* **140:**332-338.

Foxman B (2003) Epidemiology of urinary tract infections: Incidence, morbidity, and economic costs. *Dis Mon* **49:**53-70.

Foxman B (2010) The epidemiology of urinary tract infection. *Nat Rev Urol* **7:**653-660.

Foxman B and Brown P (2003) Epidemiology of urinary tract infections: transmission and risk factors, incidence, and costs. *Infect Dis Clin North Am* **17:**227-241.

Foxman B and Frerichs RR (1985) Epidemiology of urinary tract infection: I. Diaphragm use and sexual intercourse. *Am J Public Health* **75:**1308-1313.

Foxman B, Gillespie B, Koopman J, Zhang L, Palin K, Tallman P, Marsh JV, Spear S, Sobel JD, Marty MJ, and Marrs CF (2000) Risk factors for second urinary tract infection among college women. *Am J Epidemiol* **151:**1194-1205.

Gales AC, Sader HS, and Jones RN (2002) Urinary tract infection trends in Latin American hospitals: report from the SENTRY antimicrobial surveillance program (1997–2000). *Diagn Microbiol Infect Dis* **44:**289-299.

Ganser GH and Hewett P (2010) An accurate substitution method for analyzing censored data. *J Occup Environ Hyg* **7:**233-244.

Ganz T (2009) Iron in innate immunity: starve the invaders. *Curr Opin Immunol* **21:**63-67.

Garcia EC, Brumbaugh AR, and Mobley HL (2011) Redundancy and specificity of *Escherichia coli* iron acquisition systems during urinary tract infection. *Infect Immun* **79:**1225-1235.

Garénaux A, Caza M, and Dozois CM (2011) The Ins and Outs of siderophore mediated iron uptake by extra-intestinal pathogenic *Escherichia coli*. *Vet Microbiol* **153:**89-98.

Garrick MD, Singleton ST, Vargas F, Kuo HC, Zhao L, Knopfel M, Davidson T, Costa M, Paradkar P, Roth JA, and Garrick LM (2006) DMT1: which metals does it transport? *Biol Res* **39:**79-85.

Geerlings SE (2008) Urinary tract infections in patients with diabetes mellitus: epidemiology, pathogenesis and treatment. *Int J Antimicrob Agents* **31 Suppl 1:**S54-57.

Geerlings SE, Brouwer EC, Gaastra W, Verhoef J, and Hoepelman AI (1999) Effect of glucose and pH on uropathogenic and non-uropathogenic *Escherichia coli*: studies with urine from diabetic and non-diabetic individuals. *J Med Microbiol* **48:**535-539.

Geerlings SE, Meiland R, van Lith EC, Brouwer EC, Gaastra W, and Hoepelman AIM (2002) Adherence of Type 1-Fimbriated *Escherichia coli* to Uroepithelial Cells. *Diabetes Care* **25:**1405-1409.

Gibaldi M and Koup JR (1981) Pharmacokinetic concepts - drug binding, apparent volume of distribution and clearance. *Eur J Clin Pharmacol* **20:**299-305.

Giesen L, Cousins G, Dimitrov B, van de Laar F, and Fahey T (2010) Predicting acute uncomplicated urinary tract infection in women: a systematic review of the diagnostic accuracy of symptoms and signs. *BMC Fam Pract* **11:**78.

Goering PL and Rehm S (1990) Inhibition of liver, kidney, and erythrocyte δ-aminolevulinic acid dehydratase (porphobilinogen synthase) by gallium in the rat. *Environ Res* **53:**135-151.

Gordon KA and Jones RN (2003) Susceptibility patterns of orally administered antimicrobials among urinary tract infection pathogens from hospitalized patients in North America:

comparison report to Europe and Latin America. Results from the SENTRY Antimicrobial Surveillance Program (2000). *Diagn Microbiol Infect Dis* **45:**295-301.

Gravel D, Taylor G, Ofner M, Johnston L, Loeb M, Roth VR, Stegenga J, Bryce E, The Canadian Nosocomial Infection Surveillance P, and Matlow A (2007) Point prevalence survey for healthcare-associated infections within Canadian adult acute-care hospitals. *J Hosp Infect* **66:**243-248.

Groessl M, Bytzek A, and Hartinger CG (2009) The serum protein binding of pharmacologically active gallium(III) compounds assessed by hyphenated CE-MS techniques. *Electrophoresis* **30:**2720-2727.

Gunshin H, Fujiwara Y, Custodio AO, Direnzo C, Robine S, and Andrews NC (2005) Slc11a2 is required for intestinal iron absorption and erythropoiesis but dispensable in placenta and liver. *J Clin Invest* **115:**1258-1266.

Gunther IV NW, Snyder JA, Lockatell V, Blomfield I, Johnson DE, and Mobley HLT (2002) Assessment of virulence of uropathogenic *Escherichia coli* type 1 fimbrial mutants in which the invertible element Is phase-locked on or off. *Infect Immun* **70:**3344-3354.

Gupta K, Hooton TM, Wobbe CL, and Stamm WE (1999) The prevalence of antimicrobial resistance among uropathogens causing acute uncomplicated cystitis in young women. *Int J Antimicrob Agents* **11:**305-308.

Hagan EC, Lloyd AL, Rasko DA, Faerber GJ, and Mobley HL (2010) *Escherichia coli* global gene expression in urine from women with urinary tract infection. *PLoS Pathog* **6:**e1001187.

Hagberg L, Engberg I, Freter R, Lam J, Olling S, and Svanborg Edén C (1983) Ascending, unobstructed urinary tract infection in mice caused by pyelonephritogenic *Escherichia coli* of human origin. *Infect Immun* **40:**273-283.

Hannan TJ, Mysorekar IU, Hung CS, Isaacson-Schmid ML, and Hultgren SJ (2010) Early severe inflammatory responses to uropathogenic *E. coli* predispose to chronic and recurrent urinary tract infection. *PLoS Pathog* **6:**e1001042.

Haraoka M, Hang L, Frendéus B, Godaly G, Burdick M, Strieter R, and Svanborg C (1999) Neutrophil recruitment and resistance to urinary tract infection. *J Infect Dis* **180:**1220-1229.

Harrington JR, Martens RJ, Cohen ND, and Bernstein LR (2006) Antimicrobial activity of gallium against virulent *Rhodococcus equi* in vitro and in vivo. *J Vet Pharmacol Ther* **29:**121-127.

Harris WR and Pecoraro VL (1983) Thermodynamic binding constants for gallium transferrin. *Biochemistry* **22:**292-299.

Hart MM and Adamson RH (1971) Antitumor activity and toxicity of salts of inorganic group IIIa metals - Aluminum, gallium, indium, and thallium *Proc Natl Acad Sci U S A* **68:**1623-&.

Heald S, Cross J, Brewe D, and Gordon R (2007) The PNC/XOR X-ray microprobe station at APS sector 20. *Nucl Instrum Meth A* **582:**215-217.

Hegge FN, Mahler DJ, and Larson SM (1977) The incorporation of Ga-67 into the ferritin fraction of rabbit hepatocytes in vivo. *J Nucl Med* **18:**937-939.

Henderson JP, Crowley JR, Pinkner JS, Walker JN, Tsukayama P, Stamm WE, Hooton TM, and Hultgren SJ (2009) Quantitative metabolomics reveals an epigenetic blueprint for iron acquisition in uropathogenic *Escherichia coli*. *PLoS Pathog* **5:**e1000305.

Herscheid JDM, Knops GHJN, Boele S, and Hoekstra A (1986) On the mechanism of gallium accumulation in tumours. Isolation of N-hydroxypeptides. *Int J Rad Appl Instrum B* **13:**63-65.

Heyns CF (2011) Urinary tract infection associated with conditions causing urinary tract obstruction and stasis, excluding urolithiasis and neuropathic bladder. *World J Urol*.

Hitchcock AP, Dynes JJ, Johansson G, Wang J, and Botton G (2008) Comparison of NEXAFS microscopy and TEM-EELS for studies of soft matter. *Micron* **39:**311-319.

Hoffer PB, Huberty J, and Khayam-Bashi H (1977) The association of Ga-67 and lactoferrin. *J Nucl Med* **18:**713-717.

Huang EH, Gabler DM, Krecic ME, Gerber N, Ferguson RM, and Orosz CG (1994) Differential effects of gallium nitrate on T lymphocyte and endothelial cell activation. *Transplantation* **58:**1216-1222.

Hubbard JA, Lewandowska KB, Hughes MN, and Poole RK (1986) Effects of iron-limitation of *Escherichia coli* on growth, the respiratory chains and gallium uptake. *Arch Microbiol* **146:**80-86.

Hunziker M, Kutasy B, D'Asta F, and Puri P (2011) Urinary tract anomalies associated with high grade primary vesicoureteral reflux. *Pediatr Surg Int*.

Hvidberg H, Struve C, Krogfelt KA, Christensen N, Rasmussen SN, and Frimodt-Møller N (2000) Development of a long-term ascending urinary tract infection mouse model for antibiotic treatment studies. *Antimicrob Agents Chemother* **44:**156-163.

Ingersoll MA, Kline KA, Nielsen HV, and Hultgren SJ (2008) G-CSF induction early in uropathogenic *Escherichia coli* infection of the urinary tract modulates host immunity. *Cell Microbiol* **10:**2568-2578.

Ishihara R, Ide-Ektessabi A, Ikeda K, Mizuno Y, Fujisawa S, Takeuchi T, and Ohta T (2002) Investigation of cellular metallic elements in single neurons of human brain tissues. *Neuroreport* **13:**1817-1820.

Jabboury K, Frye D, Holmes FA, Fraschini G, and Hortobagyi G (1989) Phase II evaluation of gallium nitrate by continuous infusion in breast cancer. *Invest New Drugs* **7:**225-229.

Jackson GE and Byrne MJ (1996) Metal ion speciation in blood plasma: gallium-67 citrate and MRJ contrast agents. *J Nucl Med* **37:**379-386.

Jakobsen L, Hammerum AM, and Frimodt-Moller N (2010) Virulence of *Escherichia coli* B2 isolates from meat and animals in a murine model of ascending urinary tract infection (UTI): evidence that UTI is a zoonosis. *J Clin Microbiol* **48:**2978-2980.

Johnson JR and Clabots C (2006) Sharing of virulent *Escherichia coli* clones among household members of a woman with acute cystitis. *Clin Infect Dis* **43:**E101-E108.

Johnson JR, Kaster N, Kuskowski MA, and Ling GV (2003) Identification of urovirulence traits in *Escherichia coli* by comparison of urinary and rectal *E. coli* isolates from dogs with urinary tract infection. *Journal of clinical microbiology* **41:**337-345.

Johnson JR, Menard M, Johnston B, Kuskowski MA, Nichol K, and Zhanel GG (2009a) Epidemic clonal groups of *Escherichia coli* as a cause of antimicrobial-resistant urinary tract infections in Canada, 2002 to 2004. *Antimicrob Agents Chemother* **53:**2733-2739.

Johnson JR, Miller S, Johnston B, Clabots C, and DebRoy C (2009b) Sharing of *Escherichia coli* sequence type ST131 and other multidrug-resistant and urovirulent *E. coli* strains among dogs and cats within a household. *J Clin Microbiol* **47:**3721-3725.

Johnson JR, Owens K, Gajewski A, and Clabots C (2008) *Escherichia coli* colonization patterns among human household members and pets, with attention to acute urinary tract infection. *J Infect Dis* **197:**218-224.

Johnson JR and Russo TA (2005) Molecular epidemiology of extraintestinal pathogenic (uropathogenic) *Escherichia coli*. *Int J Med Microbiol* **295:**383-404.

Johnson JR, Stell AL, Delavari P, Murray AC, Kuskowski M, and Gaastra W (2001) Phylogenetic and pathotypic similarities between *Escherichia coli* isolates from urinary tract infections in dogs and extraintestinal infections in humans. *J Infect Dis* **183:**897-906.

Justice SS, Hunstad DA, Seed PC, and Hultgren SJ (2006) Filamentation by *Escherichia coli* subverts innate defenses during urinary tract infection. *Proc Natl Acad Sci USA* **103:**19884-19889.

Kamitsubo H (1998) *First commissioning of SPring-8*. Ieee, New York.

Kaneko Y, Thoendel M, Olakanmi O, Britigan BE, and Singh PK (2007) The transition metal gallium disrupts *Pseudomonas aeruginosa* iron metabolism and has antimicrobial and antibiofilm activity. *J Clin Invest* **117:**877-888.

Karlowsky JA, Kelly LJ, Thornsberry C, Jones ME, and Sahm DF (2002) Trends in antimicrobial resistance among urinary tract infection isolates of *Escherichia coli* from female outpatients in the United States. *Antimicrob Agents Chemother* **46:**2540-2545.

Karlowsky JA, Lagace-Wiens PR, Simner PJ, DeCorby MR, Adam HJ, Walkty A, Hoban DJ, and Zhanel GG (2011) Antimicrobial resistance in urinary tract pathogens in Canada from 2007 to 2009: CANWARD surveillance study. *Antimicrob Agents Chemother* **55:**3169-3175.

Kau AL, Hunstad DA, and Hultgren SJ (2005) Interaction of uropathogenic *Escherichia coli* with host uroepithelium. *Curr Opin Microbiol* **8:**54-59.

Kaye D (1968) Antibacterial activity of human urine. *J Clin Invest* **47:**2374-2390.

Kaznacheyev K, Osanna A, Jacobsen C, Plashkevych O, Vahtras O, Ågren, Carravetta V, and Hitchcock AP (2002) Innershell absorption spectroscopy of amino acids. *J Phys Chem A* **106:**3153-3168.

Kaznatcheev K, Karunakaran C, Lanke U, Urquhart S, Obst M, and Hitchcock A (2007) Soft X-ray spectromicroscopy beamline at the CLS: Commissioning results. *Nucl Instrum Meth A* **582:**96-99.

Kerrn MB, Struve C, Blom J, Frimodt-Møller N, and Krogfelt KA (2005) Intracellular persistence of *Escherichia coli* in urinary bladders from mecillinam-treated mice. *J Antimicrob Chemother* **55:**383-386.

Khandelwal P, Abraham SN, and Apodaca G (2009) Cell biology and physiology of the uroepithelium. *Am J Physiol Renal Physiol* **297:**F1477-F1501.

Khasriya R, Khan S, Lunawat R, Bishara S, Bignal J, Malone-Lee M, Ishii H, O'Connor D, Kelsey M, and Malone-Lee J (2010) The inadequacy of urinary dipstick and microscopy as surrogate markers of urinary tract infection in urological outpatients With lower urinary tract symptoms without acute frequency and dysuria. *J Urol* **183:**1843-1847.

King MM and Chou WT (1993) Nuclear Data Sheets Update for A = 73. *Nuclear Data Sheets* **69:**857-901.

Klausner JS, Osborne CA, and Stevens JB (1976) Clinical evaluation of commercial reagent strips for detection of significant bacteriuria in dogs and cats. *Am J Vet Res* **37:**719-722.

Klumpp DJ, Rycyk MT, Chen MC, Thumbikat P, Sengupta S, and Schaeffer AJ (2006) Uropathogenic *Escherichia coli* induces extrinsic and intrinsic cascades to initiate urothelial apoptosis. *Infect Immun* **74:**5106-5113.

Koeijers JJ, Kessels AGH, Nys S, Bartelds A, Donker G, Stobberingh EE, and Verbon A (2007) Evaluation of the Nitrite and Leukocyte Esterase Activity Tests for the Diagnosis of Acute Symptomatic Urinary Tract Infection in Men. *Clin Infect Dis* **45:**894-896.

Krakoff IH, Newman RA, and Goldberg RS (1979) Clinical toxicologic and pharmacologic studies of gallium nitrate. *Cancer* **44:**1722-1727.

Krämer SD (1999) Absorption prediction from physicochemical parameters. *Pharm Sci Technol Today* **2:**373-380.

Krause MO (1979) Atomic radiative and radiationless yields for K and L shells. *J Phys Chem Ref Data* **8:**307-327.

Kreutzer MF, Kage H, Gebhardt P, Wackler B, Saluz HP, Hoffmeister D, and Nett M (2011) Biosynthesis of a complex yersiniabactin-like natural product via the mic locus in phytopathogen *Ralstonia solanacearum*. *Appl Environ Microbiol* **77:**6117-6124.

Krewulak KD and Vogel HJ (2008) Structural biology of bacterial iron uptake. *Biochim Biophys Acta* **1778:**1781-1804.

Krewulak KD and Vogel HJ (2011) TonB or not TonB: is that the question? *Biochem Cell Biol* **89:**87-97.

Kurazono H, Nakano M, Yamamoto S, Ogawa O, Yuri K, Nakata K, Kimura M, Makino S, and Nair GB (2003) Distribution of the usp gene in uropathogenic *Escherichia coli* isolated from companion animals and correlation with serotypes and size-variations of the pathogenicity island. *Microbiol Immunol* **47:**797-802.

Lagacé-Wiens PRS, Simner PJ, Forward KR, Tailor F, Adam HJ, DeCorby M, Karlowsky J, Hoban DJ, and Zhanel GG (2011) Analysis of 3789 in- and outpatient *Escherichia coli* isolates from across Canada—results of the CANWARD 2007–2009 study. *Diagn Microbiol Infect Dis* **69:**314-319.

Lambert LA (2012) Molecular evolution of the transferrin family and associated receptors. *Biochim Biophys Acta* **1820:**244-255.

Lambert LA, Perri H, Halbrooks PJ, and Mason AB (2005) Evolution of the transferrin family: Conservation of residues associated with iron and anion binding. *Comp Biochem Physiol B Biochem Mol Biol* **142:**129-141.

Lane DR and Takhar SS (2011) Diagnosis and management of urinary tract infection and pyelonephritis. *Emerg Med Clin North Am* **29:**539-552.

Laupland KB, Bagshaw SM, Gregson DB, Kirkpatrick AW, Ross T, and Church DL (2005) Intensive care unit-acquired urinary tract infections in a regional critical care system. *Crit Care* **9:**R60-65.

Laupland KB, Ross T, Pitout JDD, Church DL, and Gregson DB (2007) Community-onset urinary tract infections: a population-based assessment. *Infection* **35:**150-153.

Lawrence JR, Swerhone GDW, Leppard GG, Araki T, Zhang X, West MM, and Hitchcock AP (2003) Scanning transmission X-ray, laser scanning, and transmission electron microscopy mapping of the exopolymeric matrix of microbial biofilms. *Appl Environ Microbiol* **69:**5543-5554.

Layer G, Reichelt J, Jahn D, and Heinz DW (2010) Structure and function of enzymes in heme biosynthesis. *Protein Sci* **19:**1137-1161.

Lee JH, Lee YM, and Cho JH (2011) Risk factors of septic shock in bacteremic acute pyelonephritis patients admitted to an ER. *J Infect Chemother*.

Legrand SB (2011) Modern management of malignant hypercalcemia. *Am J Hosp Palliat Care* **28:**515-517.

Leman P (2002) Validity of urinalysis and microscopy for detecting urinary tract infection in the emergency department. *Eur J Emerg Med* **9:**141-147.

Levison ME and Levison JH (2009) Pharmacokinetics and pharmacodynamics of antibacterial agents. *Infect Dis Clin North Am* **23:**791-815, vii.

Lewis TA, Munson AE, and McCoy KL (1996) Gallium arsenide selectively suppresses antigen processing by splenic macrophages for CD4+ T cell activation. *J Pharmacol Exp Ther* **278:**1244-1251.

Leyland-Jones B (2004) Treating cancer-related hypercalcemia with gallium nitrate. *J Support Oncol* **2:**509-516.

Ling GV (1984) Therapeutic strategies involving antimicrobial treatment of the canine urinary tract. *J Am Vet Med Assoc* **185:**1162-1164.

Ling GV, Norris CR, Franti CE, Eisele PH, Johnson DL, Ruby AL, and Jang SS (2001) Interrelations of organism prevalence, specimen collection method, and host age, sex, and breed among 8,354 canine urinary tract infections (1969-1995). *J Vet Intern Med* **15:**341-347.

Ling GV, Rohrich PJ, Ruby AL, Johnson DL, and Jang SS (1984) Canine urinary tract infections: a comparison of in vitro antimicrobial susceptibility test results and response to oral therapy with ampicillin or with trimethoprim-sulfa. *J Am Vet Med Assoc* **185:**277-281.

Lipinski CA, Lombardo F, Dominy BW, and Feeney PJ (1997) Experimental and computational approaches to estimate solubility and permeability in drug discovery and development settings. *Adv Drug Deliv Rev* **23:**3-25.

Llinas M, Wilson DM, and Neilands JB (1973) Effect of metal binding on the conformation of enterobactin. A proton and carbon-13 nuclear magnetic resonance study. *Biochemistry* **12:**3836-3843.

Lloyd AL, Rasko DA, and Mobley HL (2007) Defining genomic islands and uropathogen-specific genes in uropathogenic *Escherichia coli*. *J Bacteriol* **189:**3532-3546.

Lombi E and Susini J (2009) Synchrotron-based techniques for plant and soil science: opportunities, challenges and future perspectives. *Plant Soil* **320:**1-35.

Loo BW, Jr., Sauerwald IM, Hitchcock AP, and Rothman SS (2001) A new sample preparation method for biological soft X-ray microscopy: nitrogen-based contrast and radiation tolerance properties of glycol methacrylate-embedded and sectioned tissue. *J Microsc* **204:**69-86.

Loughman JA and Hunstad DA (2011) Attenuation of human neutrophil migration and function by uropathogenic bacteria. *Microbes Infect* **13:**555-565.

Low DA, Braaten BA, Ling GV, Johnson DL, and Ruby AL (1988) Isolation and comparison of *Escherichia coli* strains from canine and human patients with urinary tract infections. *Infect Immun* **56:**2601-2609.

Lumachi F, Brunello A, Roma A, and Basso U (2008) Medical treatment of malignancy-associated hypercalcemia. *Curr Med Chem* **15:**415-421.

MacKenzie EL, Iwasaki K, and Tsuji Y (2008) Intracellular iron transport and storage: from molecular mechanisms to health implications. *Antioxid Redox Signal* **10:**997-1030.

Maiden MCJ, Bygraves JA, Feil E, Morelli G, Russell JE, Urwin R, Zhang Q, Zhou J, Zurth K, Caugant DA, Feavers IM, Achtman M, and Spratt BG (1998) Multilocus sequence typing: A portable approach to the identification of clones within populations of pathogenic microorganisms. *Proc Natl Acad Sci USA* **95:**3140-3145.

Malaviya R, Ikeda T, Abraham SN, and Malaviya R (2004) Contribution of mast cells to bacterial clearance and their proliferation during experimental cystitis induced by type 1 fimbriated *E. coli*. *Immunol Lett* **91:**103-111.

Malfetano JH, Blessing JA, and Adelson MD (1991a) A phase II trial of gallium nitrate (NSC #15200) in previously treated ovarian carcinoma. A Gynecologic Oncology Group Study. *Am J Clin Oncol* **14:**349-351.

Malfetano JH, Blessing JA, and Homesley HD (1995) A phase II trial of gallium nitrate (NSC #15200) in nonsquamous cell carcinoma of the cervix. A Gynecologic Oncology Group study. *Am J Clin Oncol* **18:**495-497.

Malfetano JH, Blessing JA, Homesley HD, and Hanjani P (1991b) A phase II trial of gallium nitrate (NSC #15200) in advanced or recurrent squamous cell carcinoma of the cervix. A Gynecologic Oncology Group study. *Invest New Drugs* **9:**109-111.

Marrs CF, Zhang L, and Foxman B (2005) *Escherichia coli* mediated urinary tract infections: Are there distinct uropathogenic *E. coli* (UPEC) pathotypes? *FEMS Microbiol Lett* **252:**183-190.

Martens RJ, Cohen ND, Fajt VR, Nerren JR, Chaffin MK, Taylor RJ, and Bernstein LR (2010) Gallium maltolate: safety in neonatal foals following multiple enteral administrations. *J Vet Pharmacol Ther* **33:**208-212.

Martens RJ, Mealey K, Cohen ND, Harrington JR, Chaffin MK, Taylor RJ, and Bernstein LR (2007) Pharmacokinetics of gallium maltolate after intragastric administration in neonatal foals. *Am J Vet Res* **68:**1041-1044.

Masinde A, Gumodoka B, Kilonzo A, and Mshana SE (2009) Prevalence of urinary tract infection among pregnant women at Bugando Medical Centre, Mwanza, Tanzania. *Tanzan J Health Res* **11:**154-159.

Matsuyama S, Shimura M, Mirnura H, Fujii M, Yumoto H, Sano Y, Yabashi M, Nishino Y, Tamasaku K, Ishikawa T, and Yamauchi K (2009) Trace element mapping of a single cell using a hard x-ray nanobeam focused by a Kirkpatrick-Baez mirror system. *X-Ray Spectrom* **38:**89-94.

McCaffrey JA, Hilton S, Mazumdar M, Sadan S, Heineman M, Hirsch J, Kelly WK, Scher HI, and Bajorin DF (1997) Phase II randomized trial of gallium nitrate plus fluorouracil versus methotrexate, vinblastine, doxorubicin, and cisplatin in patients with advanced transitional-cell carcinoma. *J Clin Oncol* **15:**2449-2455.

McCown DA, Woodward LL, and Pool ML (1948) Radioactive isotopes of Ga and Ge. *Phys Rev* **74:**1311-1314.

McKellar QA, Sanchez Bruni SF, and Jones DG (2004) Pharmacokinetic/pharmacodynamic relationships of antimicrobial drugs used in veterinary medicine. *J Vet Pharmacol Ther* **27:**503-514.

Medina-Bombardo D and Jover-Palmer A (2011) Does clinical examination aid in the diagnosis of urinary tract infections in women? A systematic review and meta-analysis. *BMC Fam Pract* **12:**111.

Medlock AE, Carter M, Dailey TA, Dailey HA, and Lanzilotta WN (2009) Product release rather than chelation determines metal specificity for ferrochelatase. *J Mol Biol* **393:**308-319.

Meitzner GD, Iglesia E, Baumgartner JE, and Huang ES (1993) The chemical state of gallium in working alkane dehydrocyclodimerization catalysts - in situ gallium K-edge x-ray absorption spectroscopy. *J Catal* **140:**209-225.

Melkerson-Watson LJ, Rode CK, Zhang L, Foxman B, and Bloch CA (2000) Integrated genomic map from uropathogenic *Escherichia coli* J96. *Infect Immun* **68:**5933-5942.

Miller MC, Parkin S, Fetherston JD, Perry RD, and DeMoll E (2006) Crystal structure of ferric-yersiniabactin, a virulence factor of *Yersinia pestis*. *J Inorg Biochem* **100:**1495-1500.

Mobley HL, Chippendale GR, Tenney JH, Hull RA, and Warren JW (1987) Expression of type 1 fimbriae may be required for persistence of *Escherichia coli* in the catheterized urinary tract. *J Clin Microbiol* **25:**2253-2257.

Moroo IKU, Ujiie M, Walker BL, Tiong JWC, Vitalis TZ, Karkan D, Gabathuler R, Moise AR, and Jefferies WA (2003) Identification of a novel route of iron transcytosis across the mammalian blood-brain barrier. *Microcirculation* **10:**457-462.

Moulin-Schouleur M, Reperant M, Laurent S, Bree A, Mignon-Grasteau S, Germon P, Rasschaert D, and Schouler C (2007) Extraintestinal pathogenic *Escherichia coli* strains of avian and human origin: link between phylogenetic relationships and common virulence patterns. *J Clin Microbiol* **45:**3366-3376.

Mouton JW, Dudley MN, Cars O, Derendorf H, and Drusano GL (2005) Standardization of pharmacokinetic/pharmacodynamic (PK/PD) terminology for anti-infective drugs: an update. *J Antimicrob Chemother* **55:**601-607.

Mulvey MA, Lopez-Boado YS, Wilson CL, Roth R, Parks WC, Heuser J, and Hultgren SJ (1998) Induction and evasion of host defenses by type 1-piliated uropathogenic *Escherichia coli*. *Science* **282:**1494-1497.

Mulvey MA, Schilling JD, and Hultgren SJ (2001) Establishment of a persistent *Escherichia coli* reservoir during the acute phase of a bladder infection. *Infect Immun* **69:**4572-4579.

Mwaka AD, Mayanja-Kizza H, Kigonya E, and Kaddu-Mulindwa D (2011) Bacteriuria among adult non-pregnant women attending Mulago hospital assessment centre in Uganda. *Afr Health Sci* **11:**182-189.

Mysorekar IU and Hultgren SJ (2006) Mechanisms of uropathogenic *Escherichia coli* persistence and eradication from the urinary tract. *Proc Natl Acad Sci USA* **103:**14170-14175.

Nagasue N (1983) Gallium scanning in the diagnosis of hepatocellular carcinoma: A clinicopathological study of 45 patients. *Clin Radiol* **34:**139-142.

Narciso A, Nunes F, Amores T, Lito L, Melo-Cristino J, and Duarte A (2011) Persistence of uropathogenic *Escherichia coli* strains in the host for long periods of time: relationship between phylogenetic groups and virulence factors. *Eur J Clin Microbiol Infect Dis*.

National Research Council Subcommittee on Laboratory Animal Nutrition (1995) *Nutrient Requirements of Laboratory Animals, Fourth Revised Edition*. The National Academies Press.

National Toxciology Program (2000) NTP Toxicology and Carcinogenesis Studies of Gallium Arsenide (CAS No. 1303-00-0) in F344/N Rats and B6C3F1 Mice (Inhalation Studies). *Natl Toxicol Program Tech Rep Ser* **492:**1-306.

Neilands JB (1995) Siderophores: Structure and function of microbial iron transport compounds. *J Biol Chem* **270:**26723-26726.

Newman RA, Brody AR, and Krakoff IH (1979) Gallium nitrate (NSC-15200) induced toxicity in the rat. A pharmacologic, histopathologic and microanalytical investigation. *Cancer* **44:**1728-1740.

Newton SM, Trinh V, Pi H, and Klebba PE (2010) Direct Measurements of the Outer Membrane Stage of Ferric Enterobactin Transport. *J Biol Chem* **285:**17488-17497.

Nicolas-Chanoine M-H, Blanco J, Leflon-Guibout V, Demarty R, Alonso MP, Caniça MM, Park Y-J, Lavigne J-P, Pitout J, and Johnson JR (2008) Intercontinental emergence of *Escherichia coli* clone O25:H4-ST131 producing CTX-M-15. *J Antimicrob Chemother* **61:**273-281.

Nielubowicz GR and Mobley HL (2010) Host-pathogen interactions in urinary tract infection. *Nat Rev Urol* **7:**430-441.

Niki M, Hirai I, Yoshinaga A, Ulzii-Orshikh L, Nakata A, Yamamoto A, Yamamoto M, and Yamamoto Y (2011) Extended-spectrum beta-lactamase-producing *Escherichia coli* strains in the feces of carriers contribute substantially to urinary tract infections in these patients. *Infection* **39:**467-471.

Nilsson LM, Yakovenko O, Tchesnokova V, Thomas WE, Schembri MA, Vogel V, Klemm P, and Sokurenko EV (2007) The cysteine bond in the *Escherichia coli* FimH adhesin is critical for adhesion under flow conditions. *Mol Microbiol* **65:**1158-1169.

Niveditha S, Pramodhini S, Umadevi S, Kumar S, and Stephen S (2012) The Isolation and the Biofilm Formation of Uropathogens in the Patients with Catheter Associated Urinary Tract Infections (UTIs). *J Clin Diagn Res* **6:**1478-1482.

Noinaj N, Guillier M, Barnard TJ, and Buchanan SK (2010) TonB-dependent transporters: regulation, structure, and function. *Annu Rev Microbiol* **64:**43-60.

Norris CR, Williams BJ, Ling GV, Franti CE, Johnson, and Ruby AL (2000) Recurrent and persistent urinary tract infections in dogs: 383 cases (1969-1995). *J Am Anim Hosp Assoc* **36:**484-492.

Nys S, Terporten PH, Hoogkamp-Korstanje JA, and Stobberingh EE (2008) Trends in antimicrobial susceptibility of Escherichia coli isolates from urology services in The Netherlands (1998-2005). *The Journal of antimicrobial chemotherapy* **62:**126-132.

Ochodnický P, Cruz CD, Yoshimura N, and Michel MC (2011) Nerve growth factor in bladder dysfunction: Contributing factor, biomarker, and therapeutic target. *Neurourol Urodyn* **30:**1227-1241.

Ogeer-Gyles J, Mathews K, Weese JS, Prescott JF, and Boerlin P (2006) Evaluation of catheter-associated urinary tract infections and multi-drug-resistant *Escherichia coli* isolates from the urine of dogs with indwelling urinary catheters. *J Am Vet Med Assoc* **229:**1584-1590.

Ohgami RS, Campagna DR, McDonald A, and Fleming MD (2006) The Steap proteins are metalloreductases. *Blood* **108:**1388-1394.

Olakanmi O, Britigan BE, and Schlesinger LS (2000) Gallium disrupts iron metabolism of mycobacteria residing within human macrophages. *Infect Immun* **68:**5619-5627.

Olakanmi O, Gunn JS, Su S, Soni S, Hassett DJ, and Britigan BE (2010) Gallium disrupts iron uptake by intracellular and extracellular *Francisella* strains and exhibits therapeutic efficacy in a murine pulmonary infection model. *Antimicrob Agents Chemother* **54:**244-253.

Oliveira FA, Paludo KS, Arend LN, Farah SM, Pedrosa FO, Souza EM, Surek M, Picheth G, and Fadel-Picheth CM (2011) Virulence characteristics and antimicrobial susceptibility of uropathogenic *Escherichia coli* strains. *Genet Mol Res* **10:**4114-4125.

Palmer BM, Vogt S, Chen Z, Lachapelle RR, and Lewinter MM (2006) Intracellular distributions of essential elements in cardiomyocytes. *J Struct Biol* **155:**12-21.

Peeters E, Nelis HJ, and Coenye T (2008) Resistance of planktonic and biofilm-grown *Burkholderia cepacia* complex isolates to the transition metal gallium. *J Antimicrob Chemother* **61:**1062-1065.

Petibois C and Cestelli Guidi M (2008) Bioimaging of cells and tissues using accelerator-based sources. *Anal Bioanal Chem* **391:**1599-1608.

Petit J, Meurice N, Kaiser C, and Maggiora G (2012) Softening the Rule of Five—where to draw the line? *Bioorg Med Chem* **20:**5343-5351.

Platt R (1983) Quantitative definition of bacteriuria. *The American Journal of Medicine* **75:**44-52.

Radunovic´ A, Ueda F, Raja KB, Simpson RJ, Templar J, King SJ, Lilley JS, Philip Day J, and Bradbury MWB (1997) Uptake of 26-Al and 67-Ga into brain and other tissues of normal and hypotransferrinaemic mice. *Biometals* **10:**185-191.

Rahmanto YS, Bal S, Loh KH, Yu Y, and Richardson DR (2012) Melanotransferrin: Search for a function. *Biochim Biophys Acta* **1820:**237-243.

Rao DV, Swapna M, Cesareo R, Brunetti A, Akatsuka T, Yuasa T, Takeda T, Tromba G, and Gigante GE (2009) Investigation of the distribution of elements in snail shell with the use of synchrotron-based, micro-beam X-ray fluorescence spectrometry. *J Trace Elem Med Biol* **23:**251-257.

Ravel B and Newville M (2005) ATHENA, ARTEMIS, HEPHAESTUS: data analysis for X-ray absorption spectroscopy using IFEFFIT. *J Synchrotron Radiat* **12:**537-541.

Reeves PR, Liu B, Zhou Z, Li D, Guo D, Ren Y, Clabots C, Lan R, Johnson JR, and Wang L (2011) Rates of mutation and host transmission for an *Escherichia coli* clone over 3 years. *PLoS One* **6:**e26907.

Regier T, Krochak J, Sham TK, Hu YF, Thompson J, and Blyth RIR (2007) Performance and capabilities of the Canadian Dragon: The SGM beamline at the Canadian Light Source. *Nucl Instrum Meth A* **582:**93-95.

Reigstad CS, Hultgren SJ, and Gordon JI (2007) Functional genomic studies of uropathogenic *Escherichia coli* and host urothelial cells when intracellular bacterial communities are assembled. *J Biol Chem* **282:**21259-21267.

Reine NJ and Langston CE (2005) Urinalysis interpretation: How to squeeze out the maximum information from a small sample. *Clin Tech Small Anim Pract* **20:**2-10.

Rocha JBT, Tuerlinckx SM, Schetinger MRC, and Folmer V (2004) Effect of Group 13 metals on porphobilinogen synthase in vitro. *Toxicol Appl Pharmacol* **200:**169-176.

Rogers BA, Sidjabat HE, and Paterson DL (2011) *Escherichia coli* O25b-ST131: a pandemic, multiresistant, community-associated strain. *J Antimicrob Chemother* **66:**1-14.

Rosen DA, Hooton TM, Stamm WE, Humphrey PA, and Hultgren SJ (2007) Detection of intracellular bacterial communities in human urinary tract infection. *PLoS Med* **4:**e329.

Roshani H, Dabhoiwala NF, Verbeek FJ, and Lamers WH (1996) Functional anatomy of the human ureterovesical junction. *Anat Rec* **245:**645-651.

Rudick CN, Billips BK, Pavlov VI, Yaggie RE, Schaeffer AJ, and Klumpp DJ (2010) Host-pathogen interactions mediating pain of urinary tract infection. *J Infect Dis* **201:**1240-1249.

Russo TA and Johnson JR (2000) Proposal for a new inclusive designation for extraintestinal pathogenic isolates of *Escherichia coli*: ExPEC. *J Infect Dis* **181:**1753-1754.

Sacks O (2003) Gallium. *Chem Eng News* **81:**88.

Sagane R (1939) Radioactive isotopes of Cu, Zn, Ga and Ge. *Phys Rev* **55:**0031-0038.

Scherberich JE and Hartinger A (2008) Impact of Toll-like receptor signalling on urinary tract infection. *Int J Antimicrob Agents* **31 Suppl 1:**S9-14.

Schilling JD, Lorenz RG, and Hultgren SJ (2002) Effect of trimethoprim-sulfamethoxazole on recurrent bacteriuria and bacterial persistence in mice infected with uropathogenic *Escherichia coli*. *Infect Immun* **70:**7042-7049.

Schito GC, Naber KG, Botto H, Palou J, Mazzei T, Gualco L, and Marchese A (2009) The ARESC study: an international survey on the antimicrobial resistance of pathogens involved in uncomplicated urinary tract infections. *Int J Antimicrob Agents* **34:**407-413.

Schwartz DJ, Chen SL, Hultgren SJ, and Seed PC (2011) Population dynamics and niche distribution of uropathogenic *Escherichia coli* during acute and chronic urinary tract infection. *Infect Immun* **79:**4250-4259.

Seguin MA, Vaden SL, Altier C, Stone E, and Levine JF (2003) Persistent urinary tract infections and reinfections in 100 dogs (1989-1999). *J Vet Intern Med* **17:**622-631.

Sekyere EO, Dunn LL, and Richardson DR (2005) Examination of the distribution of the transferrin homologue, melanotransferrin (tumour antigen p97), in mouse and human. *Biochim Biophys Acta* **1722:**131-142.

Senderowicz AM, Reid R, Headlee D, Abornathy T, Horti J, Lush RM, Reed E, Figg WD, and Sausville EA (1999) A phase II trial of gallium nitrate in patients with androgen-metastatic prostate cancer. *Urol Int* **63:**120-125.

Shimizu K, Takamatsu M, Nishi K, Yoshida H, Satsuma A, and Hattori T (1996) Influence of local structure on the catalytic activity of gallium oxide for the selective reduction of NO by CH_4. *Chem Commun***:**1827-1828.

Smith YC, Rasmussen SB, Grande KK, Conran RM, and O'Brien AD (2008) Hemolysin of uropathogenic *Escherichia coli* evokes extensive shedding of the uroepithelium and hemorrhage in bladder tissue within the first 24 hours after intraurethral inoculation of mice. *Infect Immun* **76:**2978-2990.

Snyder JA, Haugen BJ, Buckles EL, Lockatell CV, Johnson DE, Donnenberg MS, Welch RA, and Mobley HLT (2004) Transcriptome of uropathogenic *Escherichia coli* during urinary tract infection. *Infect Immun* **72:**6373-6381.

Solomon D, Lehmann J, Kinyangi J, Liang BQ, Heymann K, Dathe L, Hanley K, Wirick S, and Jacobsen C (2009) Carbon (1s) NEXAFS spectroscopy of biogeochemically relevant reference organic compounds. *Soil Sci Soc Am J* **73:**1817-1830.

Spencer JD, Hains DS, Porter E, Bevins CL, DiRosario J, Becknell B, Wang H, and Schwaderer AL (2012) Human alpha defensin 5 expression in the human kidney and urinary tract. *PLoS One* **7:**e31712.

Srinivas S, Beck JT, Vesole D, McEwen C, Bhatnagar A, and Valone F (2002) Phase I study of oral gallium maltolate in patients with refractory malignancies. *European Journal of Cancer* **38:**S48-S48.

Stahlhut SG, Tchesnokova V, Struve C, Weissman SJ, Chattopadhyay S, Yakovenko O, Aprikian P, Sokurenko EV, and Krogfelt KA (2009) Comparative structure-function analysis of mannose-specific FimH adhesins from *Klebsiella pneumoniae* and *Escherichia coli*. *J Bacteriol* **191:**6592-6601.

Stenutz R, Weintraub A, and Widmalm G (2006) The structures of *Escherichia coli* O-polysaccharide antigens. *FEMS Microbiol Rev* **30:**382-403.

Sterrett SP, Penniston KL, Wolf Jr JS, and Nakada SY (2008) Acetazolamide Is an effective adjunct for urinary alkalization in patients With uric acid and cystine stone formation recalcitrant to potassium citrate. *Urology* **72:**278-281.

Stojiljkovic I, Kumar V, and Srinivasan N (1999) Non-iron metalloporphyrins: potent antibacterial compounds that exploit haem/Hb uptake systems of pathogenic bacteria. *Mol Microbiol* **31:**429-442.

Streit JM, Jones RN, Sader HS, and Fritsche TR (2004) Assessment of pathogen occurrences and resistance profiles among infected patients in the intensive care unit: report from the SENTRY Antimicrobial Surveillance Program (North America, 2001). *Int J Antimicrob Agents* **24:**111-118.

Sun HZ, Li HY, and Sadler PJ (1999) Transferrin as a metal ion mediator. *Chem Rev* **99:**2817-2842.

Sung J and Skoog S (2011) Surgical management of vesicoureteral reflux in children. *Pediatr Nephrol*.

Swenson CL, Boisvert AM, Kruger JM, and Gibbons-Burgener SN (2004) Evaluation of modified Wright-staining of urine sediment as a method for accurate detection of bacteriuria in dogs. *J Am Vet Med Assoc* **224:**1282-1289.

Taganna J, de Boer AR, Wuhrer M, and Bouckaert J (2011) Glycosylation changes as important factors for the susceptibility to urinary tract infection. *Biochem Soc Trans* **39:**349-354.

Tam VH, Schilling AN, and Nikolaou M (2005) Modelling time-kill studies to discern the pharmacodynamics of meropenem. *J Antimicrob Chemother* **55:**699-706.

Thompson AC and Vaughan D (2001) *X-ray Data Booklet*. Lawrence Berkeley National Laboratory, University of California.

Thornton SJ, Wong IT, Neumann R, Kozlowski P, and Wasan KM (2011) Dietary supplementation with phytosterol and ascorbic acid reduces body mass accumulation and alters food transit time in a diet-induced obesity mouse model. *Lipids Health Dis* **10:**107.

Thumbikat P, Berry RE, Ge Z, Billips BK, Yaggie RE, Zaichuk T, Tung-Tien S, Schaeffer AJ, and Klumpp DJ (2009) Bacteria-induced uroplakin signaling mediates bladder response to infection. *PLoS Pathog* **5:**1-17.

Toner B, Fakra S, Villalobos M, Warwick T, and Sposito G (2005) Spatially resolved characterization of biogenic manganese oxide production within a bacterial biofilm. *Appl Environ Microbiol* **71:**1300-1310.

Toutain PL and Bousquet-Melou A (2004a) Bioavailability and its assessment. *J Vet Pharmacol Ther* **27:**455-466.

Toutain PL and Bousquet-Melou A (2004b) Plasma clearance. *J Vet Pharmacol Ther* **27:**415-425.

Toutain PL and Bousquet-Melou A (2004c) Plasma terminal half-life. *J Vet Pharmacol Ther* **27:**427-439.

Toutain PL and Bousquet-Melou A (2004d) Volumes of distribution. *J Vet Pharmacol Ther* **27:**441-453.

Tsan MF (1985) Mechanism of gallium-67 accumulation in inflammatory lesions. *J Nucl Med* **26:**88-92.

Turnidge J, Bell J, Biedenbach DJ, and Jones RN (2002) Pathogen occurrence and antimicrobial resistance trends among urinary tract infection isolates in the Asia-Western Pacific Region: report from the SENTRY Antimicrobial Surveillance Program, 1998–1999. *Int J Antimicrob Agents* **20:**10-17.

United States Pharmacopeia (2005) Gallium Nitrate (Systemic), in: *United States Pharmacopeia Drug Information: Drug Information for the Health Care Professional* (Pharmacopeia US ed), pp 1508-1509, Thompson Micromedex.

Vail DM, Allen TA, and Weiser G (1986) Applicability of leukocyte esterase test strip in detection of canine pyuria. *J Am Vet Med Assoc* **189:**1451-1453.

van den Bosch J, Postma P, van Brenk D, Guinée P, de Graaff J, and MacLaren D (1981) Virulence of *Escherichia coli* strains isolated from urine of patients with acute cystitis and from faeces of healthy women. *Antonie Van Leeuwenhoek* **47:**97-106.

Verron E, Loubat A, Carle GF, Vignes-Colombeix C, Strazic I, Guicheux J, Rochet N, Bouler JM, and Scimeca JC (2012) Molecular effects of gallium on osteoclastic differentiation of mouse and human monocytes. *Biochem Pharmacol* **83:**671-679.

Verron E, Masson M, Khoshniat S, Duplomb L, Wittrant Y, Baud'huin M, Badran Z, Bujoli B, Janvier P, Scimeca JC, Bouler JM, and Guicheux J (2010) Gallium modulates osteoclastic bone resorption in vitro without affecting osteoblasts. *Br J Pharmacol* **159:**1681-1692.

Vigil PD, Alteri CJ, and Mobley HL (2011) Identification of in vivo-induced antigens including an RTX family exoprotein required for uropathogenic *Escherichia coli* virulence. *Infect Immun* **79:**2335-2344.

Vincent C, Boerlin P, Daignault D, Dozois CM, Dutil L, Galanakis C, Reid-Smith RJ, Tellier PP, Tellis PA, Ziebell K, and Manges AR (2010) Food reservoir for *Escherichia coli* causing urinary tract infections. *Emerg Infect Dis* **16:**88-95.

Wagenlehner F, Cek M, Naber K, Kiyota H, and Bjerklund-Johansen T (2011a) Epidemiology, treatment and prevention of healthcare-associated urinary tract infections. *World J Urol***:**1-9.

Wagenlehner FM, Hoyme U, Kaase M, Funfstuck R, Naber KG, and Schmiemann G (2011b) Uncomplicated urinary tract infections. *Dtsch Arztebl Int* **108:**415-423.

Wagner D, Maser J, Moric I, Boechat N, Vogt S, Gicquel B, Lai B, Reyrat JM, and Bermudez L (2005) Changes of the phagosomal elemental concentrations by *Mycobacterium tuberculosis* Mramp. *Microbiology* **151:**323-332.

Walker RD and Dowling PM (2006) Chapter 17: Fluoroquinolones, in: *Antimicrobial Therapy in Veterinary Medicine* (Giguère S, Prescott JF, Baggot JD, Walker RD, and Dowling PM eds), pp 263-284, Iowa State University Press, Ames, Iowa.

Wang H, Liang FX, and Kong XP (2008) Characteristics of the phagocytic cup induced by uropathogenic *Escherichia coli*. *J Histochem Cytochem* **56:**597-604.

Wang J and Pantopoulos K (2011) Regulation of cellular iron metabolism. *Biochem J* **434:**365-381.

Warrell RP, Bockman RS, Coonley CJ, Isaacs M, and Staszewski H (1984) Gallium nitrate inhibits calcium resorption from bone and is effective treatment for cancer-related hypercalcemia. *J Clin Invest* **73:**1487-1490.

Warrell RP, Coonley CJ, Straus DJ, and Young CW (1983) Treatment of patients with advanced malignant lymphoma using gallium nitrate administered as a seven-day continuous infusion. *Cancer* **51:**1982-1987.

Wasielewski E, Tzou DL, Dillmann B, Czaplicki J, Abdallah MA, Atkinson RA, and Kieffer B (2008) Multiple conformations of the metal-bound pyoverdine PvdI, a siderophore of *Pseudomonas aeruginosa*: a nuclear magnetic resonance study. *Biochemistry* **47:**3397-3406.

Watson RE and Perlman ML (1978) Seeing with a New Light: Synchrotron Radiation. *Science* **199:**1295-1302.

Weber DJ, Sickbert-Bennett EE, Gould CV, Brown VM, Huslage K, and Rutala WA (2011) Incidence of catheter-associated and non-catheter-associated urinary tract infections in a healthcare system. *Infect Control Hosp Epidemiol* **32:**822-823.

Webster LK, Olver IN, Stokes KH, Sephton RG, Hillcoat BL, and Bishop JF (2000) A pharmacokinetic and phase II study of gallium nitrate in patients with non-small cell lung cancer. *Cancer Chemother Pharmacol* **45:**55-58.

Weiner RE (1996) The mechanism of 67Ga localization in malignant disease. *Nucl Med Biol* **23:**745-751.

Weiner RE, Avis I, Neumann RD, and Mulshine JL (1996) Transferrin dependence of Ga $(NO_3)_3$ inhibition of growth in human-derived small cell lung cancer cells. *J Cell Biochem Suppl* **24:**276-287.

Weng TI, Wu HY, Lin PY, and Liu SH (2009) Uropathogenic *Escherichia coli*-induced inflammation alters mouse urinary bladder contraction via an interleukin-6-activated inducible nitric oxide synthase-related pathway. *Infect Immun* **77:**3312-3319.

Wetzstein HG (2005) Comparative mutant prevention concentrations of pradofloxacin and other veterinary fluoroquinolones indicate differing potentials in preventing selection of resistance. *Antimicrob Agents Chemother* **49:**4166-4173.

Whelan HT, Williams MB, Bajic DM, Segura AD, McAuliffe TL, and Chitambar CR (1994) Prevention of gallium toxicity by hyperhydration in treatment of medulloblastoma. *Pediatr Neurol* **10:**217-220.

Wierup M (1978) Bacteriological examination of urine specimens from non-catheterized and catheterized dogs with symptoms of urinary tract infection. *Nordisk veterinaermedicin* **30:**318-323.

Wiles TJ, Kulesus RR, and Mulvey MA (2008) Origins and virulence mechanisms of uropathogenic *Escherichia coli*. *Exp Mol Pathol* **85:**11-20.

Wilke M, Farges F, Petit PE, Brown GE, and Martin F (2001) Oxidation state and coordination of Fe in minerals: An FeK-XANES spectroscopic study. *Am Mineral* **86:**714-730.

Wilson ML and Gaido L (2004) Laboratory diagnosis of urinary tract infections in adult patients. *Clin Infect Dis* **38:**1150-1158.

Wiwanitkit V, Udomsantisuk N, and Boonchalermvichian C (2005) Diagnostic value and cost utility analysis for urine Gram stain and urine microscopic examination as screening tests for urinary tract infection. *Urol Res* **33:**220-222.

Wooley RE and Blue JL (1976) Quantitative and bacteriological studies of urine specimens from canine and feline urinary tract infections. *J Clin Microbiol* **4:**326-329.

Wu X-R, Kong X-P, Pellicer A, Kreibich G, and Sun T-T (2009) Uroplakins in urothelial biology, function, and disease. *Kidney Int* **75:**1153-1165.

Wu XR, Lin JH, Walz T, Häner M, Yu J, Aebi U, and Sun TT (1994) Mammalian uroplakins. A group of highly conserved urothelial differentiation-related membrane proteins. *J Biol Chem* **269:**13716-13724.

Wu XR, Sun TT, and Medina JJ (1996) In vitro binding of type 1-fimbriated *Escherichia coli* to uroplakins Ia and Ib: relation to urinary tract infections. *Proceedings of the National Academy of Sciences* **93:**9630-9635.

Xia X, Meng J, McDermott PF, and Zhao S (2011) *Escherichia coli* from retail meats carry genes associated with uropathogenic *Escherichia coli*, but are weakly invasive in human bladder cell culture. *J Appl Microbiol* **110:**1166-1176.

Yamamoto S (2007) Molecular epidemiology of uropathogenic *Escherichia coli*. *J Infect Chemother* **13:**68-73.

Yamamoto S, Higuchi Y, and Nojima M (2010) Current therapy of acute uncomplicated cystitis. *Int J Urol* **17:**450-456.

Yang J-L and Chen H-C (2003a) Effects of gallium on common carp (*Cyprinus carpio*): acute test, serum biochemistry, and erythrocyte morphology. *Chemosphere* **53:**877-882.

Yang JL and Chen HC (2003b) Growth Retardation and Histopathology of Common Carp (*Cyprinus carpio*) Exposed to Gallium. *Bull Environ Contam Toxicol* **71:**0240-0247.

Yeh JJ, Huang YC, Teng WB, Huang YF, Chuang YW, and Hsu CC (2011) The role of gallium-67 scintigraphy in comparing inflammatory activity between tuberculous and nontuberculous mycobacterial pulmonary diseases. *Nucl Med Commun* **32:**392-401.

Zasloff M (2007) Antimicrobial peptides, innate immunity, and the normally sterile urinary tract. *J Am Soc Nephrol* **18:**2810-2816.

Zhanel GG, Hisanaga TL, Laing NM, DeCorby MR, Nichol KA, Palatnik LP, Johnson J, Noreddin A, Harding GK, Nicolle LE, and Hoban DJ (2005) Antibiotic resistance in outpatient urinary isolates: final results from the North American Urinary Tract Infection Collaborative Alliance (NAUTICA). *Int J Antimicrob Agents* **26:**380-388.

Zhanel GG, Hisanaga TL, Laing NM, DeCorby MR, Nichol KA, Weshnoweski B, Johnson J, Noreddin A, Low DE, Karlowsky JA, and Hoban DJ (2006) Antibiotic resistance in *Escherichia coli* outpatient urinary isolates: final results from the North American Urinary Tract Infection Collaborative Alliance (NAUTICA). *Int J Antimicrob Agents* **27:**468-475.

Zhao J, Wang Z, Chen X, Wang J, and Li J (2011) Effects of intravesical liposome-mediated human beta-defensin-2 gene transfection in a mouse urinary tract infection model. *Microbiol Immunol* **55:**217-223.

Zhao X and Drlica K (2002) Restricting the selection of antibiotic-resistant mutant bacteria: measurement and potential use of the mutant selection window. *J Infect Dis* **185:**561-565.

Zhou G, Mo W-J, Sebbel P, Min G, Neubert TA, Glockshuber R, Wu X-R, Sun T-T, and Kong X-P (2001) Uroplakin Ia is the urothelial receptor for uropathogenic *Escherichia coli*: evidence from in vitro FimH binding. *J Cell Sci* **114:**4095-4103.

Zhou Q, Cao Z, Sun Y, Zhang J, Zhang L, and Chen C (2000) The magnet design of the SSRF storage ring and booster. *IEEE Trans Appl Supercond* **10:**256-259.

Zhou X, Heigl F, Ko J, Murphy M, Zhou J, Regier T, Blyth R, and Sham T (2007a) Origin of luminescence from Ga2O3 nanostructures studied using x-ray absorption and luminescence spectroscopy. *Physical Review B* **75**.

Zhou XT, Heigl F, Ko JYP, Murphy MW, Zhou JG, Regier T, Blyth RIR, and Sham TK (2007b) Origin of luminescence from Ga2O3 nanostructures studied using x-ray absorption and luminescence spectroscopy. *Physical Review B* **75:**-.

Appendix 1. **Near-edge x-ray absorption spectroscopy at the gallium K-edge for gallium reference compounds**

A library of near-edge x-ray absorption spectra at the gallium K-edge was assembled for gallium reference compounds to confirm that the compounds could be distinguished spectroscopically.

Gallium nitrate, gallium oxide, gallium maltolate, and tris (8-hydroxyquinolinato) gallium (III) were mounted on carbon tape. Gallium-transferrin was synthesized from human apo-transferrin, mouse transferrin and gallium nitrate as previously described, and ultraviolet absorption difference spectra were monitored to confirm the production of gallium-transferrin. Excess gallium nitrate was removed by rinsing and centrifugal filtration. Gallium K-edge x-ray absorption spectra were collected for all compounds using the PNC/XSD 20-BM beamline at the Advanced Photon Source.

A sharp increase in x-ray absorption around the gallium K-edge energy of 10.37 keV was observed in all samples (Figure A.1.). Post-edge peak locations and width varied between reference compounds, indicating that gallium K-edge x-ray absorption spectroscopy can allow identification of gallium compounds of potential biological relevance.

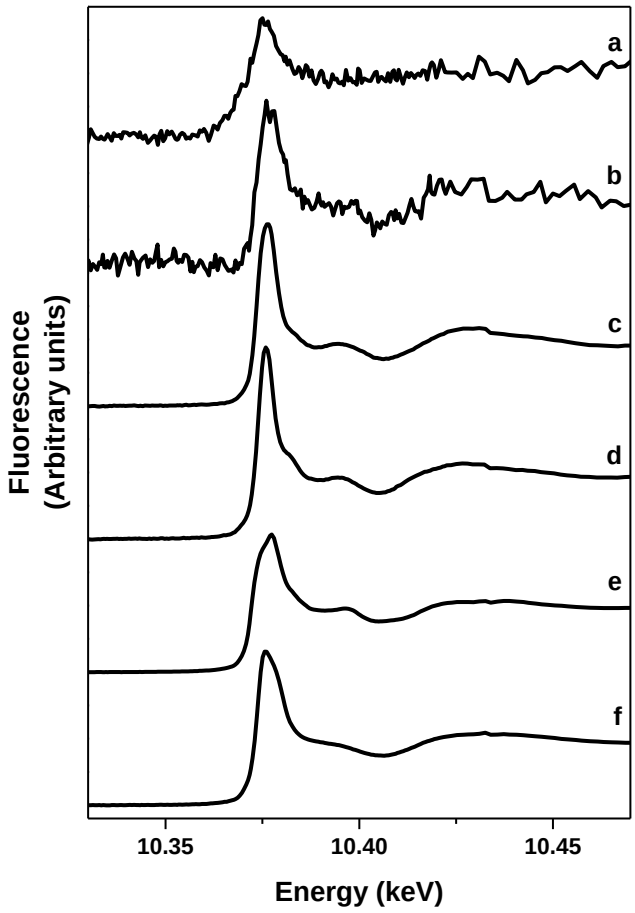

Figure A.1 X**-ray absorption near-edge spectra at the gallium K-edge for selected gallium compounds.**

Letters above the spectra indicate the compound evaluated: a, mouse gallium-transferrin; b, human gallium-transferrin; c, gallium maltolate; d, tris (8-hydroxyquinolinato) gallium; e, gallium oxide; f, gallium nitrate.